Multi-partite quantum optical systems for quantum information processing

Aurél Gábris

ÉRTEKEZÉS

a

DOKTORI (Ph.D)

fokozat megszerzéséhez

Fizikából

Gábris Aurél

Többrészű kvantumoptikai rendszerek alkalmazása a kvantuminformatikában

témavezető:
Prof. Janszky József
a fizika tudomány doktora,
az MTA rendes tagja
MTA Szilárdtestfizikai és Optikai Kutatóintézet

konzultáns:
Prof. Girish S. Agarwal
Oklahoma State University

Szegedi Tudománygyetem
Szeged, 2007

DISSERTATION

for the degree of

DOCTOR OF PHILOSOPHY

in

Physics

by

Aurél Gábris

Multi-partite quantum optical systems for quantum information processing

supervisor:

Prof. József Janszky

Research Institute for Solid State Physics and Optics,
Hungarian Academy of Sciences

consultant:

Prof. Girish S. Agarwal

Oklahoma State University

University of Szeged
Szeged, 2007

This dissertation is submitted in partial satisfaction of the requirements for the degree of doctor of philosophy in physics at the University of Szeged.

The majority of research work presented here has been carried out in the Research Institute for Solid State Physics and Optics, Hungarian Academy of Sciences, Budapest.

Jelen értekezés a Szegedi Tudományegyetem fizika doktori (Ph.D.) fokozatának megszerzése céljából készült.

Az értekezés alapjául szolgáló eredmények többsége a Magyar Tudományos Akadémia Szilárdtestfizikai és Optikai Kutatóintézetében folytatott kutatómunka során születtek.

"If the laws of physics did not support computational universality, they would be decreeing their own unknowability."

Quote from Ref. [63]

Contents

Introduction

Quantum optics is concerned with the study of light, and the interaction of light with matter, in the quantum regime [1–6]. Starting from the completely classical description of light–matter interactions [7], and reducing thermal fluctuations, usually accompanied by decreasing light intensities or the number of atoms, quantum effects can be made more dominant. In the fully quantum regime, both the electromagnetic field and the atoms that build up matter must be treated quantum mechanically. In between the two descriptions there are two intermediate limits. When only the quantum nature of light plays an important role, matter may be regarded as bulk, classical substance. A typical example of this treatment is (quantum) optics, where the employed light exhibits very small thermal fluctuations (i.e. it has strong coherence), and the various optical elements, such as mirrors, beam splitters, and half-wave plates, behave as completely classical objects. In the other intermediate limit, certain degrees of freedom of the atoms are treated quantum mechanically, and light modes are regarded as classical electromagnetic waves [8]. This limit is known as semi-classical description, and it is particularly useful in situations involving few weakly interacting atoms, and relatively strong light sources. The theory of classical lasers is a good example of the success of the semi-classical approach. The full quantum mechanical treatment is used when both the electromagnetic and the atomic system maintain strong internal coherences, and their mutual interaction is much stronger than the interaction with the environment. In this work all these three limits are used in an effort to demonstrate application of quantum optics to quantum information processing. We cannot limit our treatment to a single quantum optical system if we aim at general quantum information processing applications. By considering composite systems, quantum mechanics is brought to a higher level, raising issues such as locality, entanglement, and more related to measurement. In the general terminology of quantum information, composite systems are generally referred to as being "multi-partite." In such case the total Hilbert space of the system that could mathematically be divided or partitioned into smaller systems in many ways, has a natural partitioning prescribed by physics. Conceptually, it is also convenient to think about these subsystems as particles, since then their most important features are conserved, such as spatial separation (i.e. locality, non-locality), individual manipulation and measurement. For quantum bits, for example, it is a general practice to think about a collection of them as a system made up of spin-1/2 particles, regardless of the actual realisation.

Quantum information is an analogue of the usual Shannon information [9] which has revolutionised our lives in the end of the 20^{th} century. In the historical perspective, for the development of quantum information theory it was necessary to point out that information is something physical rather than a purely theoretical concept [10]. The science of quantum information and quantum computing is relatively young, however, there are now several good review books available on this topic [11–17], and we have listed an excellent introductory text book also under Ref. [18].

The basic unit of quantum information is the quantum bit [19], and it plays a sim-

ilar role as the bit in classical information theory [9, 20]. According to the convention, throughout this work the quantum bit is usually abbreviated to qubit, and to stress the classical nature, the bit is often given the epithet "classical." A quantum bit may be represented by a single two-level quantum system. Following the analogy from classical to quantum information, the two levels are conventionally denoted by the states $|0\rangle$ and $|1\rangle$ that are orthogonal, i.e. in a classical sense they are "mutually exclusive." In a physical realization these states may correspond to two orthogonal polarisations of a photon, two distinct electronic levels of an atom, opposite directions of a nuclear spin, etc. A quantum bit, and especially a collection of quantum bits, behaving according to quantum mechanics [21–26], display much more diverse properties than a classical bit that is subject to the laws of the classical theory.

The most important rule applying to the quantum bit is the superposition principle, and it says that the state of a quantum bit may be both $|0\rangle$ and $|1\rangle$ simultaneously. This is very different from the case of a deterministic classical bit that can only be either 0 or 1. The superposition principle is also the essence of many interesting features of quantum behaviour. It is notable that for the full description of a given general state of a quantum bit, infinitely many classical bits would be required. Due to the nature of quantum measurement, however, this sort of "information" cannot be extracted from the quantum state [23, 27, 28]. The consistent definition of information content of a quantum system can be done [19] using the von Neumann entropy [27].

Another important and peculiar consequence of the superposition principle is entanglement [29]. Entanglement between two quantum systems is generally marked by correlations between measurement outcomes that cannot be explained by any local classical theory [30, 31]: it seems as if the measurement of one party affected the measurement outcomes of the other in a non-local way. This property of quantum mechanics has been a subject of many debates. In particular, Einstein, Podolsky and Rosen termed entanglement as a paradox of quantum theory in their famous paper [32], and used it as an argument to why quantum theory was an incomplete theory in their sense. Entanglement receives enormous attention even today. The questions addressed include, criteria for entanglement [30, 31, 33, 34], finding a unique measure [35–39], detection [40, 41], and creation [42–45] of entanglement. Indeed its role in quantum computing and most other quantum information processing protocols is not yet fully understood although extensively studied [46–48].

Naturally the question arises, can we perform computation on quantum bits, just as we do on classical bits? And if so, can it be more efficient? The same questions can be asked with regard to communication. In general the answer to all these questions is yes. The algorithms invented by Deutsch [49, 50], Shor [51–55] and Grover [56, 57] demonstrate striking improvement compared to the best known classical algorithms. Also, these days quantum cryptography [58–62] systems are already commercially available. It is generally argued that the extra power of going quantum comes from the superposition principle. In case of quantum computation [63–69], the superposition of many different inputs of

a calculation lead to quantum parallelism allowing exponential speedup on certain problems. Today's quantum cryptography protocols either directly or indirectly all draw their unprecedented security from features of entanglement. Hence we see that employing quantum bits to encode information yields tremendous advantages over the classical practice. However, there is a price to pay: in accordance with quantum mechanics, our operations must be unitary ("reversible"). This rules out most of our favourite operations, including the duplication of bits and even the ordinary NOT operation. Nevertheless, there is always some kind of a workaround for such problems. Indeed, it has been shown that every (probabilistic) classical circuit can be simulated with quantum circuits [70]. The science of quantum information processing is concerned with harnessing the potential power of using quantum systems to encode information. Be it the development of complex quantum algorithms that solve a given problem, or the construction of quantum gates that are the basic building blocks of the logic for quantum bits, or the transmission of quantum information in special ways, they all fall under the umbrella of quantum information processing.

The difficulties in quantum information processing are not only theoretical or conceptual, there are a great deal of fundamental experimental challenges also. The problem is that the non-classical properties of quantum bits, that we wish to exploit, are lost very rapidly during the interaction with the environment. The naïve solution is to find a quantum system that is perfectly isolated from its environment. However, the problem is two-sided: quantum system weakly coupled to their environment are generally also difficult to manipulate and measure, thus feeding in the input, performing calculations, and reading out the results is very inefficient. Therefore we must always deal with some level of error being introduced into our system. The processes when errors are introduced by the environment or by unwanted interaction of quantum bits are collectively termed decoherence [71–77]. Fortunately, there exist several techniques to suppress the impact of decoherence. These include quantum error correction [78–84], encoding qubits in decoherence free subspaces. However, at the current state of technology decoherence prohibits realizations of large scale quantum information processing applications. Many believe that our technology just needs further refinement to be able to suppress the level of decoherence below an acceptable level. On the other hand, it is still not well understood whether the limitation is only technical and can be resolved by increasing precision, or something inherently contained in the nature of quantum errors.

In this work we approach quantum information processing from the direction of quantum optics. After a brief review of quantum optics and quantum information processing, we present part of our work related to the pure optical limit when only the electromagnetic field is regarded as quantised. We consider quantum bits corresponding to certain subspaces of the Hilbert space of light. Our initial attention is focused on a special class of states of light, the coherent states. These states are formally the same as the coherent states of a quantum harmonic oscillator, and these are the "most classical" quantum states of light also. The quasi-distribution function [85] of coherent states for example,

may be interpreted as a classical distribution function in phase space, and it evolves the same way in time as the corresponding classical distribution. Since an ideal laser is the source of a coherent state, it can, up to reasonable accuracy, be prepared in a laboratory. A property of coherent states, that somewhat complicates problems, is that they are not orthogonal to each other. This also means that they cannot be used as a computational basis. They can, however, still be used for representation of quantum states, because they span the complete Hilbert space. In particular, we can also use them to describe states of quantum bits. The non-orthogonality of coherent states only implies that the representation may be ambiguous. This ambiguity, however, can be removed by imposing certain conditions on the representation. In the present dissertation, we use the one-dimensional coherent state representation as the starting point for our calculations related to coherent states. First we generalise the representation to two modes, hence making it possible to represent entangled states in a similar manner. Since the representation is through functions defined on a complex plane, we term this representation one-complex-plane representation [86, 87]. We show its completeness by expressing a complete orthonormal basis using the notion of two-mode squeezing. The applicability of this representation has already demonstrated by elegantly reformulating [88] quantum teleportation of continuous variables [89, 90] in Hilbert space formalism. We believe that it may also be useful in description of other problems where coherent states have a special role, such as coherent state quantum computing [91, 92], or optical systems in the presence of significant decoherence.

As an application for the one-complex-plane representation, by discretising such a representation of two-mode squeezed vacuum, we derive a two-mode generalisation of optical Schrödinger cat states. We calculate the entanglement between the two modes using a formalism we have developed for this purpose. To demonstrate a possible use of this resource, we also propose a scheme for teleporting coherent state qubits [93]. This proposal works for a four-level (two quantum bits) subspace of the electromagnetic field, which is in contrast to earlier proposals [91, 94], which work only for a single quantum bit.

In the simplest case of coherent state quantum information processing protocols, we take two non-identical coherent states. These states, although not orthogonal, nevertheless span a two dimensional Hilbert space. If we choose, as it is often done, the coherent amplitudes of the two coherent states to be related to each other by a minus sign, then the optical Schrödinger cat states can be used as a computational basis [92, 95]. In contrast to the original pair of coherent states, the Schrödinger cat basis states are particularly prone to decoherence. In a case of a simple read-out problem, when the only results can be the two basis states, and no superpositions are permitted, we are required to distinguish Schrödinger cat states. If there is decoherence during the read-out procedure, its effect is that this discrimination cannot be done unambiguously with any measurement scheme. According to the Quantum Sanov Theorem [96], the maximum efficiency achievable by quantum measurements are given by quantum relative entropy [38, 97]. We analyse how

the preparation of the environment in a special state, i.e. squeezed vacuum, affects the distinguishablity of the two different possible outputs. We deduce the optimal relative phases for maximal suppressing of the effect of decoherence, and based on numerical calculations we give the optimal value of squeezing with respect to the average number of photons in the original basis states [98].

Light has proven itself an excellent media for sending quantum information [99], thanks to its weak coupling to the environment. In addition, interaction between two electromagnetic modes is also negligible. This latter property is rather bad news for quantum information processing. We know from universality theorems that to realize every quantum operation on quantum bits, possessing unitary control over individual quantum bits is not sufficient: in addition we need at least one suitable two qubit quantum operation [100]. Usually two qubit quantum operations can be derived from the interaction between the two quantum bits, or from the interaction of the two quantum bits with a third system. For efficient quantum computing the strength of the interaction is crucial. We must be able to finish our calculation before decoherence demolishes the state of the system, and the number of operations we can carry out in a given time depends on the strength of interactions that the operations are based on. In all-optical implementations, we would need non-linear elements to induce interactions between different modes of light [101–103]. However, to reduce the effect of decoherence the applied intensities are so low that the needed magnitude of optical non-linearities is well beyond the capabilities of presently available bulk non-linear materials. There is a solution to overcome this problem, it is however a little cumbersome: use only linear elements, and introduce non-linearities through conditional measurements [104].

One may find, however, very strong interactions in a high quality optical cavity between atoms and the electromagnetic field. This may offer a good test bed for implementing quantum operations involving two light modes [105], a light mode and an atom [106], or several atoms [107]. The theory that describes optical cavities and their interactions with atoms according to quantum mechanics is cavity quantum electrodynamics, or cavity QED for short [108–110]. There is an intuitive explanation to why an optical cavity enhances the strength of interaction so greatly. Such a cavity consists of two mirrors placed facing each other, allowing a photon to travel several round-trips between the two mirror walls, and interact repeatedly with the atoms located inside. The higher the quality factor of the cavity is, the more round-trips a photon can complete before it leaks out. The internal volume of the cavity plays and important role also: small resonator volumes yield strong interactions, and in the limit of infinite volume we get the free-space case.

In the present dissertation we consider cavity QED systems of several atoms localised in the same optical cavity. By considering such systems we would like to demonstrate how two major difficulties of traditional cavity QED realisations of quantum computing can be overcome. The first problem addressed is scalability. We formulate our first proposal [111] such that no theoretical limit seems to appear on the number of quantum bits, although

there are several technical limits at present. Our scheme consists of four level atoms of doubly degenerate ground state, and similarly degenerate excited states interacting with a two-mode cavity. We consider the two orthogonal circular polarisation modes of nearly the same frequency. We assume sufficient detuning of the cavity frequency from the atomic transition such that no direct excitations occur, and then we can reduce our treatment to the doubly degenerate ground states of the atoms. Further we assume a single photon in the cavity field. With these assumptions we can designate each atom and the cavity field as separate quantum bits, and we find an Ising type interaction between quantum bits ($\sigma_z^{(i)}\sigma_z^{(j)}$ terms in the Hamiltonian). The interaction can be visualised on a star shaped diagram, where the central node represents the cavity qubit, vertices symbolise coupling, and all other nodes represent the atoms which are connected only to the central node. We adopt a technique well-known in nuclear magnetic resonance to effectively cancel unwanted couplings, and we show that with external control of individual quantum bits a universal set of quantum operations can be generated in this system. The calculations also show that the operation of the apparatus does not get significantly more complicated with increasing the number of atoms: the number of additional laser pulses scales linearly with the number of additional atoms. As a side-effect of limiting our treatment to the ground states of the atoms, we have greatly reduced the effect of atomic decay, and the most significant source of decoherence remains the leakage of photons from the cavity.

Finally we consider a cavity QED system with identical localised two level atoms and a single mode electromagnetic field. We show that with sufficient detuning of the cavity resonance frequency from the atomic resonance, a robust implementation of quantum computing is achievable using this system [112]. The principle of operation relies on the vacuum shifts caused by the cavity. The vacuum shifts affect all atoms simultaneously, and the atoms perturb the cavity also, therefore the cavity acts as a mediator between the atoms. When the cavity's relaxation is fast compared to its coupling[1] to the atoms, the cavity state can be averaged out, leaving us only with the atoms which we identify as our quantum bits. The real strength of the scheme is that the requirements on the cavity lifetime are quite relaxed. Our scheme tolerates relatively high escape rates from the cavity, and one only pays the price through increased operation times. Even thermal excitations of the cavity field can be easily compensated using the same technique of laser pulses that is used to carry out single qubit operations. The interaction between the atoms may be written in terms of collective spin operators in a simple form. However, with the inclusion of single qubit operations, a rather complicated set of equations must be solved to obtain a desired transformation. Up to three atoms, we present explicit constructions of the essential two qubit operation, the CNOT gate. These constructions demonstrate the universality of the system up to three quantum bits. Higher quantum bit constructions would be an interesting theoretical challenge, however, they would yet be of limited practical use, as today's cavities and trapping apparata would allow localisation of at most two or three atoms in the same cavity. In our treatment we do not take into

[1] We note that the coupling depends also on the detuning that can be well controlled.

account the atomic decay. On the other hand, the techniques generally used to suppress atomic decay rely on introduction of additional levels, usually boil down to an effective two level system. Therefore the application of the modified configurations is possible along the lines worked out for the two-level atoms.

The structure of this dissertation is the following. In Chapter 1 briefly recall the necessary fundamentals of quantum optics and quantum information processing. We present in Chapter 2 our results concerning coherent state quantum bits. In Section 2.1 we develop the one-complex-plane representation. We define entangled Schrödinger cat states in Section 2.2 by discretisation of the one-complex-plane representation, and devise a quantum teleportation scheme to illustrate its applicability. In Section 2.3 we apply the multi-partite approach to the case of decoherence of Schrödinger cat states, and we calculate the optimal parameters when the environment can be prepared in a squeezed state. We turn to cavity QED systems in Chapter 3, and develop two examples of atom–cavity schemes for quantum computing. In Section 3.1 we propose a scheme that uses the collective interaction between the atoms and the cavity field, and yet turn out to be scalable at least on theoretical grounds. Next, in Section 3.2, we propose a scheme that is particularly robust against the strongest source of decoherence, the cavity losses.

Chapter 1

Quantum optics and quantum information processing

1.1 Quantum states of light in an optical cavity

This section is dedicated to a brief review of the quantum theory of light in an ideal cavity. We recall the quantisation of the free electromagnetic field based on the notion of normal modes. By the introduction of normal modes we are able to draw an analogy between a quantum harmonic oscillator and an electromagnetic mode. The notion of energy eigenstates leads us to the definition of the Fock basis, which is related to the exact number of photons in the mode, and therefore it provides a good deal of insight to the quantum nature of light. Following, we mention certain properties of polarisation modes and multi-mode cavities. We finally turn to the coherent states of light, and discuss the basic properties of coherent states, squeezed states. We also discuss simple superpositions of coherent states such as the optical Schrödinger cat states, as well as certain continuous superpositions such as those showing up in the one-dimensional coherent state representation.

1.1.1 Normal modes of the electromagnetic field in cavities

Here, and through the present work, we stay within the framework of non-relativistic quantum mechanics. It is therefore essential that implications which may follow from these results must be handled with care in relativistic situations. Such situation may be the question of causality in a Bell experiment. In these cases a Lorenz invariant quantisation and full quantum field theoretical treatment should be used.

In the following we shall discuss the mode structure of a one dimensional cavity. This is very well just an abstraction, and in a three dimensional cavity both the shapes of the modes and their structure can be very different. Nevertheless, certain modes of a real cavity may still be well approximated by those derived for the simplified system. When only those modes play significant role in an interaction, the following results can be applied directly.

For the quantisation of the electromagnetic field, we must find the appropriate canonical coordinates on which the quantisation rules can be prescribed. We choose the canonical coordinates associated to the normal modes of the cavity for this purpose. Our treatment starts from the Maxwell equations of the free classical field:

$$\nabla \times \mathbf{H} = \frac{\partial \mathbf{D}}{\partial t}, \tag{1.1}$$

$$\nabla \times \mathbf{E} = -\frac{\partial \mathbf{B}}{\partial t}, \tag{1.2}$$

$$\nabla \cdot \mathbf{B} = 0, \tag{1.3}$$

$$\nabla \cdot \mathbf{D} = 0, \tag{1.4}$$

where we have $\mathbf{B} = \mu_o \mathbf{H}$ and $\mathbf{D} = \varepsilon_0 \mathbf{E}$. It follows from Eqs. (1.1–1.4) that $\mathbf{E}$ must satisfy the wave equation

$$\nabla^2 \mathbf{E} - \frac{1}{c^2} \frac{\partial^2 \mathbf{E}}{\partial t^2} = 0. \tag{1.5}$$

The boundary condition for this differential equation follows from the assumption of an ideal cavity: the components of $\mathbf{E}$ parallel to the surface must vanish at the cavity mirrors. If we take the cavity axis to be parallel to the z axis, the boundary conditions become

$$E_{x,y}|_{\text{mirrors}} = 0. \tag{1.6}$$

The basic stationary solutions of the wave equation (1.5) with the boundary conditions (1.6) are called the normal modes, and can be written

$$\mathbf{E}_{\lambda,\nu}(x, y, z) = \hat{\mathbf{e}}_\lambda \sin(k_\nu z), \tag{1.7}$$

where $\hat{\mathbf{e}}_{\lambda=1,2}$ is the polarisation unit vector that can take two orthogonal values in the x–y plane, and $k_\nu = \nu\pi/L$, $\nu = 1, 2, \ldots$, with L denoting the length of the cavity. If we restrict our treatment to the x and z directions, a general solution of Eq. (1.5) can be expanded as

$$E_x(z, t) = \sum_\nu A_\nu q_\nu(t) \sin(k_\nu z), \tag{1.8}$$

with $A_\nu = \sqrt{2\omega_\nu^2 m_\nu / V_c \varepsilon_0}$, where V_c is the volume enclosed by the cavity mirrors, and $\omega_\nu = \nu\pi c/L$ the ν^{th} cavity eigenfrequency. The introduction of m_ν, a quantity of mass dimension, is inspired by the correspondence to a harmonic oscillator to which we conclude later. For convenience we assume $m_\nu = 1$. We notice that the functions $q_\nu(t)$ completely characterise the time evolution of our system (we may see this explicitly e.g. by performing a Fourier transformation on the z coordinate). We therefore identify the canonical position coordinates of the electromagnetic field in a cavity to be q_ν. Using the formula for the energy of the free electromagnetic field, we may write the Hamiltonian as

$$\mathscr{H} = \frac{1}{2} \int_{V_c} \varepsilon_0 E_x^2 + \mu_0 H_y^2 dV, \tag{1.9}$$

where H_y is the only non-vanishing component of the magnetic field, and according to the dynamical equations it is

$$H_y = \sum_\nu A_\nu \left(\frac{\dot{q}_\nu \varepsilon_0}{k_\nu} \right) \cos(k_\nu z). \tag{1.10}$$

Therefore we can express the Hamiltonian using only the q_ν functions as

$$\mathscr{H} = \frac{1}{2} \sum_\nu (m_\nu \omega_\nu^2 q_\nu + m_\nu \dot{q}_\nu^2). \tag{1.11}$$

Using the Hamiltonian (1.11) in the canonical equations we get $p_\nu = m_\nu \dot{q}_\nu$ for the canonical momentum, and hence we obtain the canonical form of the Hamiltonian of the free electromagnetic field in the cavity

$$\mathscr{H} = \sum_\nu \left(\frac{p_\nu^2}{2m_\nu} + \frac{1}{2} m_\nu \omega_\nu^2 q_\nu \right). \tag{1.12}$$

This expression demonstrates that each mode is dynamically equivalent to a harmonic oscillator, therefore that the electromagnetic field of a cavity can be regarded as a collection of infinitely many independent harmonic oscillators.

1.1.2 Quantisation of normal modes

Now that we have found the canonical coordinates q_ν and p_ν of the classical electromagnetic field, we may proceed to its quantisation. We prescribe the commutation relations:

$$[q_\nu, p_{\nu'}] = i\hbar \delta_{\nu\nu'}, \tag{1.13}$$

$$[q_\nu, q_{\nu'}] = [p_\nu, p_{\nu'}] = 0. \tag{1.14}$$

For convenience we introduce the ladder operators

$$a_\nu = \frac{1}{\sqrt{2m_\nu \hbar \omega_\nu}} (m_\nu \omega_\nu q_\nu + i p_\nu), \tag{1.15}$$

$$a_\nu^\dagger = \frac{1}{\sqrt{2m_\nu \hbar \omega_\nu}} (m_\nu \omega_\nu q_\nu - i p_\nu), \tag{1.16}$$

and with these we can write the quantum version of Hamiltonian (1.12) as

$$\mathscr{H} = \hbar \sum_\nu \omega_\nu \left(a_\nu^\dagger a_\nu + 1/2 \right). \tag{1.17}$$

In the Heisenberg picture, the time evolution of the ladder operators (1.15,1.16) is simply

$$a_\nu(t) = a_\nu \, \mathrm{e}^{-i\omega_\nu t}, \tag{1.18}$$

$$a_\nu^\dagger(t) = a_\nu^\dagger \, \mathrm{e}^{i\omega_\nu t}. \tag{1.19}$$

Therefore the quantised electric and magnetic fields (1.8, 1.10) can be written

$$E_x(z,t) = \sum_\nu \mathcal{E}_\nu \left(a_\nu \, \mathrm{e}^{-i\omega_\nu t} + a_\nu^\dagger \, \mathrm{e}^{i\omega_\nu t} \right) \sin k_\nu z, \tag{1.20}$$

$$H_y(z,t) = -i\varepsilon_0 c \sum_\nu \mathcal{E}_\nu \left(a_\nu \, \mathrm{e}^{-i\omega_\nu t} - a_\nu^\dagger \, \mathrm{e}^{i\omega_\nu t} \right) \cos k_\nu z, \tag{1.21}$$

where

$$\mathcal{E}_\nu = \sqrt{\frac{\hbar\omega_\nu}{\varepsilon_0 V_c}}. \tag{1.22}$$

We note, that inspired by the expansions in Eqs. (1.20-1.21), we may introduce the classical complex dynamical variable defined using the classical canonical variables q_ν and p_ν as

$$\alpha_\nu = \frac{1}{\sqrt{2\hbar\omega_\nu}}(\omega_\nu q_\nu + i p_\nu), \tag{1.23}$$

and its complex conjugate α_ν^*. This allows us to express the classical field as a Fourier expansion similar to Eqs. (1.20-1.21), with $m_\nu = 1$ for convenience.

1.1.3 Quantisation of travelling waves

Quantisation of the electromagnetic field in unbounded free space can be treated analogously. In this case we look for running-wave solutions and replace the boundary conditions (1.6) imposed by the ideal cavity mirrors by periodic boundary conditions. The basis solutions of the differential equation (1.5) are then plane waves, and the quantisation can be done on the canonical variables associated to each plane wave. We label the plane waves with the wave vector $\mathbf{k}$, that satisfies

$$\mathbf{k} = 2\pi\mathbf{n}/L, \qquad \text{with } \mathbf{n} \in \mathbb{Z}, \tag{1.24}$$

where L is the linear size of the volume with the periodic boundary conditions. In the limit of $L \to \infty$ the $\mathbf{k}$ vectors fill $\mathbb{R}^3$ continuously. In addition, to each $\mathbf{k}$ there are two polarisation labels $\lambda = 1, 2$ corresponding to two orthogonal polarisation vectors $\hat{\mathbf{e}}_\mathbf{k}^{(\lambda)}$ such that

$$\hat{\mathbf{e}}^{(\lambda)}\mathbf{k} = 0. \tag{1.25}$$

In terms of the ladder operators that correspond to (1.15,1.16), the quantisation relations become

$$[a_{\mathbf{k}\lambda}, a^\dagger_{\mathbf{k}'\lambda'}] = \delta_{\mathbf{k}\mathbf{k}'}\delta_{\lambda\lambda'}, \tag{1.26}$$

with all other commutators vanishing. The operators for electric and magnetic fields can then be written

$$\mathbf{E}(\mathbf{r},t) = \sum_{\mathbf{k},\lambda} \mathcal{E}_\mathbf{k}\hat{\mathbf{e}}^{(\lambda)} \left(a_{\mathbf{k}\lambda}\,\mathrm{e}^{-i\omega_k t + i\mathbf{k}\mathbf{r}} + a^\dagger_{\mathbf{k}\lambda}\,\mathrm{e}^{i\omega_k t - i\mathbf{k}\mathbf{r}}\right), \tag{1.27}$$

$$\mathbf{H}(\mathbf{r},t) = \frac{1}{\mu_0}\sum_{\mathbf{k},\lambda} \mathcal{E}_\mathbf{k}\frac{\mathbf{k}\times\hat{\mathbf{e}}_\mathbf{k}^{(\lambda)}}{\omega_k} \left(a_{\mathbf{k}\lambda}\,\mathrm{e}^{-i\omega_k t + i\mathbf{k}\mathbf{r}} + a^\dagger_{\mathbf{k}\lambda}\,\mathrm{e}^{i\omega_k t - i\mathbf{k}\mathbf{r}}\right), \tag{1.28}$$

where $\omega_k = c|\mathbf{k}|$, $\mathcal{E}_\mathbf{k} = \sqrt{\frac{\hbar\omega_k}{2\varepsilon_0 V_c}}$. And the Hamiltonian

$$\mathscr{H} = \sum_{\mathbf{k}\lambda} \hbar\omega_k (a^\dagger_{\mathbf{k}\lambda} a_{\mathbf{k}\lambda} + 1/2), \tag{1.29}$$

is completely analogous to what we have for the cavity field in Eq. (1.17), except that there the direction of the $\mathbf{k}$ modes is fixed by the cavity geometry, and that we have not explicitly included the polarisation labels there. Therefore the conclusion that the free electromagnetic field is dynamically equivalent to a collection of non-interacting harmonic oscillators holds for the unbounded case also. To avoid complications, in the following we shall not make any formal distinction between modes of a cavity and the free space unless the actual spatial dependence is important.

1.1.4 Fock states

Here and in the next sections we give a brief overview of certain states of the quantum harmonic oscillator that are important from the point of quantum optics.

The well-known Hamiltonian of a quantum harmonic oscillator can be written as

$$H = \hbar\omega(a^\dagger a + 1/2), \tag{1.30}$$

which is formally equivalent to the Hamiltonian of a normal mode of the electromagnetic field, appearing in the sum in Eq. (1.17).

The eigenstates of the harmonic oscillator Hamiltonian Eq. (1.30) are termed Fock states. Using only the commutation relations of the ladder operators

$$[a, a^\dagger] = 1, \tag{1.31}$$

and the positivity of H, we find

$$\begin{aligned} a^\dagger |n\rangle &= \sqrt{n+1}\,|n+1\rangle\,, \\ a\,|n\rangle &= \sqrt{n}\,|n-1\rangle\,, \end{aligned} \tag{1.32}$$

where $|n\rangle$ are defined as

$$H\,|n\rangle = \hbar\omega(n+1/2)\,|n\rangle\,,\ n = 0, 1, 2, \ldots, \tag{1.33}$$

or equivalently: $a^\dagger a\,|n\rangle = n\,|n\rangle$. Eq. (1.32) also tells us that the eigenstates can be generated as

$$|n\rangle = \frac{(a^\dagger)^n}{\sqrt{n!}}\,|0\rangle \tag{1.34}$$

from $|0\rangle$ that is called the ground state, or vacuum in case the harmonic oscillator corresponds to a normal mode of the electromagnetic wave.

Turning to optics, we identify each excitation of the Harmonic oscillator with a photon, and we say that the Fock state $|n\rangle$ corresponds to n photons in the mode. This identification is in accordance with Einstein's notion of light quanta those each carry the energy of $\hbar\omega$, thus the energy of a field with n photons must be $\hbar\omega n$. For travelling waves we have similar results regarding physical momentum, which can be defined for a mode characterised by the wave vector $\mathbf{k}$ as $\mathbf{P} = \hbar\mathbf{k}(a^\dagger a + 1/2)$. Referring to the interpretation of n being the number of photons, the Fock states $|n\rangle$ are also called number states, and

$$N = a^\dagger a \tag{1.35}$$

the number operator.

Because the Fock states are the eigenvectors of a Hermitian operator, they form an orthogonal basis of the Hilbert space, that is, in this case the state space of the harmonic oscillator. Together with their straight-forward physical interpretation this makes them an excellent basis to expand quantum states of the electromagnetic field. The expansion of states in the Fock basis is termed Fock representation, and in fact it is perhaps the most widely used representation in quantum optics. In the subsequent sections whenever a new representation or basis is introduced, it will also be compared to the Fock representation.

In the light of the above results, the calculation of eigenstates of the Hamiltonian (1.17) is straight-forward. We interpret the complete Hilbert space $\mathcal{H}$ as the tensor product of the oscillator Hilbert spaces $\mathcal{H}_{\mathrm{HO}}$:

$$\mathcal{H} = \bigotimes_{\nu} \mathcal{H}_{\mathrm{HO}}^{(\nu)}. \tag{1.36}$$

And since the oscillators are independent of each other, the multi-mode Fock states, denoted

$$|n_1\rangle|n_2\rangle\cdots|n_\nu\rangle\cdots \quad \text{or} \quad |n_1 n_2 \ldots n_\nu \ldots\rangle\,, \tag{1.37}$$

and constructed from the vacuum as

$$|n_1 n_2 \ldots n_\nu \ldots\rangle = \prod_{\nu} \left(\frac{(a^\dagger)^{n_\nu}}{\sqrt{n_\nu!}}\right)|0\rangle\,, \tag{1.38}$$

become eigenvectors of the Hamiltonian (1.17) with eigenvalues $\sum_\nu n_\nu$. Here we used the notation $|0\rangle$ for the general vacuum. Sometimes the number of modes is explicitly included in the notation for the vacuum state, and it is written as $|00\ldots\rangle$ using the appropriate number of zeros.

1.1.5 Polarisation modes

Recall that in section 1.1.1 in solving the wave equation (1.5) we restricted ourselves to two spatial directions x and z. The full three dimensional problem can be treated, however, introducing the notion of polarisation same way as it was used in Sec. 1.1.3. In a cavity with axis parallel to the z axis, the polarisation vectors must satisfy

$$\hat{\mathbf{e}}_\lambda \hat{\mathbf{z}} = 0, \tag{1.39}$$

$$\hat{\mathbf{e}}_\lambda \hat{\mathbf{e}}_{\lambda'} = \delta_{\lambda\lambda'}, \tag{1.40}$$

where $\hat{\mathbf{z}}$ is the unit vector in the z direction, and the indices λ, λ' may take the values $1, 2$.

Another possible choice of polarisation basis is the circular polarisation. The two vectors corresponding to positive and negative helicity are

$$\hat{\mathbf{e}}_{+1} = -\frac{1}{\sqrt{2}}(\hat{\mathbf{e}}_1 + i\hat{\mathbf{e}}_2), \tag{1.41}$$

$$\hat{\mathbf{e}}_{-1} = \frac{1}{\sqrt{2}}(\hat{\mathbf{e}}_1 - i\hat{\mathbf{e}}_2), \tag{1.42}$$

in terms of the unit vectors of linear polarisation. These vectors still satisfy both Eqs. (1.39) and (1.40), however, they no longer correspond to any physical vector because of the imaginary component. The same construction can be done for travelling waves starting from the expressions (1.25).

Starting from a pair of ladder operators for orthogonal linearly polarised modes of the same normal mode or plane wave (a_1 and a_2), the ladder operators for the circular polarisations may be expressed

$$a_{+1} = -\frac{1}{\sqrt{2}}(a_1 + ia_2), \tag{1.43}$$

$$a_{-1} = \frac{1}{\sqrt{2}}(a_1 - ia_2). \tag{1.44}$$

In the usual terminology the two polarisations are denoted by σ^+ and σ^-, and photons in each mode carry $\hbar$ and $-\hbar$ angular momentum [113], respectively. This fact that photons can carry angular momentum will become important in 1.3.4 when we treat atom–photon interactions. In those cases it will be important that the total angular momentum is conserved during an atomic transition.

It is often convenient to speak of two polarisation states of a single photon. In that case a general state may be written as a linear combination of two orthogonal polarisation states. For example, in a linearly polarised basis

$$|\psi\rangle = \sin\vartheta\,|\updownarrow\rangle + \mathrm{e}^{i\varphi}\cos\vartheta\,|\leftrightarrow\rangle\,, \tag{1.45}$$

or when in a circularly polarised basis

$$|\psi\rangle = \sin\vartheta'\,|\sigma^+\rangle + \mathrm{e}^{i\varphi'}\cos\vartheta'\,|\sigma^-\rangle\,. \tag{1.46}$$

We can match this notation to the multi-mode Fock state formalism by setting

$$|\updownarrow\rangle = |1\rangle|0\rangle \quad \text{and} \quad |\leftrightarrow\rangle = |0\rangle|1\rangle\,, \tag{1.47}$$

and then accordingly we have

$$|\sigma^+\rangle = -\frac{1}{\sqrt{2}}(|1\rangle|0\rangle + i\,|0\rangle|1\rangle) \quad \text{and} \quad |\sigma^-\rangle = \frac{1}{\sqrt{2}}(|1\rangle|0\rangle - i\,|0\rangle|1\rangle). \tag{1.48}$$

The polarisation states of travelling photons can easily be manipulated by passive elements such as polarisation beam-splitters, and quarter-wave and half-wave plates. Therefore the polarisation states have found wide applications in quantum information processing. It is not by chance that the first experimental demonstration [114] of quantum teleportation [89] was done using polarised photons. A number of implementations of quantum cryptography protocols employ polarised photons.

1.1.6 Wigner representation

A representation that may come handy in visualising and interpreting processes in quantum optics is the Wigner representation. It is analogous to the phase space distribution

function description of classical ensembles. However, the Wigner function must fulfil different conditions than a classical distribution function. We define the Wigner function of a density operator ϱ as

$$W(q,p) = \frac{1}{2\pi}\int_{\mathbb{R}} \mathrm{e}^{ipx}\,\langle q - x/2|\varrho|q + x/2\rangle\,\mathrm{d}x, \tag{1.49}$$

where $|q \pm x/2\rangle$ now denotes the position eigenket. In other words, the Wigner function can be obtained from the position representation of the state by Fourier transformation. Since this transformation is invertible, the correspondence between the density matrix ϱ and the Wigner function $W(q,p)$ in formula (1.49) is one-to-one.

The Wigner function shares the normalisation property with the classical distribution function. However, a Wigner function is not necessarily positive, and it may contain negative regions. In addition, a Wigner function representing a pure state also satisfies $-1 \leq W(q,p) \leq 1$. Because of its negativity W cannot be interpreted as a joint probability distribution of position and momentum, and this is in perfect agreement with the uncertainty principle. On the other hand, the marginals of the Wigner function satisfy all criteria of a probability distribution, e.g.

$$P(q) = \int_{\mathbb{R}} W(q,p)\,\mathrm{d}p \tag{1.50}$$

gives the probability distribution of a measurement of the position coordinate.

For the electromagnetic field, since the canonical position and momentum operators have no direct physical meaning, it is customary to introduce the dimensionless quadrature operators

$$X = \frac{1}{2}(a + a^\dagger), \tag{1.51}$$

$$Y = \frac{1}{2i}(a - a^\dagger), \tag{1.52}$$

those inherit the commutation relation $[X,Y] = i/2$. The operators differ from the canonical position and momentum operators in constant factors, and therefore can always be interchanged with them. In particular, we may express the Wigner function (1.49) using the quadrature eigenvalues x and y as labels. Using these eigenvalue labels, we introduce the complex parameter $\alpha = x + iy$, and assign $W(x,y) \equiv W(\alpha)$. The definition of this complex parameter suggests a connection between the argument α and the annihilation operator a. We note that the direct measurement of the quadrature operators is possible, see Sec. 1.2.3 for details.

We have plotted the Wigner function of the vacuum on Fig. 1.1. This function is a Gaussian with variance $\frac{1}{2}$ in each quadrature direction which means that the uncertainty relation

$$\Delta X\,\Delta Y \leq \frac{1}{4}, \tag{1.53}$$

is satisfied with an equal sign. Here $\Delta A = (\langle A^2\rangle - \langle A\rangle^2)^{1/2}$ is the standard deviation of the measurement probability distribution. This property will become important in the following section.

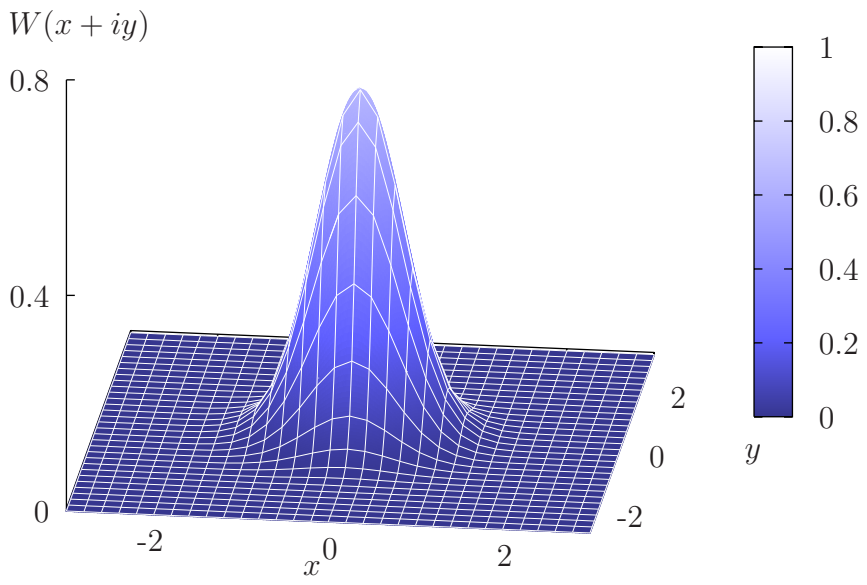

Figure 1.1: Wigner function for the vacuum (ground) state. It is a Gaussian distribution centered on the origin with half width 1/2.

To discuss all important features of Wigner functions is beyond the scope of the present dissertation. For a complete treatment refer to e.g. [115], [116] or [3].

1.1.7 Coherent states

Coherent states constitute another special class of states of the quantum harmonic oscillator. We adopt the definition of coherent states that says that these are the eigenstates of the annihilation operator a. More precisely,

$$a\,|\alpha\rangle = \alpha\,|\alpha\rangle\,, \tag{1.54}$$

where α is a complex number, and $|\alpha\rangle$ denotes the coherent state. To avoid ambiguity, Fock states are usually given Latin indices, while coherent states are labelled with Greek letters. If we would like to write down a coherent state with a particular amplitude we shall use a notation analogous to the expression

$$|\alpha = 0\rangle = |0\rangle\,, \tag{1.55}$$

that states the fact that the vacuum state (Fock state 0) is a coherent state with coherent amplitude zero. The generator for coherent states is the so-called displacement operator $D(\alpha)$, and it works by applying it to the vacuum state (1.55):

$$|\alpha\rangle = D(\alpha)\,|0\rangle\,, \quad D(\alpha) = \mathrm{e}^{\alpha a^\dagger - \alpha^* a}\,. \tag{1.56}$$

In can be shown that the effect of displacement on the Wigner functions is a translation

$$W(\alpha) \xrightarrow{D(\beta)} W(\alpha+\beta). \tag{1.57}$$

Therefore, we can deduce that a coherent state $|\alpha\rangle$ has the same Gaussian form as the vacuum, only they are centered at α on the complex plane. This also means that the uncertainly relation (1.53) is satisfied as an equality for all coherent states.

Another one of the important features of coherent states is that they maintain their shape during the free evolution of the harmonic oscillator

$$\mathrm{e}^{-\frac{i}{\hbar}Ht}\,|\alpha\rangle = |\mathrm{e}^{-i\omega t}\,\alpha\rangle\,. \tag{1.58}$$

Pictorially, Eq. (1.58) means that an initial Gaussian quasi-distribution function, similar to Fig. 1.1 but displaced, circumambulates the origin with frequency ω. Indeed, if we considered a classical harmonic oscillator, and started with a similar Gaussian distribution function, we could observe the exact same behaviour. This connection to the classical dynamics is a major reason why coherent states are considered the "most classical" quantum states of the quantum harmonic oscillator.

Although we used the Wigner functions of coherent states to gain a good insight into their nature, for practical calculations we shall turn to their Fock state representation. In the Fock state basis a coherent state is expanded as

$$|\alpha\rangle = \mathrm{e}^{-|\alpha|/2}\sum_{n=0}^{\infty}\frac{\alpha^n}{\sqrt{n!}}\,|n\rangle\,. \tag{1.59}$$

It can be easily verified that this formula complies with all previous statements on coherent states. Moreover, we can use it to calculate the average number of photons in a coherent state, by taking the expectation value of the number operator, see Eq. (1.35),

$$\langle\alpha|N|\alpha\rangle = |\alpha|^2\,. \tag{1.60}$$

It can also be efficiently used to verify the scalar product of two coherent states

$$\langle\alpha|\beta\rangle = \mathrm{e}^{\alpha^*\beta-\frac{|\alpha|^2}{2}-\frac{|\beta|^2}{2}}\,. \tag{1.61}$$

Hence we just found that there are no two coherent states that are orthogonal to each other. We also see, however, that the overlap, $|\langle\alpha|\beta\rangle|^2 = \mathrm{e}^{-|\alpha-\beta|^2}$, between two coherent states decreases exponentially with the distance. The non-orthogonality of coherent states did not come as unexpected, since the coherent states are eigenstates of a non-Hermitian operator. Despite this, however, the coherent states turn out to be linearly spanning the entire Hilbert space, i.e. we can decompose any state into a (continuous) superposition of coherent states. In particular, the decomposition of the identity operator into coherent states can be written as

$$\mathbb{1} = \frac{1}{\pi}\int_{\mathbb{C}}|\alpha\rangle\langle\alpha|\,\mathrm{d}^2\alpha. \tag{1.62}$$

Since the decomposition of states into coherent states is not unique, the coherent states, we say that these constitute an *over complete* basis.

In order to define a unique representation using coherent states, one has to make restrictions on which kind of decompositions are valid. There are several ways to do this. In particular the most widely used is Glauber's analytic representation [117]. In the present work we shall also use the one-dimensional coherent state representation [118] as a starting point for the one-complex plane representation [86, 87] of Sec. 2.1, therefore we present a brief summary for this in Sec. 1.1.10.

We mention here, that the relation of coherent states to the usual definition coherence of the electromagnetic radiation has been first worked out extensively by Glauber in Ref. [119].

1.1.8 Squeezed states

We have seen that the vacuum state and all coherent states are minimum uncertainty states. We also understand that since the coherent states correspond to a displaced vacuum, they have the exact same uncertainty properties. Naturally the question arises, can we go below the vacuum uncertainty? The answer is in the affirmative. However, there is a trade-off between the two conjugate variables which appear in the uncertainty relation (1.53). If we reduce the standard deviation of one variable, the standard deviation in the other variable must increase.

This effect leads us to the notion of squeezing. Let us introduce the rotated quadrature operators

$$d_1(\varphi) = (a\,\mathrm{e}^{-i\varphi} + a^\dagger\,\mathrm{e}^{i\varphi})/2, \tag{1.63}$$

$$d_2(\varphi) = (a\,\mathrm{e}^{-i\varphi} - a^\dagger\,\mathrm{e}^{i\varphi})/2i, \tag{1.64}$$

which satisfy $[d_1(\varphi), d_2(\varphi)] = i/2$ for any φ. Using the quadrature operators (1.52), we may write $d_1(\varphi) = X\cos\varphi + Y\sin\varphi$ and $d_2 = Y\cos\varphi - X\sin\varphi$. If a state for some φ (and l) satisfies

$$\Delta d_l(\varphi) < \frac{1}{2}, \tag{1.65}$$

the state is called squeezed. If in addition, it is also a minimal uncertainty state, it is termed an ideal squeezed state. In the present work we shall mostly consider ideal squeezed states, and therefore when we write "squeezed state", we will usually mean an ideal squeezed state. A Wigner function of an ideal squeezed state is plotted on Fig. 1.2.

It can be shown that every minimum uncertainty state has a Gaussian form. This means that also every ideally squeezed state is a Gaussian state (for a complete definition of Gaussian states see e.g. [120]). This allows us to relate coherent states to squeezed states via a unitary operator. This operator is called squeezing operator and is defined as

$$S(\zeta) = \exp\left(\frac{1}{2}\zeta a^{\dagger 2} - \frac{1}{2}\zeta^* a^2\right), \tag{1.66}$$

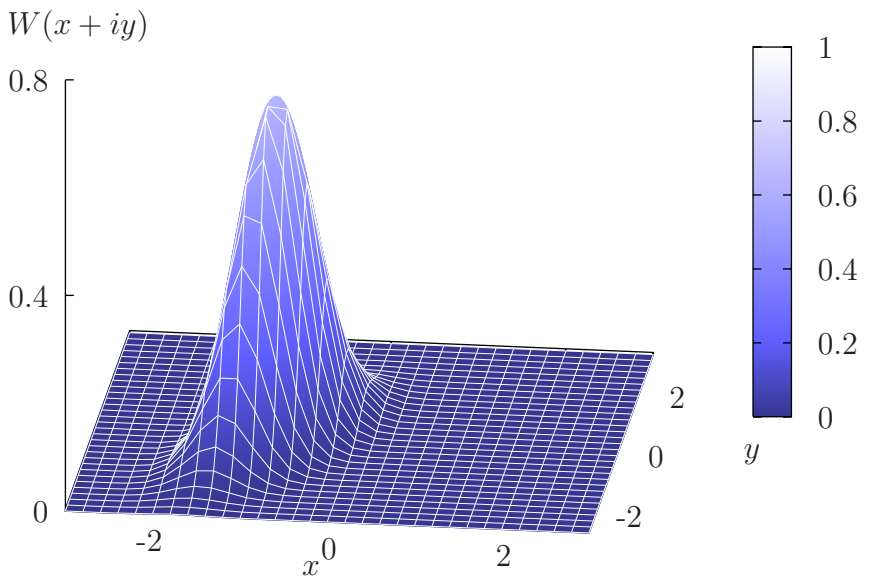

Figure 1.2: Wigner function for the squeezed coherent state $\left|\alpha = \mathrm{e}^{i9\pi/8}\right\rangle$ with squeezing parameter $r = 0.5$ and direction $\vartheta = -2\pi/9$.

where the complex parameter is often written as $\zeta = r\,\mathrm{e}^{i\vartheta}$. The parameter ϑ defines the angle of squeezing in the phase space, and r sets the amount of squeezing e^{-r} in one direction and the spread-out e^r in the perpendicular direction (if we assume $r \geq 0$).

The effect of S on the annihilation operator is

$$S(\zeta)^\dagger a S(\zeta) = a\cosh r + a^\dagger\,\mathrm{e}^{i\vartheta}\sinh r, \tag{1.67}$$

and it is customary to introduce $u = \cosh r$, $v = \mathrm{e}^{i\vartheta}\sinh r$. Using this notation, following Ref. [1] the Fock state expansion of a squeezed coherent state can therefore be written as

$$|\zeta,\alpha\rangle = S(\zeta)D(\alpha)\,|0\rangle = \frac{1}{\sqrt{v}}\,\mathrm{e}^{-\frac{1}{2}\left(|\alpha|^2 - \frac{u^*}{v}\alpha^2\right)}\sum_{n=0}^{\infty}\frac{1}{2^n\sqrt{n!}}\left(\frac{u}{v}\right)^{\frac{n}{2}} H_n\left(\frac{\alpha}{\sqrt{2uv}}\right)|n\rangle\,, \tag{1.68}$$

where H_n denotes the Hermite polynomials. We shall see later that the Hermite polynomials play an important role in one-mode squeezing. It is also worth pointing out that due to the properties of the Hermite polynomials, the squeezed vacuum state $|\zeta, 0\rangle$ contains only even photon numbers in its Fock basis expansion.

1.1.9 Optical Schrödinger cat states

In Schrödinger's famous gedanken experiment [29] the peculiarities of quantum mechanics is demonstrated by preparing a quantum superposition of two macroscopical, i.e. classical states. Before opening the box, our system is in the superposition of two states, one

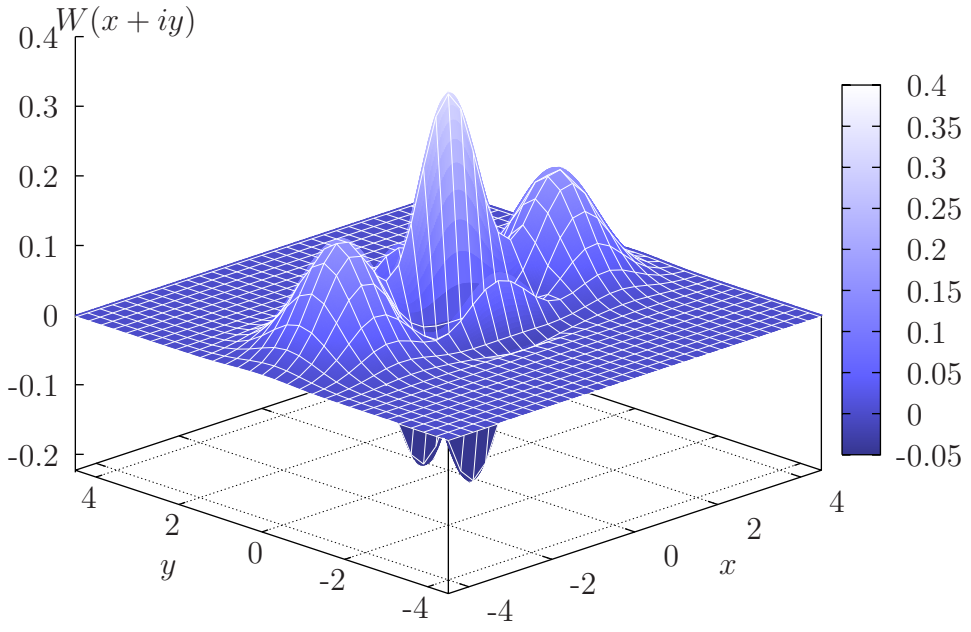

Figure 1.3: Wigner function of the even Schrödinger cat state $|\alpha, +\rangle$, with $\alpha = 2.6$. The original humps of the two constituting coherent states are clearly visible. The central peak is due to quantum interference, and its height tends to zero as the separation between the coherent states increase.

containing a live cat, and the other a dead cat. Of course this experiment has not yet been carried out successfully, and no cats have been hurt. In quantum optics, however, preparation of similar superpositions is almost a routine task. The two "macroscopical" states involved in the superposition are two coherent states, which we can consider the most classical states of the electromagnetic field. Although the complexity of these states is definitely below of those involving live cats, the usage of terminology "Schrödinger cat state" is widespread in the quantum optics community. Some authors, however, prefer to call a special (though most often used) sub-class of Schrödinger cat states "even" and "odd coherent states." Their meaning will be explained shortly.

Although the superposition of any two coherent states would be a state corresponding to the original Schrödinger cat states, most often a special selection is made. The most widely used definition for optical Schrödinger cat states is to take a coherent amplitude α and form the equal weight superpositions

$$|\alpha, \pm\rangle = \frac{1}{\mathcal{N}_{\pm}(\alpha)} \left(|\alpha\rangle \pm |-\alpha\rangle\right), \tag{1.69}$$

with the two normalisation factors being $\mathcal{N}_{\pm}(\alpha) = \sqrt{2}\sqrt{1 \pm \exp(-2|\alpha|^2)}$. These normalisation factors differ from $\sqrt{2}$ because the coherent states are non-orthogonal.

The above definition of Schrödinger cat states gives us two Schrödinger cat states for every coherent amplitude α. A short analysis of the Fock state expansion of the states

(1.69) shows that $|\alpha,+\rangle$ contains only even, while $|\alpha,-\rangle$ contains only odd Fock states. This property is the basis for the terminology "even coherent state" and "odd coherent state" for $|\alpha,+\rangle$ and $|\alpha,-\rangle$, respectively.

1.1.10 One-dimensional coherent state representations

The over completeness of coherent states has already been mentioned in Sec. 1.1.7, along with its implications to representations. In this section we briefly recall the fundamental idea behind coherent state representations, the varieties of one-dimensional coherent state representations, and the basic definitions for the straight-line representation. The straight-line representation will serve as model construction for the later generalisation to entangled states.

The discovery of the fundamental property of coherent states that stands behind the one-dimensional representations is due to Cahill [121]. According to his theorem, if a sequence of complex numbers α_n has a limit point in $\mathbb{C}$, the corresponding set of coherent states $\{|\alpha_n\rangle\}$ spans the entire Hilbert space. In particular, if we take the set of points making up a continuous curve in the complex plane, to every point in the curve there exists a sequence in this set that converges to this point, therefore any element of this set is a limit point. This implies that the linear hull of the corresponding set of coherent states is the entire Hilbert space.

Here we mention two examples for representations based on coherent states constituting a continuous line in phase space. It has been shown in [118] that if we take any straight line across the origin, any state of the harmonic oscillator can be expressed as a continuous superposition of the states on this line. For example, if we take the line along the x axis, any state can be expressed as

$$|\psi\rangle = \int_{\mathbb{R}} f(x)\,|x\rangle\,\mathrm{d}x, \tag{1.70}$$

where now $|x\rangle$ denotes a coherent state with real coherent amplitude x. Similar construction holds for any other straight line, and we have the freedom to choose the direction that best suits our calculations. In certain cases a proper selection can make a great difference, since the symbol f is generally not just a complex valued function, but rather a distribution. From the formal point of view this does not cause any complications, since our f only appears under an integration sign in every observable. For practical purposes, however, we may prefer to work with nice looking functions.

Another example worked out in [122], is the expansion in terms of coherent states on a circle centered at the origin. In this representation, also the uniqueness of the representation function can be easily ensured. It can be shown that if we require that the Laurent series of the function g in the formula

$$|\psi\rangle = \frac{\exp(R^2/2)}{2\pi i} \oint_{|\alpha|=R} g(\alpha)\,|\alpha\rangle\,\mathrm{d}\alpha, \tag{1.71}$$

does not contain any regular part, then the mapping defined by (1.71) is one-to-one (R is the radius of the circle chosen for the actual representation). The relations between

the analytic and the Fock representation can also be given in terms of the coefficients of the Laurent series of g. We note here, that similarly to the straight line representation, g exists only as a distribution. As a rule of thumb, g is a proper function only if the state "does not extend too far" beyond the circle line.

Returning to the straight line representation [118], we shall discuss its relation to squeezing. We first note that the straight-line representation is a rather natural representation of the squeezed vacuum. With the choice of the direction of the line being the same as the direction of squeezing, we have the expression

$$|\zeta, 0\rangle = \frac{\sqrt[4]{\gamma^2+1}}{\gamma\sqrt{\pi}} \int_{\mathbb{R}} \mathrm{e}^{-x^2/\gamma^2} \, |x\,\mathrm{e}^{i\vartheta}\rangle \, \mathrm{d}x, \tag{1.72}$$

where ϑ and γ is related to the squeezing parameter as $\zeta = -1/2 \ln(\gamma^2+1)\,\mathrm{e}^{i2\vartheta}$. Based on this expression, with the help of the Hermite polynomials it is possible to construct a complete set of orthonormal basis as

$$|h_n(\zeta)\rangle = \mathcal{N}_n(\gamma) \int_{\mathbb{R}} H_n(\mu x)\,\mathrm{e}^{-x^2/\gamma^2} \, |x\,\mathrm{e}^{\vartheta}\rangle \, \mathrm{d}x, \tag{1.73}$$

where $\mathcal{N}_n(\gamma)$ is a normalisation factor, and $\mu = \sqrt{2(1+\gamma^2)/(2+\gamma^2)}/\gamma$. With the definition of this basis, the expansion of any state is unique:

$$|\psi\rangle = \sum_n C_n(\gamma)\,|h_n(\zeta)\rangle\,, \tag{1.74}$$

which makes the representation function f of Eq. (1.70) also unique. We shall use the same line of thought at the construction of a complete representation for entangled states in Sec. 2.1.

1.2 Linear optics

In the previous section we have discussed several quantum states of the electromagnetic field, but nothing has been said about how the manipulation of light can be done. In the present section we shall discuss this problem in the framework of linear optics under which we mean the use of beam-splitters, phase shifters and photo detectors. Despite the simplicity of the tools available to linear optics, it is actually a very powerful paradigm for the manipulation of light. It is in fact possible to simulate quantum computers using only linear optical elements [123], and even more with cleverly designed measurement schemes [104].

In the present section we recall the definition of the beam-splitter. Then discuss the possibilities of linear optics in creating entanglement, assuming that coherent states or low photon number Fock states are available to the experimenter as initial states. Then we shall discuss the detection techniques generally available in the laboratory.

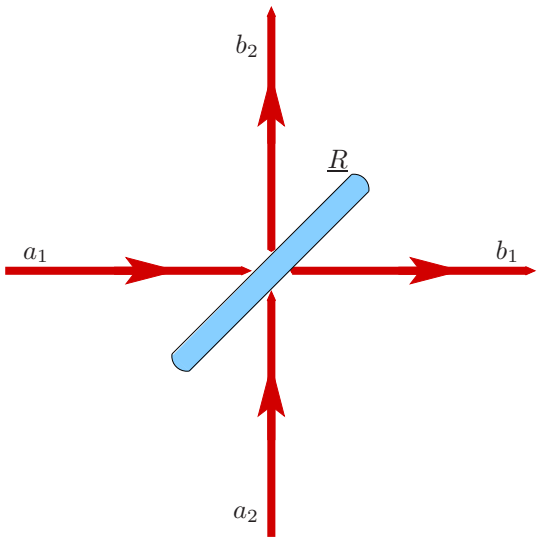

Figure 1.4: Schematic figure of a beam splitter or partially reflecting mirror. The two input modes are labelled a_1 and a_2, the output modes are b_1 and b_2. The interaction between the two modes is described by an $SU(2)$ matrix that defines the relation between the annihilation operators of the input and output modes.

1.2.1 Beam splitters

We follow the customary description of beam splitters that was first worked out in [124]. The beam splitter (or partially reflecting mirror) is an optical element with two input modes. The input modes interact on the beam splitter, and produce two output modes. This process is depicted on Fig. 1.4, with the two input modes labelled as a_1 and a_2, and the output modes labelled with b_1 and b_2. We also denote the respective annihilation operators of the input and output modes with a_1, a_2, b_1 and b_2. This notation is convenient because the effect of the beam splitter is described by a unitary transformation of the annihilation operators:

$$\begin{pmatrix} b_1 \\ b_2 \end{pmatrix} = \begin{pmatrix} t & r \\ -r^* & t^* \end{pmatrix} \begin{pmatrix} a_1 \\ a_2 \end{pmatrix} = \underline{R} \begin{pmatrix} a_1 \\ a_2 \end{pmatrix}, \tag{1.75}$$

where the unitary matrix R is conventionally taken to have unit determinant, i.e. $|t|^2 + |r|^2 = 1$. Hence we can parametrise the $SU(2)$ matrix R as

$$t = \mathrm{e}^{i\varphi_t} \cos\tau, \tag{1.76a}$$
$$r = \mathrm{e}^{i\varphi_r} \sin\tau. \tag{1.76b}$$

In a classical picture we may think of r as a reflection coefficient and t as transmission coefficient. In fact, coherent states transform exactly according to this rule:

$$U_{\mathrm{R}} |\alpha\rangle |\beta\rangle = |t\alpha + r\beta\rangle |t^*\beta - r^*\alpha\rangle . \tag{1.77}$$

Of course beam splitters may be combined by directing their outputs to the input ports of another beam splitter and so on. It has been shown that the networks produced using only beam splitters (and phase shifters) are sufficient to realize any unitary operation connecting N input modes with N output modes [100]. This result actually points much beyond quantum optics, and establishes a solid background for decomposition of $SU(N)$ operations into a succession of $SU(2)$ operations, and in turn this problem is of fundamental importance in the theory of quantum computational complexity.

1.2.2 Entanglement and linear optics

Although a beam splitter transforms coherent states as simple as in Eq. (1.77), it not so even for the most simple superpositions of coherent states. For example, a Schrödinger cat state (1.69) along with the vacuum on a $50-50\%$ anti-symmetric beam splitter transforms as

$$U_R \left|\sqrt{2}\alpha, -\right\rangle |0\rangle = \mathcal{N}_+(\sqrt{2}\alpha)^{-1} \left(|\alpha\rangle \left|-\alpha\right\rangle - \left|-\alpha\right\rangle |\alpha\rangle\right), \tag{1.78}$$

which is an entangled state (input state is scaled only for convenience). Entanglement is discussed in more detail in Sec. 1.4.2.

The beam splitter can be used to generate a whole variety of entangled states. For example, from squeezed vacuum state and vacuum, we can generate the two-mode squeezed vacuum state, which plays the role of the quantum channel in the teleportation of continuous variables [90]. We shall see another example in Sec. 2.2, where we demonstrate that the two mode Schrödinger state could be prepared in a procedure involving a beam splitter. Moreover, it has been shown [125] that a single beam splitter can be used to test the non-classicality of an arbitrary quantum state via the entanglement generated.

1.2.3 Optical detection schemes

In optics, the natural detection techniques are destructive, i.e. the photon is absorbed during the measurement process. The basic measurement device is the photo detector, which is based on the photoelectric effect. In quantum optics, two types of photo detectors are used. The so-called single-photon detector produces a click whenever an incoming photon is detected. Conventionally single-photon photo detectors are not expected to differentiate between different non-vacuum Fock states, i.e. they produce the same click for an incoming $|1\rangle$ and $|2\rangle$ Fock state. More formally phrased, an ideal realistic photo detector projects the incoming state onto two linear subspaces: the vacuum and its orthogonal complement. There are also examples of more sensitive photo detectors that produce three distinct outputs, and can distinguish between the vacuum, $|1\rangle$, and the rest of the Fock-states.

The more traditional photo detectors producing photoelectric currents proportional to the incoming intensity find very important application in homodyne detection. There are two versions of homodyne detection, as depicted on Fig. 1.5. The principle of both is

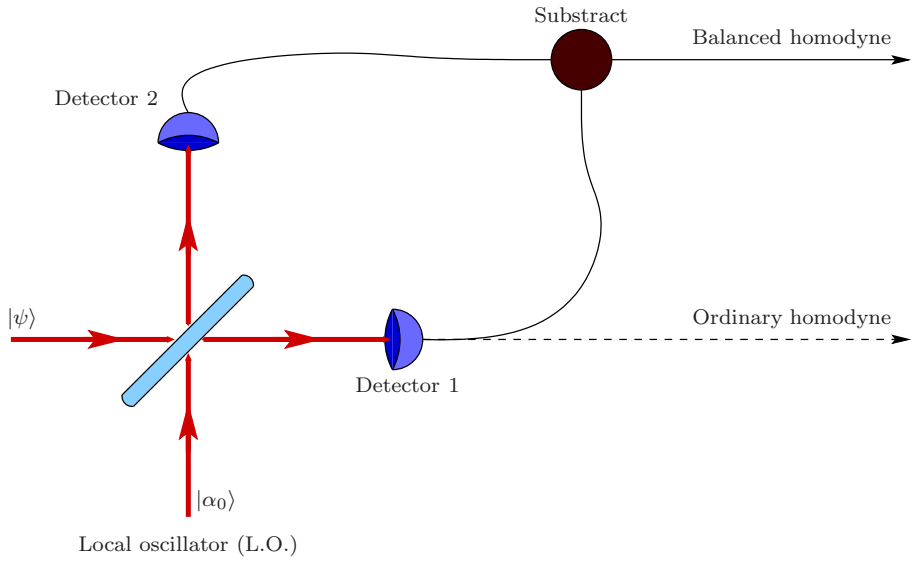

Figure 1.5: Schematic representation of two homodyne detection arrangements. For each setup the measurement signal is drawn only from one of the leads, as indicated here.

mixing the input state with a strong coherent beam on a beam splitter. This auxiliary coherent field is conventionally called local oscillator or L.O. for short.

In case of the ordinary homodyne detection scheme, an almost perfectly transmitting mirror ($t \gg r$) is used, and the measurements are recorded only on detector 1. There are contributions to the photo current from the transmitted input state, the reflected L.O. field and the interference terms between the input and the L.O. At sufficiently high intensity of the L.O., the direct contribution of the input can be neglected and the expectation value of the photon number measurement may be expressed as

$$\langle n_1 \rangle \approx (1-t)|\alpha_0|^2 - 2\sqrt{t(1-t)}\,|\alpha_0|\,\langle\psi|d_1(\varphi_0+\pi/2)|\psi\rangle\,, \tag{1.79}$$

where $d_1(\varphi)$ is the "rotated" quadrature (1.63), and φ_0 is the phase of the local oscillator relative to the input source, or a common reference. Since the first term is an independent background over the interference contribution it may be subtracted, and the expectation value $\langle\psi|d_1(\varphi_0+\pi/2)|\psi\rangle$ can be recorded while varying the phase φ_0.

Balanced homodyning provides the measurement of the same operators, however, in a more robust way. For the balanced setup, the beam splitter is replaced by a $50-50\%$ symmetric beam splitter ($\tau = \pi/2$, $\varphi_t = 0$, $\varphi_r = \pi/2$), and the difference between the two photo currents is recorded. The signal thus obtained is directly proportional to the expectation value

$$\langle n_{12} \rangle = -2|\alpha_0|^2\,\langle\psi|d_1(\varphi_0+\pi/2)|\psi\rangle\,. \tag{1.80}$$

Therefore the requirements on the stability of the local oscillator are less stringent.

In both cases the homodyne measurement with a fixed φ_0 may be regarded as a measurement projecting onto the eigenstates of the rotated quadrature operator $d_1(\varphi_0+$

$\pi/2$). Although these states are unnormalisable, they can be written as

$$|\Phi = \varphi_0 + \pi/2\rangle = \lim_{r\to\infty} |\zeta = r\,\mathrm{e}^{i\varphi_0}, 0\rangle\,. \tag{1.81}$$

These states may be regarded as a kind of phase states, as they each have a well-defined phase and completely undefined amplitude [126].

1.3 Interaction with matter

So far, in the description of beam splitters, we have used a classical phenomenon and generalised it to quantised light. In the present section we follow a different approach in the description of light–matter interactions. We start from the microscopical description of a simple atom, and consider its interaction with the electromagnetic field in the dipole approximation.

We shall formulate for our purposes the fundamental equations of atom–field interaction for a classically treated light in Sec. 1.3.2, and for the fully quantised treatment in Sec. 1.3.3. We also discuss in Sec. 1.3.4 the phenomenon of Raman transitions which are also fundamental for interpreting our results in Chapter 3.

1.3.1 The two-level atom

The basic setup considered in quantised light–matter interactions is an electromagnetic mode at certain frequency ω_0 and an atom with transition frequency ω_A close to ω_0. In order for the following approximations to work, we must assume that the rest of the transition frequencies of the atom much farther from resonance with ω_0.

At optical frequencies the transition of the atom is usually associated with two electronic states. For the purpose we shall term the lower electronic state "ground" state, and the upper electronic state "excited" state. Since we do not consider any other internal states of the atom the Hamiltonian may be written in terms of these two states as

$$H_A = \frac{1}{2}\hbar\omega_A(|e\rangle\langle e| - |g\rangle\langle g|) = \frac{1}{2}\hbar\omega_A\sigma_z, \tag{1.82}$$

where $|e\rangle$ and $|g\rangle$ denotes the excited and ground states, respectively. In the above formula we have also introduced one of the σ operators. These operators are represented by the usual Pauli σ matrices in the $\{|g\rangle, |e\rangle\}$ basis, i.e.

$$\underline{\sigma}_z = \begin{pmatrix} 1 & 0 \\ 0 & -1 \end{pmatrix} \quad \leftrightarrow \quad |e\rangle\langle e| - |g\rangle\langle g| = \sigma_z, \tag{1.83a}$$

$$\underline{\sigma}_x = \begin{pmatrix} 0 & 1 \\ 1 & 0 \end{pmatrix} \quad \leftrightarrow \quad |e\rangle\langle g| + |g\rangle\langle e| = \sigma_x, \tag{1.83b}$$

$$\underline{\sigma}_y = \begin{pmatrix} 0 & -i \\ i & 0 \end{pmatrix} \quad \leftrightarrow \quad -i\,|e\rangle\langle g| + i\,|g\rangle\langle e| = \sigma_y. \tag{1.83c}$$

It is also useful to define the two operators

$$\sigma_{\pm} = \frac{1}{2}(\sigma_x \pm i\sigma_y). \tag{1.84}$$

We consider the interaction of the two level atom (TLA) with the electromagnetic field in the dipole approximation. This approximation holds whenever the vector potential $A(\mathbf{r})$ does not change significantly over the size of the atom, and the momentum of the atom is small. Thus we write the interaction term as

$$V = -\mathbf{d} \cdot \mathbf{E}(\mathbf{R}_A, t), \tag{1.85}$$

where $\mathbf{d}$ is the electric dipole moment of the atom. The electric dipole moment can classically be expressed as $\mathbf{d} = e\mathbf{r}$, where $\mathbf{r}$ is the position of the electron relative to the nucleus. In the quantised case this becomes

$$\mathbf{d} = e\mathbf{r}_{eg}(\sigma_+ + \sigma_-), \tag{1.86}$$

where $\mathbf{r}_{eg} = \langle e|\mathbf{r}|g\rangle$ is the matrix element of the position operator, and it has been set to be real by suitably choosing the phases of the basis vectors. The complete Hamiltonian of the system is therefore

$$H = \frac{1}{2}\hbar\omega_A\sigma_z - e\mathbf{r}_{eg}(\sigma_+ + \sigma_-)\mathbf{E}(\mathbf{R}_A, t) + H_{\text{Field}}. \tag{1.87}$$

1.3.2 Semi-classical treatment

In the semi-classical limit of the atom–field interaction we use the above quantum treatment of the atom, but still use classical equations to describe the dynamics of the electromagnetic field.

Using Eq. (1.23) we expand the single mode of the electromagnetic field at the position of the atom R_A as

$$E(\mathbf{R}_A, t) = \sqrt{\frac{\omega_0}{2\hbar\varepsilon V_c}}\mathbf{E}_M(\mathbf{R}_A)\left(\alpha(t) + \alpha^*(t)\right). \tag{1.88}$$

Upon substituting this expression into the interaction term of Eq. (1.87) we apply the so-called "rotating wave approximation." In the spirit of this approximation first we associate the rotating factors $\mathrm{e}^{-i\omega_A t}$ and $\mathrm{e}^{-i\omega_0}$that correspond to the free evolution with σ_+ and α, respectively. Second we assume $\omega_A \approx \omega_0$, and imply that the terms of double frequencies $\omega_0 + \omega_A \gg |\omega_A - \omega_0|$ and therefore average out quickly. The interaction term (1.85) may therefore be written

$$V = -\hbar g(\sigma_+\alpha + \sigma_-\alpha^*), \tag{1.89}$$

where the coupling constant is

$$g = \sqrt{\frac{\omega_0}{2\hbar\varepsilon V_c}}e\mathbf{r}_{eg}\mathbf{E}_M(\mathbf{R}_A). \tag{1.90}$$

We may solve the Hamiltonian (1.87) with the interaction term (1.90) assuming a strong external pump that is effectively not affected by the atom. After going to a rotating frame described by the operator $T = \exp(i\omega_0 t\sigma_z/2)$, the only non-trivial time evolution is of the two-level quantum system. The unitary operator describing this evolution may be written in matrix form in the $|g\rangle$ and $|e\rangle$ basis as

$$\underline{U}(t) = \begin{pmatrix} \cos\Omega_{\text{eff}}t - i\dfrac{\delta}{2\Omega_{\text{eff}}}\sin\Omega_{\text{eff}}t & i\,\mathrm{e}^{-i\varphi}\dfrac{\Omega}{\Omega_{\text{eff}}}\sin\Omega_{\text{eff}}t \\ i\,\mathrm{e}^{i\varphi}\dfrac{\Omega}{\Omega_{\text{eff}}}\sin(\Omega_{\text{eff}}t) & \cos\Omega_{\text{eff}}t + i\dfrac{\delta}{2\Omega_{\text{eff}}}\sin\Omega_{\text{eff}}t \end{pmatrix}, \tag{1.91}$$

where $\Omega = g|\alpha|$ is called Rabi frequency, $\varphi = \arg\alpha$ is the initial phase of the field, $\delta = \omega_0 - \omega_A$ is called detuning, and $\Omega_{\text{eff}} = \sqrt{\Omega^2 + \delta^2/4}$ denotes the effective Rabi frequency. Clearly if $\delta = 0$ then $\Omega_{\text{eff}} = \Omega$, and $U(t)$ realizes rotation operators. For special cases of φ we have:

$$U(t) = \begin{cases} \mathbb{1}\cos\Omega t - \sigma_x i\sin\Omega t = R_x(\Omega t/2) & \text{if } \varphi = \pi, \\ \mathbb{1}\cos\Omega t - \sigma_y i\sin\Omega t = R_y(\Omega t/2) & \text{if } \varphi = -\pi/2. \end{cases} \tag{1.92}$$

We shall discuss rotation operators in Sec. 1.4.4.

1.3.3 The Jaynes–Cummings model

In this section we briefly overview the fundamental equations of the fully quantised atom–field interaction. We again assume the validity of the dipole approximation and the rotating wave approximation. The fully quantum Hamiltonian can therefore be written

$$H = \sum_{\mathbf{k}} \hbar\omega_k a_{\mathbf{k}}^\dagger a_{\mathbf{k}} + \frac{1}{2}\hbar\omega_A\sigma_z + \hbar\sum_{\mathbf{k}} g_{\mathbf{k}}(\sigma_+ a_{\mathbf{k}} + a_{\mathbf{k}}^\dagger\sigma_-). \tag{1.93}$$

In the case of a single resonant mode (i.e. $\delta = 0$) the notion of dressed states may be introduced. The dressed states may be expressed as

$$|\pm, n\rangle = \frac{1}{\sqrt{2}}(|e, n\rangle \pm |g, n+1\rangle), \tag{1.94}$$

and they are the eigenstates of the interaction picture Hamiltonian $H_I = \hbar g(\sigma_+ a + \sigma_- a^\dagger)$.

The Hamiltonian (1.93) is often referred to as Jaynes–Cummings Hamiltonian, and serves as a basis for many quantum optical calculations.

1.3.4 Degenerate two-level atoms

In the previous sections we considered the simplest possible model of atom–field interactions. This model very well describes certain resonances of circular Rydberg atoms such as the ^{87}Rb. In a more general case, however, the ground and excited states are split into degenerate Zeeman sub-levels. Each Zeeman sub-level is associated with certain angular momentum, just like each circular polarisation of the photon carries some. Assuming conservation of angular momentum, this explains intuitively the polarisation dependence of resonances. A full explanation is possible by examining the Clebsch–Gordan coefficients.

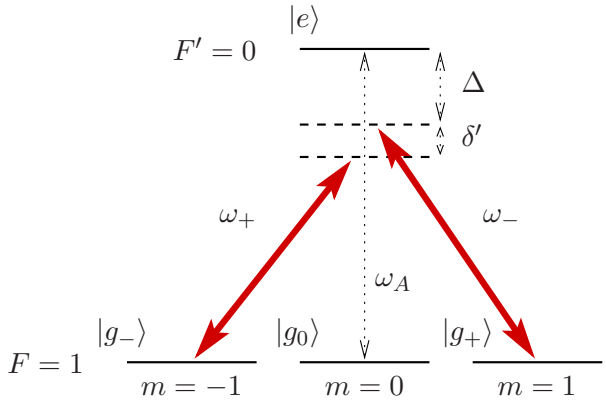

Figure 1.6: Diagram representing a virtual transition between two lower Zeeman sublevels using two pump lasers. In the limit of large detunings, $|\Delta| \gg |g|$, the system may be reduced to an effective two level system containing only $|g_+\rangle$ and $|g_-\rangle$. The effective coupling constant being $g' = g^2/\Delta$, with $\Delta = \omega_+ - \omega_A$, and the effective detuning $\delta' = \omega_+ - \omega_-$.

An entirely new phenomena in degenerate two level atoms are virtual or Raman transitions [107, 127]. The essence of these transitions is that we achieve coupling between two levels that are not directly connected by the dipole interaction, but there is an intermediate level to which they could both be directly coupled. The point of making virtual transitions is that the intermediate level need not be directly excited, i.e. both pump lasers may be detuned from the respective transitions. A possible configuration is depicted on Fig. 1.3.4. If we assume large detuning ($|\Delta| \gg |g|$) and no initial population on the intermediate level, the Hamiltonian may be reduced to an effective two-level system, with the coupling strength depending on the overall detuning of the two pumps from the transition, and the frequency difference between the two pumps playing similar role as the detuning $\delta = \omega_0 - \omega_A$ of section Sec. 1.3.3. In the notations of Fig. 1.3.4, the effective Hamiltonian may be expressed

$$H_{\text{eff}} = -\hbar g'(|g_-\rangle\langle g_-|\, a_+^\dagger a_+ + |g_+\rangle\langle g_+|\, a_-^\dagger a_-) - \hbar g'(|g_-\rangle\langle g_+|\, a_+^\dagger a_- + |g_+\rangle\langle g_-|\, a_-^\dagger a_+) + \hbar\delta'\,|g_+\rangle\langle g_+|\,, \quad (1.95)$$

with $\delta' = \omega_+ - \omega_-$, $\Delta = \omega_+ - \omega_A$ and $g' = g^2/\Delta$. The unitary operator describing the time evolution in the $|g_-\rangle$, $|g_+\rangle$ basis has the same matrix as in Eq. (1.91), however, with the $\delta \to \delta'$ and $g \to g'$ substitutions.

1.4 Quantum information processing

This section is devoted to a brief recollection of the fundamentals of quantum information and quantum information processing. First we introduce the notion of quantum bit and

its properties that make it a fascinating subject of research from the perspective of information processing. Then we review the basics of manipulation of quantum information within the quantum gate paradigm, that is the quantum analog of classical boolean logic network. In this paradigm we start with a given initial state that encodes our input, and to attain the desired output, we apply unitary transformations chosen from a limited set. The unitary transformations in this set are generally referred to as quantum gates. Along with measurements performed on the output (or intermediate) quantum bits, this is all that we can use to realize quantum algorithms.

From the computational perspective, we are often faced with the problem that a quantum algorithm requires a certain unitary transformation to be constructed from the available quantum gates. The first problem is that such a construction does not necessary exists. Only the second problem is that of actual decomposition. We shall recollect some answers to these problems in sections 1.4.4 and 1.4.5.

We close the section with the discussion of the problem of constructing sets of quantum gates from the Hamiltonian time evolution of a physical system. The solution to this kind of problems is generally non-trivial and requires a great deal of insight and experience with the given physical system. The major source of difficulties is the limited and imprecise physical control of the system. To attain success a physical system suitable for the given problem must be found, and ways of sufficiently precise manipulation must be devised.

1.4.1 The quantum bit

The usual definition of a quantum bit is a two-level quantum system. In analogy with the convention of classical bit, the two distinct levels are labelled $|0\rangle$ and $|1\rangle$. However, since this is a quantum system, an arbitrary pure state of a quantum bit may be a superposition, e.g.

$$|\psi\rangle = \cos\vartheta\,|0\rangle + \mathrm{e}^{i\varphi}\sin\vartheta\,|1\rangle\,. \tag{1.96}$$

We realize that a quantum bit may be described using two (continuous) real variables ϑ and φ. Therefore we may argue that to represent a quantum bit in a classical information processing system, we would need infinitely many classical bits. This may make us believe that a quantum bit "contains" infinite information. This statement is, however, not true. In order to quantify the information "contained" in a quantum system we have to go back to the original definitions of information in the classical theory [9], and build up quantum information theory along the same lines.

The central quantity the classical theory is the Shannon entropy that is defined as

$$H(x) = -\sum_{x_i\in\mathscr{X}} p(x_i)\log_2 p(x_i), \tag{1.97}$$

for a source that produces the signals x_i from the alphabet $\mathscr{X}$ with probability $p(x_i)$. The base 2 of the logarithm sets the scale of this quantity to be $\log_2 N$ in case of an N letter alphabet and uniform distribution p. Hence, according to the *noiseless coding theorem*, $H(x)$ gives the average number of two state systems (bits) required to code the

output of the source using an ideal code. Therefore $H(x)$ is usually just referred to as the information content of the source, and is measured in bits.

The Shannon entropy has a striking formal analogy with statistical entropy, and indeed statistical entropy may be interpreted as the number of bits required to describe the micro state of the system. The statistical entropy of a quantum system has been introduced by von Neumann in Ref. [27] as

$$S(\varrho) = -\operatorname{Tr} \varrho \log_2 \varrho, \tag{1.98}$$

where ρ is the density operator describing the state of the quantum system, and Tr denotes taking the trace of the arguments. It is clear that $S(\varrho) = H(\lambda_i)$, where λ_i's denote the eigenvalues of ϱ. It has been shown by Schumacher [19] that in the quantum generalisation of the *coding theorem* this von Neumann entropy gives the average number of two state systems — this case quantum bits in the sense of Eq. (1.96) — required for an ideal coding.

We have certain freedom in defining states $|0\rangle$ and $|1\rangle$ of Eq. (1.96). The only requirement is that they have to be orthogonal states. A valid identification for example, are two orthogonal polarisation states of a photon, or the spin z eigenstates of a spin-$\frac{1}{2}$ particle. However, equally good would be the spin x eigenstates of the same particle, which are superpositions of spin z eigenstates. Therefore the $|0\rangle$ and $|1\rangle$ basis must be fixed at the beginning of any calculations. This basis is generally referred to as *computational basis*.

In case of multiple qubits, the tensor product notation may be abbreviated, e.g.

$$|0\rangle \otimes |1\rangle \otimes |1\rangle \equiv |011\rangle = |3\rangle\,, \tag{1.99}$$

where the right hand side equality is made valid by interpreting the binary string "011" as a binary number. We shall denote the space of a qubit by $\mathcal{H}_2$, and the space of N qubits by $\mathcal{H}_2^{\otimes N}$.

1.4.2 Bipartite pure state entanglement

Entanglement has raised a vast number of issues and therefore its literature is immense. For the purposes of the upcoming text, however, understanding the basic concepts of bipartite pure state entanglement is sufficient.

A pure state of a composite system of two subsystems, or bipartite system for short, is termed separable if it can be written as a tensor product

$$|\psi_{12}\rangle = |\psi\rangle \otimes |\varphi\rangle\,. \tag{1.100}$$

If a state $|\psi\rangle$ is non-separable, it is called entangled. There is a unique measure for this kind of entanglement. If using the proper basis for both subsystems any state of the composite system may be expanded as

$$|\psi_{12}\rangle = \sum_{j=1}^{\min\{d_1,d_2\}} \sqrt{\lambda_j}\,|e_j\rangle\,|f_j\rangle\,, \tag{1.101}$$

where all λ_j are non-negative real numbers, and d_1 and d_2 denotes the dimensionality of the first and the second subsystem, respectively. The expansion (1.101) is called the Schmidt decomposition, and the bases $|e_j\rangle$ and $|f_j\rangle$ are sometimes referred to as the Schmidt bases. Note that a separable state has one λ_j equal to 1, and the rest zero. If separable states are the least entangled states, then maximally entangled states are expected to have $\lambda_j = 1/\min\{d_1, d_2\}$. Maximally entangled states in this sense also exhibit the highest degree of non-locality, hence the intuitive expectations coincide.

The measure of bipartite pure state entanglement can be formulated in terms of its Schmidt coefficients as

$$E(|\psi_{12}\rangle) = -\sum_j \lambda_j \log_2 \lambda_j, \tag{1.102}$$

which resembles the Shannon entropy (1.97) of λ_j as a probability distribution. An alternative formulation is also possible, by taking the von Neumann entropy (1.98) of the reduced density matrix of either subsystems:

$$E(|\psi_{12}\rangle) = S(\varrho_1) = S(\varrho_2). \tag{1.103}$$

The reduced density matrices for one subsystem, e.g. 1, is defined as

$$\varrho_1 = \mathrm{Tr}_2 \, |\psi_{12}\rangle\langle\psi_{12}| \,, \tag{1.104}$$

where Tr_2 denotes taking the partial trace on subsystem 2. The entanglement measure (1.102) gives the degree of entanglement in units of ebits, and it may range from 0 to $\log_2 \min\{d_1, d_2\}$. Hence in case of two qubits, maximally entangled states possess 1 ebit of entanglement.

1.4.3 Quantum gates and quantum circuits

Now that we have seen the definition Eq. (1.96) of the quantum bit is in accordance with the information theoretical approach, we may safely proceed in making use of the quantum bit just as we do with classical bits. One way, initiated by Deutsch [65], is to follow an adaptation of standard Boolean network paradigm to quantum bits. In the classical model we start with several input bits that are fed into a Boolean network consisting of several elementary logic gates, and finally read out the output to find out the transformation committed by the network.

To generalise this to quantum bits we must determine the class of possible transformations on the quantum bits. As it turns out, these transformations can only be unitary. This fact has several implications, the most important perhaps being the so called *no-cloning theorem*, that states that a single qubit cannot be copied (or *cloned*).

The quantum analogs of logic gates are therefore simple unitary transformations termed "quantum gates." Besides quantum gates, we are also allowed to use measurements and the classical data from them in the construction of quantum circuits. However, considering the linearity of both measurements and quantum gates it is easy to show that every measurement that we would commit inside the circuit, can always be postponed to

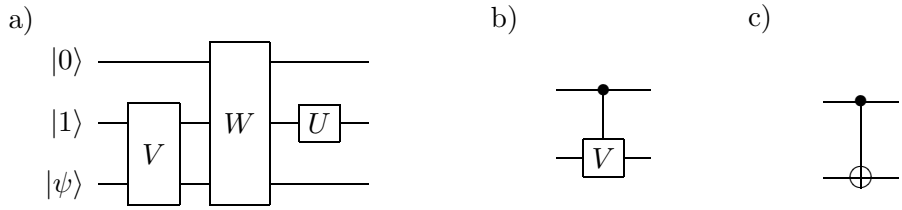

Figure 1.7: Examples of the standard quantum circuit formalism. a) Quantum circuit acting on three input qubits. The diagram may be formally written as $(\mathbb{1} \otimes U \otimes \mathbb{1})W(\mathbb{1} \otimes V)\,|0\rangle\,|1\rangle\,|\psi\rangle$, where U, V and W are one, two and three qubit unitaries, respectively. This expression is the output state itself. b) A controlled V gate with the first bit as control, and second as target. V can be any unitary. c) Controlled NOT gate, with first bit as control, second as target.

the end of the procedure. Therefore in the construction of networks realizing a certain transformation we can divide the problem into the construction of a unitary operation, followed by the design of proper measurements.

There is a standardised representation of quantum circuits that we shall follow. We now only recall the basic notations, for a complete listing refer to Ref. [18].

We provide an example of a simple quantum circuit on Fig. 1.7a. According to the convention, such diagram should be read from left to right. On the most left hand side, at start of the solid lines are the input quantum bits. The boxes denote the indicated unitary transformations that act on their input quantum bits that as given by the solid lines. These solid lines represent the quantum leads, and they are used to specify which qubits are being transformed by a certain quantum gate, and then to clearly identify their outputs. At the end of the leads on the right hand side we will have the output state of the network which is both available for further processing, or measurements.

There are certain, or certain type of quantum gates that are often used, and therefore have special notation. A large class of quantum gates is the set of so called controlled operations. For example, a two qubit controlled operation is shown on Fig. 1.7b. This depicts an operation that's control bit is the first qubit, and its target is the second qubit. Its action is to apply the operation V to the target bit when the control bit is $|1\rangle$, and leave the target bit as it is otherwise. The gate works on superpositions accordingly. Fig. 1.7c shows the famous controlled NOT gate. This gate is particularly important in the problem of universality that will be addressed in the next section. Because of its importance, here we explicitly list the action of CNOT on the basis states:

$$\begin{aligned} |00\rangle &\rightarrow |00\rangle\,, \\ |01\rangle &\rightarrow |01\rangle\,, \\ |10\rangle &\rightarrow |11\rangle\,, \\ |11\rangle &\rightarrow |10\rangle\,. \end{aligned} \tag{1.105}$$

As we can see, this gate performs a "bit flip" operation on the second quantum bit (target) when the first quantum bit (control) is in the state $|1\rangle$, but leaves it intact when it is

$|0\rangle$. This gate can be applied to any superposition of the input states, which produces an output state of a similar superposition with the (1.105) substitution in effect. In otherwords, both the control and the target bit may be in a superposition.

These controlled gates can be used to create entanglement. For example, from the separable state $1/\sqrt{2}(|0\rangle+|1\rangle)\,|0\rangle$ the CNOT produces $1/\sqrt{2}(|00\rangle+|11\rangle)$ which is maximally entangled.

1.4.4 Universality

In loose terms we call a set $\mathscr{G}$ of gates universal, if for any N bit transformation S there exists a network consisting only of elements of $\mathscr{G}$ that realizes the transformation S to arbitrary precision. In classical logic such universal sets are known long ago. An example is the NAND gate, which by itself is sufficient to construct any boolean network. There is, however, a catch in this statement: the use of the fan-in (joining leads) and fan-out (spliting leads) gates is implicitly assumed. Therefore the NAND gate (and the likes) are not universal gates themselves, they are only part of a universal gate set that includes fan-in and fan-out. Since the fan-in and fan-out gates correspond to splitting and joining of leads, they have no quantum mechanical equivalents. On the other hand, Fredkin and Toffoli have found three bit universal gates for reversible classical logic [128]. These gates are known as the Fredkin and Toffoli gate, and both have found applications in quantum computing also.

In classical logic there exist universal sets of gates with countable number of elements such that any transformation S can be realized exactly. This, however, is not possible in quantum computing, since the set of transformations on N qubits is a continuum set. Therefore, using any discrete set, we may only expect to be able to approximate any S to *arbitrary precision.* In this sense it has been shown, that almost any unitary acting on two quantum bits (also termed two-level unitary) is in fact universal, according to Ref. [67].

Another possibility is to define a continuum universal set, that will be universal in the exact sense. An example is the set consisting of the single qubit unitaries and the controlled-NOT (CNOT) gate. The proof of universality of this set comes from a quantum optics problem [100]. The speciality of the proof is that it is constructive, i.e. an algorithm is given that can be used to determine a decomposition of a given unitary S into a network of the elementary quantum gates. It takes away some of the beauty of the construction that it does not give the optimal decomposition. Nevertheless, due to its reliability, it serves as a good benchmark for other methods. The other part that may seem to be problematic at first sight is the requirement of all possible single qubit unitaries. Fortunately, any 2×2 unitary may be expressed as

$$U = \mathrm{e}^{i\alpha} R_z(\beta) R_y(\gamma) R_z(\delta), \tag{1.106}$$

where R_z and R_y are the rotation operators, generated from the Pauli sigma operators Eq. (1.83) as

$$R_i(\vartheta) = \mathrm{e}^{-i\sigma_i \vartheta/2}, \quad (i = x, y, z). \tag{1.107}$$

Of course the notation for the basis states is arbitrary, and in this case we imply the identification $|0\rangle \equiv |g\rangle$, $|1\rangle \equiv |e\rangle$. For similar reasons, the two rotation operators do not have to be around z and y but any two non-parallel direction. (It is, however, preferable to stick to orthogonal directions.)

In conclusion, the CNOT and the single qubit rotation operators around two orthogonal axes form a universal set of quantum gates. We may add, however, that if we restrict to the CNOT, Hadamard (H), phase (S) and the T gate, we still get an "approximately" universal set. The these gates are represented in the computational basis by the following matrices:

$$H = \frac{1}{\sqrt{2}} \begin{pmatrix} 1 & 1 \\ 1 & -1 \end{pmatrix}, \tag{1.108a}$$

$$S = \begin{pmatrix} 1 & 0 \\ 0 & i \end{pmatrix}, \tag{1.108b}$$

$$T = \begin{pmatrix} 1 & 0 \\ 0 & \mathrm{e}^{i\pi/4} \end{pmatrix}. \tag{1.108c}$$

The universality of these gates is mostly of theoretical importance, since no efficient way is known to carry out task of constructing a quantum circuit that performs a given transformation. For this reason, it is preferable to have all single qubit rotations in a quantum logic realization.

1.4.5 Invariants of quantum gates

We have mentioned the difficulty of finding an optimal decomposition of a unitary into elementary gates. For two-qubit gates, however, there are efficient algorithmic ways to carry this out due to Bremner et al. [129] and also Makhlin [130]. In present dissertation we shall use the latter method, and in the following we briefly reformulate it.

Quantum gates can be classified on the basis of "local equivalence." In the context of two-qubit quantum gates, we call two gates M and L *equivalent* or *locally equivalent* if there exist single qubit gates O_1, O_2, O_1' and O_2' such that

$$(O_1' \otimes O_2') M (O_1 \otimes O_2) = L, \tag{1.109}$$

where the expression $O_1 \otimes O_2$ denotes that operation O_1 is applied to the first qubit, and O_2 is applied to the second qubit. The use of the term "local equivalence" is justified by the fact that the classification seems to have deep connections to entanglement, where the bipartite state is spatially separated, hence we may speak of non-local operations that affect the amount of entanglement, and local operations that do not affect it.

It is clear that the definition (1.109) is an equivalence relation, that means e.g. that if M_1 is equivalent to M_2, and M_2 is equivalent to M_3, then M_1 is equivalent to M_3 as well. With the help of the invariants presented in [130], this classification of two-qubit quantum

gates becomes straight-forward. The invariants can be calculated in the entangled basis defined by the matrix

$$\underline{Q} = \frac{1}{\sqrt{2}} \begin{pmatrix} 1 & 0 & 0 & i \\ 0 & i & 1 & 0 \\ 0 & i & -1 & 0 \\ 1 & 0 & 0 & -i \end{pmatrix}. \tag{1.110}$$

The speciality of this basis is that a matrix in this basis corresponds to a local operation ($O = O_1 \otimes O_2$) if and only if its matrix is orthogonal.

Let our two-qubit quantum gate be represented by the matrix $\underline{M}$ in the computational basis, and $\underline{M}_B$ in the alternative Bell-basis defined by (1.110). The invariants may be expressed using the matrix $\underline{m} = \underline{M}_B^{\mathrm{T}} \underline{M}_B$, as

$$[\mathrm{Tr}^2\, \underline{m}/16 \det \underline{M}, (\mathrm{Tr}^2\, \underline{m} - \mathrm{Tr}\, \underline{m}^2)/4 \det \underline{M}], \tag{1.111}$$

with the superscript $^{\mathrm{T}}$ denoting real transposition, and the constant factors having been introduced for later convenience.

These definitions can also be used to efficiently find the single qubit rotations $O = O_1 \otimes O_2$ and $O' = O_1' \otimes O_2'$ of Eq. (1.109) as follows. First, find $\underline{O}_M$ and $\underline{O}_L$ orthogonal matrices such that $\underline{m} = \underline{O}_M^{\mathrm{T}} \underline{d}_M \underline{O}_M$ ($\underline{l} = \underline{O}_L^{\mathrm{T}} \underline{d}_L \underline{O}_L$), where $\underline{d}_M$ ($\underline{d}_L$) is a diagonal matrix. Then O and O' correspond to

$$\underline{O} = \underline{O}_M \underline{O}_L^{\mathrm{T}}, \tag{1.112a}$$

$$\underline{O}' = \underline{O}_L^{\mathrm{T}} \underline{O}^{\mathrm{T}} \underline{M}_B^{\dagger}, \tag{1.112b}$$

in the computational basis.

In case, two gates L and A are not in the same class, i.e. their invariants (1.111) are not equal, the construction (1.112) is invalid. However, we can use the invariants to speed up our search. First we try find O_f such that $M := AO_fA$ is equivalent to L and then use (1.112). It must be noted that we may fail to find M this way. In that case we may try higher order products such as $AO_fAO_f'A$, or use the method of Ref. [129].

1.4.6 Quantum gates from Hamiltonian evolution

As mentioned before, quantum gates are unitary operators. It is obvious that by choosing a Hamiltonian, just by controlling the time t, a manifold of quantum gates may be generated. However, a single Hamiltonian is never enough to generate a universal gate set. A solution can be to quickly "switch" between Hamiltonians, via some external control of the system. In case of an NMR quantum computer this corresponds to switching on and off an external magnetic field [131, 132]. Therefore, in this sense we may introduce the notion of universality in the context of Hamiltonians. According to [63, 133] (and [134]), for a set of Hamiltonians $\mathscr{H}$ of an N qubit system to be universal it is necessary and sufficient that it is the generator of the entire $U(2^N)$ Lie group through commutation. We refer the reader to the works of Bremner et al. for universality criteria of Hamiltonians when all single qubit gates are available [129, 135–138].

In certain cases, it is possible to make an approximation to keep the algebra generated by $\mathscr{H}$ simple. In NMR for example, the Hamiltonian can be written as the sum of internal and external parts

$$H = H_{\text{int}} + \lambda H_{\text{ext}}, \tag{1.113}$$

of which H_{int} cannot be controlled, while the external part can be varied to a great extent. (We represented this variability here by the factor λ.) Then we may define two Hamiltonians $H_A = H_{\text{int}}$ and $H_B = H_{\text{int}} + \lambda H_{\text{ext}}$ and "switch" between them in time by controlling the value of λ. When the two parts satisfy that all eigenvalues of $\lambda H_{\text{ext}} - H_{\text{int}}$ are much greater than 0 for sufficiently large λ. Then for practical purposes we have $H_B \approx \lambda H_{\text{ext}}$, and the "switching" is between H_{int} and λH_{ext}.

1.5 Optical quantum teleportation

Quantum teleportation can be a very useful quantum communication primitive. Depending on the demands, it may be used to transmit quantum information to distant place, with the speed essentially limited by the classical part of the communication. Another possible application is the transfer of an unknown state of one system to another, each of different physical nature. An example would be the transfer of a photon polarisation state to a two level atom.

In the present section we briefly summarise the original idea of Bennett et al. for quantum teleportation [89], then recall the teleportation scheme of Braunstein and Kimble [90] that is more fitted to the continuous nature of the electromagnetic field. Finally, we mention a teleportation scheme based on coherent states [94] that is somewhere in between the two other schemes.

1.5.1 Discrete quantum teleportation

The essence of quantum teleportation is a pair of quantum systems in an entangled state. The protocol described in Ref. [89] uses the singlet state of two spin-$\frac{1}{2}$ particles, however, the scheme works with any maximally entangled qubit state, after minor modifications. Entanglement plays special role in the measurement also, since the projection has to be done onto a basis entirely consisting of maximally entangled states. In general, the measurement basis must be *matched* to the entangled pair for optimal results [139, 140].

The setup of quantum teleportation is well-known in the quantum physics community. Here we just quickly recollect the basic notations. In the original problem, Alice has an unknown quantum state $|\psi_{\text{in}}\rangle$ that she wants to send to Bob. Initially an entangled (known) state is split between them, and Alice is allowed to send classical information to Bob. To describe the protocol, let us introduce the entangled basis,

$$|\Psi_\pm\rangle = \frac{1}{\sqrt{2}}(|0\rangle|1\rangle \pm |1\rangle|0\rangle), \tag{1.114a}$$

$$|\Phi_\pm\rangle = \frac{1}{\sqrt{2}}(|0\rangle|0\rangle \pm |1\rangle|1\rangle), \tag{1.114b}$$

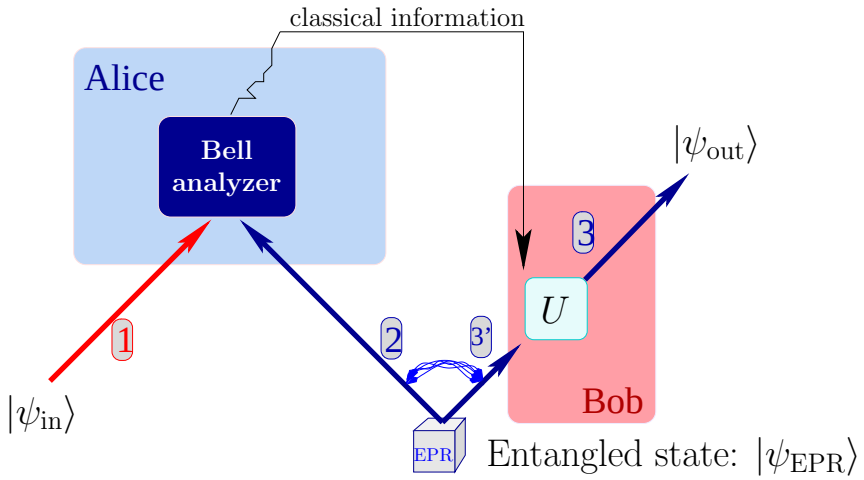

Figure 1.8: Quantum teleportation

that is called Bell basis. We choose $|\Psi_-\rangle$ as the entangled (EPR) pair $|\psi_{\text{EPR}}\rangle$. Note that if the computational basis is a spin z eigenbasis, then $|\Psi_-\rangle$ is a singlet state, and the rest of the Bell states (1.114) are triplet states.

Now Alice's task is to make a joint measurement on the unknown state $|\psi_{\text{in}}\rangle$ and her share of the entangled state $|\psi_{\text{EPR}}\rangle$, such that she projects them onto the Bell basis states. As the result of her measurement, Bob's end of the entangled state will be projected into some state $|\psi'_{\text{out}}\rangle$. However, due to the entanglement of $|\psi_{\text{EPR}}\rangle$, this state will be related to the initial state $|\psi_{\text{in}}\rangle$ via a unitary operator U that depends only on the outcome of Alice's measurement. The four possible operators are

$$U_{00} = -\begin{pmatrix} 1 & 0 \\ 0 & 1 \end{pmatrix}, \qquad U_{01} = \begin{pmatrix} -1 & 0 \\ 0 & 1 \end{pmatrix}, \qquad U_{10} = \begin{pmatrix} 0 & 1 \\ 1 & 0 \end{pmatrix}, \qquad U_{11} = \begin{pmatrix} 0 & 1 \\ -1 & 0 \end{pmatrix}. \tag{1.115}$$

Therefore, Alice has to send the outcome of her measurement, that will indicate to Bob which unitary has to be applied to his state $|\psi'_{\text{out}}\rangle$. For example, if Alice's measurement projects onto $|\Psi_-\rangle$, she must send 00 to Bob, who in turn applies the correct unitary U_{00}.

Optics took a leading role in quantum communication with the first experimental demonstration of quantum teleportation, using polarisation states of photons [114].

1.5.2 Continuous variable quantum teleportation

The continuous variable teleportation scheme differs from the discrete version at several points. First of all, instead of qubits, the protocol aims at teleporting the full quantum state of an electromagnetic mode. This implies the second feature: maximal entanglement requires that all Schmidt coefficients in Eq. (1.101) are equal, however, in the infinite dimensional case, this criterion cannot be fulfilled together with the requirement

of normalisation. Therefore, there does not exist any maximally entangled state of two electromagnetic modes, and the teleportation cannot be perfect in general.

In the scheme described by Braunstein and Kimble [90] the entangled state is a two-mode squeezed vacuum state. In the Fock representation this state can be written

$$|\psi_{\mathrm{EPR}}\rangle = \frac{1}{u}\sum_{n=0}^{\infty}\left(-\frac{v}{u}\right)^n |n\rangle|n\rangle\,, \tag{1.116}$$

with $u = \cosh r$ and $v = \mathrm{e}^{i\varphi}\sinh r$, where $\zeta = r\,\mathrm{e}^{i\varphi}$ is the squeezing parameter. It is clear that for any finite value of r its entanglement is finite. However, the entanglement goes to infinity as r tends to infinity, and state also becomes unnormalisable.

If we ignore the problem of non maximal entanglement for a moment, we find that the Bell state analysis and reconstruction is surprisingly simple in this case. The realization of the Bell state measurement requires only a beam splitter and two homodyne detectors measuring two perpendicular quadratures. The classical information to be sent to Bob are simply the detector currents from the homodyne measurements, and Bob's reconstruction consists of applying a coherent displacement with real and imaginary part corresponding to the appropriate classical currents. This protocol has been realized first by Furusawa et al. [141].

Unfortunately, the non maximal entanglement distorts this beautiful picture. It turns out that there is no matching measurement that guarantees perfect teleportation for every state. In case we do not modify the original protocol, this error manifests itself in a Gaussian smearing of the original input state, the variance of the Gaussian depending on the entanglement on the EPR state, and the position depending on the measurement outcome. Since the inverse of the smearing introduced by the protocol is an unphysical process, the error cannot be removed.

1.5.3 Teleportation with coherent states

The principle of operation for teleporting coherent states [94] is not very different from the original protocol by Bennett et al. The most important difference lies in the entangled state that is used as quantum channel, that is a superposition of coherent states. Along the lines of Sec. 1.1.9, we choose two coherent states with opposite sign as basis: $|\alpha\rangle$ and $|-\alpha\rangle$. This is not an orthogonal basis, but we can define one using the Schrödinger cat states (1.69). It turns out, that some maximally entangled states can be expressed in a very simple manner:

$$|\Psi_{\mathrm{EPR}}\rangle = \frac{1}{\sqrt{\mathcal{N}}}(|\alpha\rangle|\alpha\rangle - |-\alpha\rangle|-\alpha\rangle\,, \tag{1.117}$$

where $\mathcal{N}$ is a normalisation factor depending on α.

A sufficiently good Bell analyser can be constructed using a 50-50% anti-symmetric beam splitter and idealistic photon counters. The possible outcomes of the photon detection are such that only one of the detectors report a non-zero number n. If n is odd, the teleportation is perfect, however, when n is even $|\Psi_{\mathrm{out}}\rangle$ relates to $|\Psi_{\mathrm{in}}\rangle$ in a non unitary (in

fact anti-unitary) way. Since the probability of detecting an odd number of photons at one of the photon counters is 1/2, the teleportation still outperforms "classical" teleportation [142, 143].

1.6 Decoherence in quantum optics

The term decoherence applies to any process that causes our observed system to lose its coherence. This is a very general terminology, and in order to understand at least partly, we must state what we mean by coherence in this context. We may get a feeling of its definition by considering the famous double slit experiment. In the quantum mechanical limit, colloquially we say that the particle crosses the two slits simultaneously. Formally we write its state as a superposition $|\psi\rangle = 1/\sqrt{2}(|\text{left}\rangle + |\text{right}\rangle)$. The interference pattern on the screen arises from the "quantum interference" of the constituting two basis states. On the other hand, a classical particle can cross only on one of the slits, however, we do not know which one. This case may be described by a distribution function, that becomes a diagonal density matrix in the quantum mechanical formalism: $\varrho_{\text{class}} = 1/2(|\text{left}\rangle\langle\text{left}| + |\text{right}\rangle\langle\text{right}|)$. If we compare the density matrices $\varrho_{\text{quant}} = |\psi\rangle\langle\psi|$ and ϱ_{class}, we find that the off-diagonal elements have disappeared in ϱ_{class} compared to ϱ_{quant}. The transition from the quantum behaviour to the classical particle behaviour is usually explained by saying that the two paths have lost their *coherence*. Therefore, the off-diagonal elements are often termed coherences, and in processes where off-diagonal elements decrease are regarded as decoherence. It must be noted, however, that general decoherence may drag the system towards a density operator diagonal in any basis.

After sketching of the notion of decoherence, we turn to the question of mechanisms leading to decoherence. The fundamental problem is that it is not possible to completely isolate a quantum system from its environment. During the observation, our quantum system will unavoidably interact with the environment. This interaction generally introduces some amount of entanglement between the observed system and the environment. However, since we can only make measurements on the observed system, we are essentially dealing not with the joint state of the system–environment system, but the reduced density operator of the observed system. Clearly, an initial pure state will eventually evolve into a mixed state due to this entanglement with the environment.

Since this time evolution is generally not unitary any more, a different dynamical equation, called master equation, has been developed to replace the Schrödinger equation. In the following section we recall its basic definition.

1.6.1 Master equation approach

While introducing the master equations to quantum mechanics, we do not violate the unitarity of its dynamics. Indeed, construction assumes a unitary time evolution of the joint state of the observed system and the environment represented by the density matrix

ϱ_{SR}. The time evolution of the density matrix is given by

$$\dot{\varrho}_{SR} = -\frac{i}{\hbar}[H_{SR}(t), \varrho_{SR}(t)], \tag{1.118}$$

where H_{SR} is the Hamiltonian of the coupled system $H_{SR} = H_S + V_{SR} + H_R$. For practical purposes the environment is considered to be much larger then the observed system and therefore often termed *reservoir*. Since this is the type of interaction we will be interested in later, we model the reservoir as a collection of bosonic modes, and in this case the self Hamiltonians can be written

$$H_S = \omega a^\dagger a, \quad \text{and} \quad H_R = \sum_i \omega_i a_i^\dagger a_i. \tag{1.119}$$

Since we are interested only in the observed system, we need an equation of motion for the reduced density operator,

$$\varrho_S(t) = \mathrm{Tr}_R\, \varrho_{SR}(t), \tag{1.120}$$

using Eq. (1.118) with the assumption that the coupling is weak. The derivation can be done by first going to the interaction picture and expanding the dynamical equation as a perturbation series. The assumption of a weak coupling allows us to drop higher orders of the interaction term (Born approximation). If we further assume that the interaction Hamiltonian is of the form

$$V_{SR} = a^\dagger R^{(+)} + a R^{(-)}, \tag{1.121}$$

where $R^{(+)} = \sum g_i a_i^\dagger$, and $R^{(-)} = R^{(+)\dagger}$, and the initial state is a tensor product

$$\varrho_{SR}(t=0) = \varrho_S^{(0)} \otimes \varrho_R^{(0)}, \tag{1.122}$$

then, under the Markov approximation, the reduced dynamical equation becomes

$$\dot{\varrho}_S = -\frac{i}{\hbar}(\omega + \Delta)[a^\dagger a, \varrho_S] - \Gamma'\{a^\dagger a, \varrho_S\} - \Gamma'\{aa^\dagger, \varrho_S\} + \Gamma'(a^\dagger \varrho_S a + a\varrho_S a^\dagger) - \frac{\Gamma}{2}\{a^\dagger a, \varrho_S\} + \Gamma a \varrho_S a^\dagger \tag{1.123}$$

in the Schrödinger picture. Here we have used the notation $\{\cdot,\cdot\}$ for the anti-commutator. The parameters Γ, Γ' and Δ depend on the spectrum of the observed system as well as the reservoir, and also the initial state Eq. (1.122).

The dynamical equation (1.123) is usually referred to as the *master equation* of the system. For a thorough treatment, and the expressions and interpretations of the various parameters, see Refs. [4] or [144].

1.6.2 Modelling decoherence with a beam-splitter

For free-space electromagnetic modes there is another model, essentially equivalent to a master equation, that is based on using a beam splitter. In this scheme, we insert a

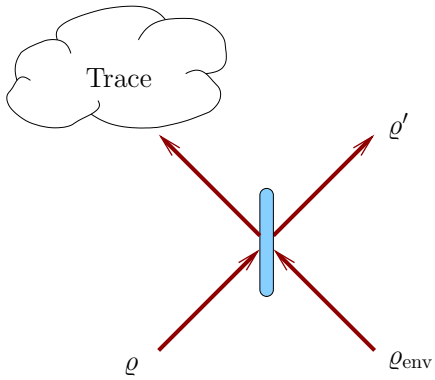

Figure 1.9: Modelling decoherence with a beam splitter. The state of the environment is represented by the external mode on the second input port of the beam splitter, the strength of interaction is set by the reflectivity of the beam splitter, and the final state after decoherence is obtained by tracing out for the reflected mode.

low reflectivity beam splitter in the way of our propagating mode, and inject vacuum, or whatever state we would like to model the environment with, on the other port. Then we trace out on the reflected mode, and obtain the state of the original mode after decoherence. The procedure is depicted on Fig. 1.9. Although this model is not based on microscopical phenomena, there is place for describing the strength of coupling through the reflectivity of the beam splitter, and the state of the reservoir by the auxiliary mode.

1.6.3 Quantum relative entropy

In the previous two sections, we dealt with the modelling of decoherence, due to interaction with the environment. In the present section we turn to the problem of quantification of decoherence, i.e. the determination of how far the final state is different from the original, prior to decoherence.

A widely used quantity is based on the overlap of the initial and the final states: $\operatorname{Tr}\varrho_{\mathrm{in}}\varrho_{\mathrm{out}}$. In this section, however, we take a more positivist approach to quantification of decoherence, one that is based on measurement statistics. At the heart of this approach lies the quantum mechanical version of Sanov theorem (theorem 8 of [38]; see also [97, 145]). This theorem relates the quantum relative entropy $S(\cdot\|\cdot)$, defined as

$$S(\sigma\|\varrho) = \operatorname{Tr}\sigma(\ln\sigma - \ln\varrho), \tag{1.124}$$

to the reliability of our measurement. It tells us that by performing measurements on n copies of the state σ, the probability of concluding that our state was some ϱ is

$$P(\sigma \to \varrho) = \mathrm{e}^{-nS(\sigma\|\varrho)}, \tag{1.125}$$

as $n \to \infty$.

We can use this definition to quantify the effect of decoherence, by considering a "read-out" problem, i.e. when we make measurements on a state undergone decoherence as if it was the original state, and we are interested in how well we can distinguish two originally orthogonal states. To achieve this, the probabilities we are interested in are $S(\sigma_0\|\sigma_1)$ and $S(\sigma_1\|\sigma_0)$, where σ_s denotes the basis state $|s = 0, 1\rangle$ undergone decoherence. In this case, we can obtain e.g. $P(\sigma_0 \to \sigma_1)$ which essentially gives us the probability of error, since we falsely identify the original outcome being $|1\rangle$ while it was actually $|0\rangle$. Since $S(.\|.)$ is not symmetric in its arguments, we need to consider a worst case scenario, and consider the combination that gives the larger probability i.e. smaller relative entropy.

Chapter 2

Coherent-state quantum bits for quantum information processing

Coherent states are interesting from the point of representations in quantum optics, and they also play an important role considering decoherence. These two features provide a legitimate basis for the search for a convenient description of entanglement, and simply formulated quantum bits, in terms of coherent states. It should also be noted, that an ideal laser would emit light in a coherent state, therefore these states are routinely available in a laboratory.

In the present chapter we address all of these aspects. With Sec. 2.1 we start with the truly bipartite problem of two-mode entanglement. We use the two-mode squeezed vacuum to develop a reduced dimensionality coherent state representation. The representation is very handy for a wide class of Gaussian states, but it can also be used for a representation of any general two-mode quantum state. We give an expression for an entangled basis based on Laguerre-2D polynomials introduced by Wünsche [146].

In Sec. 2.2 we make use of the representation of Sec. 2.1 by deriving a simplified superposition possessing high degree of entanglement. We demonstrate its applicability for coherent state based quantum information processing by devising a setup where this entangled state plays the role of the quantum channel. We show that this channel is capable of assisting the transfer of two qubits of quantum information at once, in a probabilistic teleportation scheme.

The last section in this chapter, Sec. 2.3, is dedicated to the analysis of the decoherence of coherent state quantum bits. We consider a read-out problem of an elementary coherent state quantum computer, where the possible outcomes of the computation are two orthogonal coherent state superpositions. Since the output states suffer decoherence as they are transfered from the quantum computer to the measurement apparatus, we must distinguish the distorted basis states. We investigate the case when we have sufficient control over the environment causing decoherence, although we cannot isolate it from our qubits. We calculate the quantum relative entropies to quantify the reliability of our results using a coherent state representation. We consider a case when the immediate

environment is somewhat under our control, and it can be prepared in a squeezed state. We present analytical and numerical results on the calculation of the optimal parameters for the squeezing of the environment.

2.1 One-complex-plane coherent state representation

The coherent states, introduced in Sec. 1.1.7, have considerable importance in quantum optics. When they are used for representations, calculations of expectation values of ladder operator polynomials is straight-forward due to the property Eq. (1.54). From the conceptual point of view, their speciality is that they can be considered to be the most classical quantum states. Another feature that supports this interpretation is their relation to decoherence. It can be shown that at optical frequencies, where the environment can be considered to be in vacuum state, an initial coherent state suffering decoherence of the type depicted on Fig. (1.9), would remain a coherent state, albeit change its coherent amplitude. This makes coherent state representations good candidates for efficient description of decoherence affected processes.

For most quantum information processing applications, entanglement plays a crucial role. In the present section we shall work out a coherent state representation of entangled states of light. Although the representation is adjusted to the most common two-mode entangled states, the two-mode squeezed vacuum, it is applicable to any possible state of the two-mode electromagnetic field. The advantage of the representation is that similarly to the one-dimensional representation of Sec. 1.1.10, it involves only a one complex dimensional sub-plane of the two complex dimensional phase space. Hence we term this representation one-complex-plane coherent state representation [86, 87].

In the development of the representation, we first discuss the one-complex-plane representation of the two-mode squeezed vacuum. Following the analogy, we further introduce an orthonormal set using Laguerre-2D polynomials [146], then show its completeness by relating it to the two-mode squeezing operator. Finally we further generalise the representation, by considering arbitrary phase of the squeezing operator. This representation has been used to describe quantum teleportation of continuous variables [88, 90, 147] .

2.1.1 Two-mode squeezed vacuum

Just like the ordinary squeezing operator, two-mode squeezing is best described in terms of the creation and annihilation operators of the involved electromagnetic modes [148]. Here, and in the following subsections, the annihilation operators of the first and the second mode are denoted by a and b, respectively. The two-mode squeezing operator is defined as

$$S^{(2)} = \mathrm{e}^{-\zeta a^\dagger b^\dagger + \zeta^* a b}, \tag{2.1}$$

where $\zeta = r\,\mathrm{e}^{i\vartheta}$ is the complex squeezing parameter analogous to Eq. (1.66). The transformation of the annihilation operators under the unitary operator $S^{(2)}$ can be written

similarly as in Eq. (1.67), as

$$a' = ua + vb^\dagger, \tag{2.2}$$
$$b' = ub + va^\dagger, \tag{2.3}$$

where $u = \cosh r$ and $v = \mathrm{e}^{i\vartheta} \sinh r$.

It is easily seen that a two mode squeezed vacuum state can be prepared from two ordinary squeezed vacuum states and a $50 - 50\%$ beam splitter with the transformation matrix

$$\underline{R} = \frac{1}{\sqrt{2}} \begin{pmatrix} 1 & 1 \\ -1 & 1 \end{pmatrix}. \tag{2.4}$$

The output state thus emerging from the beam splitter can be written

$$|\psi\rangle = U\,|0\rangle|0\rangle = U_R S(\zeta_1) \otimes S(\zeta_2)\,|0\rangle|0\rangle = U_R S(\zeta_1) \otimes S(\zeta_2) U_R^\dagger U_R\,|0\rangle|0\rangle\,, \tag{2.5}$$

however, $U_R\,|0\rangle|0\rangle = |0\rangle|0\rangle$ since the beam splitter has no effect on the vacuum state. Also, since the ladder operators a and b of the two squeezing operators commute, their exponents can be brought together, hence we arrive at

$$U = U_R \exp(\zeta_1 a^{\dagger 2} - \zeta_1 a^2 + \zeta_2 b^{\dagger 2} - \zeta_2 b^2) U_R^\dagger. \tag{2.6}$$

Using Eq. (1.67), we can verify that with $\zeta_1 = -r/2\,\mathrm{e}^{i\vartheta}$ and $\zeta_2 = r/2\,\mathrm{e}^{i\vartheta}$, where r and ϑ are real parameters, we have

$$U = S^{(2)}(2r\,\mathrm{e}^{i\vartheta}), \tag{2.7}$$

therefore $|\psi\rangle = |\zeta, \{0,0\}\rangle$. We note that these two values ζ_1 and ζ_2 correspond to squeezing along two orthogonal directions. For example if $\vartheta = 0$, they correspond to the Y and the X directions, respectively.

2.1.2 Basis using Laguerre-2D polynomials

Our goal is to find a two-mode generalisation of the one dimensional coherent state representation. We observe that the one dimensional coherent state representation used exactly half of the available dimensionality of the phase space. As a special case, this one dimensional manifold is a proper subspace, e.g. a straight line. Therefore, we concentrate our attention on a subspace which may be parametrised by a single complex parameter α, and characterised by two angles ϱ_a and ϱ_b:

$$S = \left\{ |\mathrm{e}^{i\varrho_a}\,\alpha\rangle|\mathrm{e}^{i\varrho_b}\,\alpha^*\rangle \;\middle|\; \alpha \in \mathbb{C} \right\}. \tag{2.8}$$

In the following, we shall show that the basis defined using the Laguerre-2D polynomials is orthogonal, and complete. The definition of the Laguerre-2D polynomials [146] read

$$l_{mn}(z, z^*) = \frac{1}{\sqrt{m!n!}} \sum_{j=0}^{\min m,n} \frac{m!n!}{j!(m-j)!(n-j)!} (-1)^j z^{*m-j} z^{n-j}. \tag{2.9}$$

The polynomials are complete and orthogonal with respect to the weight function $w(z,z^*) = \mathrm{e}^{-zz^*}$, i.e.

$$\frac{1}{\pi}\int_{\mathbb{C}} \mathrm{e}^{-zz^*}\, l_{kl}(z,z^*) l_{mn}(z,z^*) \mathrm{d}^2 z = \delta_{km}\delta_{ln}. \tag{2.10}$$

Therefore, we define the countable set $\mathcal{L}$ that consists of the states

$$|l_{mn}(\gamma)^{\{\varrho\}}\rangle := \mathcal{N}_{mn}(\gamma)\int_{\mathbb{C}} \mathrm{e}^{-|\alpha|^2/\gamma^2}\, l_{mn}(\mu\alpha,\mu\alpha^*)\, |\mathrm{e}^{i\varrho_a}\,\alpha\rangle |\mathrm{e}^{i\varrho_b}\,\alpha^*\rangle\, \mathrm{d}^2\alpha, \tag{2.11}$$

where

$$\mathcal{N}_{mn}(\gamma) = \frac{\sqrt{1+2\gamma^2}}{\gamma^2\pi}\left(\frac{1+\gamma^2}{\gamma^2}\right)^{\frac{m+n}{2}}, \text{ and} \tag{2.12a}$$

$$\mu = \sqrt{\frac{1+2\gamma^2}{\gamma^2(\gamma^2+1)}}. \tag{2.12b}$$

The orthogonality of these states can be demonstrated easily using the definitions, and the integral identity ($\mu > 0$),

$$\int_{\mathbb{C}} l_{mn}(z,z^*)\, \mathrm{e}^{-\mu|z|^2+\lambda z+\nu z^*}\, \mathrm{d}^2 z = \frac{\pi}{\mu}\left(\frac{\mu-1}{\mu}\right)^{\frac{m+n}{2}} \exp\left(-\frac{(\mu-\frac{1}{2})\lambda\nu}{\mu(\mu-1)}\right) l_{mn}\left(\nu/\sqrt{\mu(\mu-1)}, \lambda/\sqrt{\mu(\mu-1)}\right). \tag{2.13}$$

We omit the details of the proof of the identity Eq. (2.13), we only mention that we make use of the more general identity

$$\int_{\mathbb{C}} z^m z^{*n}\, \mathrm{e}^{-\mu|z|^2+\lambda z+\nu z^*}\, \mathrm{d}^2 z = \frac{\pi}{\mu}\,\frac{\partial^m}{\partial\lambda'^m}\frac{\partial^n}{\partial\nu'^n}\, \mathrm{e}^{\frac{\lambda'\nu'}{\mu}}\Big|_{\substack{\lambda'=\lambda\\ \nu'=\nu}}. \tag{2.14}$$

To demonstrate the orthogonality, we must show that the scalar product $\langle l_{kl}(\gamma)^{\{\varrho\}} | l_{mn}(\gamma)^{\{\varrho\}}\rangle$ vanishes whenever $k \neq m$ and $l \neq n$. We expand this scalar product and arrive at

$$\langle l_{kl}(\gamma)^{\{\varrho\}} | l_{mn}(\gamma)^{\{\varrho\}}\rangle = \mathcal{N}_{kl}(\gamma)\mathcal{N}_{mn}(\gamma)\int_{\mathbb{C}^2} l_{kl}(\mu\alpha,\mu\alpha^*)^*\, \mathrm{e}^{-|\alpha|^2/\gamma^2}\, l_{lm}(\mu\beta,\mu\beta^*)\, \mathrm{e}^{-|\beta|^2/\gamma^2} \times \langle \mathrm{e}^{i\varrho_a}\,\alpha|\, \mathrm{e}^{i\varrho_a}\,\beta\rangle \langle \mathrm{e}^{i\varrho_b}\,\alpha^*|\, \mathrm{e}^{i\varrho_b}\,\beta^*\rangle\, \mathrm{d}^2\alpha\, \mathrm{d}^2\beta, \tag{2.15}$$

and we notice that the phase factors ϱ_a and ϱ_b get cancelled out in the scalar product. We first evaluate the β integral. Leaving only the β dependent terms under the integration sign, we are left with

$$I = \int_{\mathbb{C}} l_{mn}(\mu\beta,\mu\beta^*)\, \mathrm{e}^{-(1/\gamma^2+1)|\beta|^2+\alpha\beta^*+\alpha^*\beta}\, \mathrm{d}^2\beta, \tag{2.16}$$

that we apply the identity (2.13) to, and obtain

$$I = \frac{\mu^2}{\mathcal{N}_{mn}(\gamma)^2}\, \mathrm{e}^{\frac{\gamma^2}{\gamma^2+1}|\alpha|^2}\, l_{mn}(\mu\alpha,\mu\alpha^*). \tag{2.17}$$

We substitute this expression into Eq. (2.15) and arrive to

$$\langle l_{kl}(\gamma)^{\{\varrho\}}|l_{mn}(\gamma)^{\{\varrho\}}\rangle = \frac{\mathcal{N}_{kl}(\gamma)}{\mathcal{N}_{mn}(\gamma)}\mu^2\int_{\mathbb{C}} \mathrm{e}^{-\mu^2|\alpha|^2}\, l_{kl}(\mu\alpha,\mu\alpha^*)^* l_{mn}(\mu\alpha,\mu\alpha^*)\mathrm{d}^2\alpha, \qquad (2.18)$$

that, according to Eq. (2.10), evaluates to $\langle l_{kl}(\gamma)^{\{\varrho\}}|l_{mn}(\gamma)^{\{\varrho\}}\rangle = \delta_{km}\delta_{ln}$, after a change of integration variable.

Now we have proven the orthogonality of the set $\mathcal{L}$. In order for $\mathcal{L}$ to be a *basis* of the two-mode system, it must also be complete. This will be shown in the next section.

2.1.3 Completeness of the Laguerre-2D basis

We shall prove the completeness of the $\mathcal{L}$ basis by explicitly showing that it is unitary equivalent to the Fock basis. The unitary transformation making the connection between the two, is the two-mode squeezing operator $S^{(2)}(\zeta)$.

To this end, we first consider the formula Eq. (2.5) starting with the initial squeezed states expressed in one-dimensional coherent state representation (1.72). The result can be written as

$$|\zeta,\{0,0\}\rangle = \mathcal{N}(\gamma)\int_{\mathbb{C}} \mathrm{e}^{-|\alpha|^2/\gamma^2}\,|\alpha\rangle|-\mathrm{e}^{i\vartheta}\,\alpha^*\rangle\,\mathrm{d}^2\alpha, \qquad (2.19)$$

with $\zeta = r\,\mathrm{e}^{i\vartheta}$ and $\gamma = \sqrt{|v|/(u-|v|)}$. In bringing Eq. (2.19) into its present form by a change in integration variables, we used the phase invariance of the Gaussian factor, and omitted the unimportant phase factor. Interestingly, if we consider $|l_{00}(\gamma)^{\{\varrho\}}\rangle$ and again use the phase invariance, we find perfect matching between it and (2.19) upon taking

$$\varrho_a + \varrho_b = \vartheta + \pi. \qquad (2.20)$$

Another crucial relation is that the basis states of different ϱ_a and ϱ_b are unitary equivalent. Namely, we can easily see that

$$|l_{mn}(\gamma)^{\{\varrho\}}\rangle = \exp(i\varrho_a a^\dagger a + i\varrho_b b^\dagger b)\,|l_{mn}(\gamma)\rangle\,, \qquad (2.21)$$

where we used $|l_{mn}(\gamma)\rangle$ to denote the state $|l_{mn}(\gamma)^{\{\varrho_a=\varrho_b=0\}}\rangle$.

Backed by these results, we now see that it is only necessary to prove for all m,n the equality

$$|l_{mn}(\gamma)\rangle = |\zeta=-r,\{m,n\}\rangle := S^{(2)}(-r)\,|m\rangle|n\rangle\,. \qquad (2.22)$$

In order to proceed, we first prove the following two identities:

$$a^{\dagger n}\,|l_{00}(\gamma)\rangle = \mathcal{N}(\gamma)\int_{\mathbb{C}} \mathrm{e}^{-|\alpha|^2/\gamma^2}\left(-\frac{u}{v}\alpha^*\right)^n|\alpha\rangle|\alpha^*\rangle\,\mathrm{d}^2\alpha = \left(-\frac{u}{v}b\right)^n|l_{00}(\gamma)\rangle\,, \qquad (2.23a)$$

$$b^{\dagger n}\,|l_{00}(\gamma)\rangle = \mathcal{N}(\gamma)\int_{\mathbb{C}} \mathrm{e}^{-|\alpha|^2/\gamma^2}\left(-\frac{u}{v}\alpha\right)^n|\alpha\rangle|\alpha^*\rangle\,\mathrm{d}^2\alpha = \left(-\frac{u}{v}a\right)^n|l_{00}(\gamma)\rangle\,, \qquad (2.23b)$$

where $u/v = \mathrm{e}^{i\vartheta}(\gamma^2-1)/\gamma^2$, but now we have to consider only the case when $\vartheta=\pi$. It is enough to show the validity of one of the equalities. First we consider the left hand side of (2.23a) in the Fock state basis:

$$a^{\dagger n}\,|l_{00}(\gamma)\rangle = \frac{1}{u}\sum_{k=0}^{\infty}\sqrt{\frac{(k+n)!}{k!}}\left(-\frac{v}{u}\right)^k|k+n\rangle|k\rangle\,. \qquad (2.24)$$

Next we substitute the Fock state expansion of the coherent state $|\alpha\rangle|\alpha^*\rangle$, and get for the central expression in Eq. (2.23a):

$$\mathcal{N}(\gamma)\int_{\mathbb{C}} \mathrm{e}^{-|\alpha|^2/\gamma^2}\left(-\frac{u}{v}\alpha^*\right)^n |\alpha\rangle|\alpha^*\rangle\ \mathrm{d}^2\alpha = \left(-\frac{u}{v}\right)^n \sum_{k,l=0}^{\infty}\frac{1}{\sqrt{k!}\sqrt{l!}}\mathcal{N}(\gamma)\left[\int_{\mathbb{C}}\alpha^k\alpha^{*l+n}\,\mathrm{e}^{-|\alpha|^2(1+1/\gamma^2)}\,\mathrm{d}^2\alpha\right]|k\rangle|l\rangle\,. \quad (2.25)$$

After evaluating the complex integral using Eq. (2.14) we obtain $\pi k!\left(\frac{|v|}{u}\right)^{k+1}\delta_{k,l+n}$, which proves the left hand side equality in Eq. (2.23a). To complete our proof, we just have to use the (1.54) definition of coherent states.

To exploit the relation between the creation and annihilation operators applied to $|l_{00}(\gamma)\rangle$, let us consider Eq. (2.22) and write it as

$$|\zeta,\{m,n\}\rangle = \frac{1}{\sqrt{m!n!}}\left(S^{(2)}(\zeta)a^\dagger S^{(2)\dagger}(\zeta)\right)^m\left(S^{(2)}(\zeta)b^\dagger S^{(2)\dagger}(\zeta)\right)^n S^{(2)}(\zeta)\,|0\rangle|0\rangle = = \frac{1}{\sqrt{m!n!}}\left(ua^\dagger+v^*b\right)^m\left(ub^\dagger+v^*a\right)^n|l_{00}(\gamma)\rangle\,. \quad (2.26)$$

Now we can apply the binomial expansion to this expression and get

$$|\zeta,\{m,n\}\rangle = \frac{1}{\sqrt{m!n!}}\sum_{k=0}^{m}\sum_{l=0}^{n}\binom{m}{k}\binom{n}{l}u^{k+l}v^{m+n-k-l}a^{\dagger k}b^{m-k}b^{\dagger l}a^{n-l}\,|l_{00}(\gamma)\rangle\,. \quad (2.27)$$

It is clear that since a and $b^\dagger$ commute, in the spirit of Eq. (2.23b) we can replace $b^{\dagger l}$ by $(-av/u)^l$. It is, however, not this simple with $a^\dagger$ since the canonical commutation relations $[a,a^\dagger]=1$ hold. In order to be able to apply Eq. (2.23a) we first have to bring it into anti-normal ordered form. For an arbitrary normal ordered monom we can use the formula

$$a^{\dagger k}a^m = \sum_{l=0}^{\min\{k,m\}}\frac{m!k!}{(m-l)!(k-l)!l!}(-1)^l a^{m-l}a^{\dagger k-l}, \quad (2.28)$$

which may be proven by induction.

In using Eq. (2.28) for evaluating Eq. (2.27), we shall limit ourselves to the case when $m\le n$. This makes possible to evaluate the minima in the upper limits of the summations, and after applications of Eqs. (2.23) and some rearrangement we obtain

$$|\zeta,\{m,n\}\rangle = \frac{1}{\sqrt{n!m!}}\left[\sum_{l=0}^{n}\binom{n}{l}\left(-\frac{u}{v}\right)^l u^l v^{n-l}\right] \times\sum_{k=0}^{m}\sum_{l=0}^{n}\binom{m}{k}\binom{n}{l}u^k v^{m-k}\frac{n!k!}{(n-j)!(k-j)!j!}(-1)^j b^{m-k}a^{n-j}\left(-\frac{u}{v}b\right)^{k-j}|l_{00}(\gamma)\rangle\,. \quad (2.29)$$

Since the calculations can be applied to the opposite case with only minor modifications, we omit them for brevity. To further simplify Eq. (2.29), we evaluate the first sum (in the

square brackets) which is just a binomial expansion. Using the property $|u|^2 - |v|^2 = 1$, it gives us the factor $(-1/v)^n$. Eventually, we can write the squeezed Fock state as

$$|\zeta, \{m,n\}\rangle = F_{mn}(a,b)\,|l_{00}(\gamma)\rangle\,, \tag{2.30}$$

where $F_{mn}(a,b)$ is a polynomial function of its arguments and can be written as

$$F_{mn}(a,b) := \frac{1}{\sqrt{m!n!}}\frac{-1}{v^n}\sum_{k=0}^{m}\sum_{j=0}^{k}\binom{m}{k}u^k v^{m-k}\left(-\frac{u}{v}\right)^{k-j}\frac{n!k!}{(n-j)!(k-j)!j!}(-1)^j b^{m-j}a^{n-j}. \tag{2.31}$$

Again using the elementary property (1.54) of coherent states, for any polynomial function $F(a,b)$ we can write

$$F(a,b)\,|l_{00}(\gamma)\rangle = \mathcal{N}(\gamma)\int_{\mathbb{C}} F(\alpha,\alpha^*)\,\mathrm{e}^{-|\alpha|^2/\gamma^2}\,|\alpha\rangle|\alpha^*\rangle\,\mathrm{d}^2\alpha, \tag{2.32}$$

which we can therefore also apply to $F_{mn}(a,b)$. After some convenient rearrangements we get

$$F(\alpha,\alpha^*) = \frac{1}{\sqrt{m!n!}}\frac{\alpha^{*m-n}}{(-v)^{m+n}}\left(\frac{v}{u}\right)\sum_{k=0}^{m}\binom{m}{k}u^{2k}v^{2(m-k)}(-1)^{m-k} \times\sum_{j=0}^{k}\binom{k}{j}\frac{n!}{(n-j)!}\left(\frac{u}{v}\right)^{n-j}(\alpha\alpha^*)^{n-j}. \tag{2.33}$$

To combine the two finite sums we first introduce the variable $x := \frac{u}{v}\alpha\alpha^*$ and write the sum over j as

$$\sum_{j=0}^{k}\binom{k}{j}\frac{n!}{(n-j)!}x^{n-j} = \left(\frac{\mathrm{d}}{\mathrm{d}x}+1\right)^k x^n. \tag{2.34}$$

We substitute this expression back into Eq. (2.33) and discover the binomial expansion of

$$F_{mn}(\alpha,\alpha^*) = \frac{1}{\sqrt{m!n!}}\frac{\alpha^{*m-n}}{(-v)^{m+n}}\left(\frac{v}{u}\right)^n\left[u^2\left(\frac{\mathrm{d}}{\mathrm{d}x}+1\right)-v^2\right]^m x^n. \tag{2.35}$$

The expression in the square brackets simplifies to $(u^2\frac{\mathrm{d}}{\mathrm{d}x}+1)$, hence we can return to a more simple binomial expansion where the differential operator can be evaluated easily:

$$\begin{aligned}F_{mn}(\alpha,\alpha^*) &= \frac{1}{\sqrt{m!n!}}\frac{\alpha^{*m-n}}{(-v)^{m+n}}\left(\frac{v}{u}\right)^n\sum_{j=0}^{m}\binom{m}{j}u^{2j}\left(\frac{\mathrm{d}}{\mathrm{d}x}\right)^j x^n \\ &= \frac{1}{\sqrt{m!n!}}\frac{1}{(-v)^{m+n}}\sum_{j=0}^{m}\frac{m!n!}{(m-j)!(n-j)!j!}\alpha^{n-j}\alpha^{*m-j}.\end{aligned} \tag{2.36}$$

As mentioned in the beginning of the calculation, the above expression holds only for $m \le n$. For the other case ($m > n$) we find that the only difference is in the upper limit

of the sum over j. We can therefore combine the two cases, and express it in a more familiar form,

$$F(\alpha,\alpha^*)=\frac{1}{\sqrt{m!n!}}\left(-\frac{u}{v}\right)^{\frac{m+n}{2}}\sum_{j=0}^{\min\{m,n\}}(-1)^j\left(\frac{\alpha}{\sqrt{-uv}}\right)^m\left(\frac{\alpha^*}{\sqrt{-uv}}\right)^n, \tag{2.37}$$

consequently, we have shown that

$$\mathcal{N}(\gamma)F_{mn}(\alpha,\alpha^*)=\mathcal{N}_{mn}(\gamma)l_{mn}(\alpha/\sqrt{-uv},\alpha^*/\sqrt{-uv}). \tag{2.38}$$

Indeed, we have proven Eq. (2.22), since $\mu=\sqrt{-uv}$, as we have taken $\mathrm{e}^{i\vartheta}=-1$. This proves the unitary equivalence of the Laguerre-2D basis and the Fock basis, and hence the completeness of the Laguerre-2D basis.

2.1.4 Conclusions

The unitary equivalence of the Laguerre-2D basis and the Fock basis imply the completeness of the one-complex plane coherent state representation. We know that every state can be expanded as

$$|\psi\rangle=\sum_{mn}C_{mn}\,|l_{mn}(\gamma)^{\{\varrho\}}\rangle\,, \tag{2.39}$$

therefore, all $|\psi\rangle$ can be written as

$$|\psi\rangle=\int_{\mathbb{C}}f(\alpha,\alpha^*)\,|\mathrm{e}^{i\varrho_a}\,\alpha\rangle|\mathrm{e}^{i\varrho_b}\,\alpha^*\rangle\,\mathrm{d}^2\alpha, \tag{2.40}$$

where $f(\alpha,\alpha^*)=\sum_{mn}\mathcal{N}_{mn}(\gamma)C_{mn}\,\mathrm{e}^{-|\alpha|^2/\gamma^2}\,l_{mn}(\alpha,\alpha^*)$.

We note, however, that this sum over m and n may not exist in the ordinary sense, but it always exists as a distribution. This means that certain states can be represented by well-behaving analytical functions, but not some others. The representation can also be useful for the description of mixed states. This has been demonstrated in Ref. [147], where the one-complex plane coherent state approach of Ref. [88] has been generalised to a case when photon losses are present.

2.2 Entangled optical Schrödinger cat states

In the present section we consider multi-mode generalisations of the usual optical Schrödinger cats (1.69). We concentrate on symmetrical constructions obtained by discretising the continuous one-complex-plane coherent state representation at four symmetrically spaced phase-space points. The similar discretisation of the appropriate one-dimensional representation leads to the usual optical Schrödingercat states [149, 150]. After the discussion of preparation, we turn to the entanglement properties of these states, and calculate it directly in the non-orthogonal coherent state basis. We determine which superposition has the most entanglement for the whole range of the continuous parameter, and devise a teleportation protocol to demonstrate its potential.

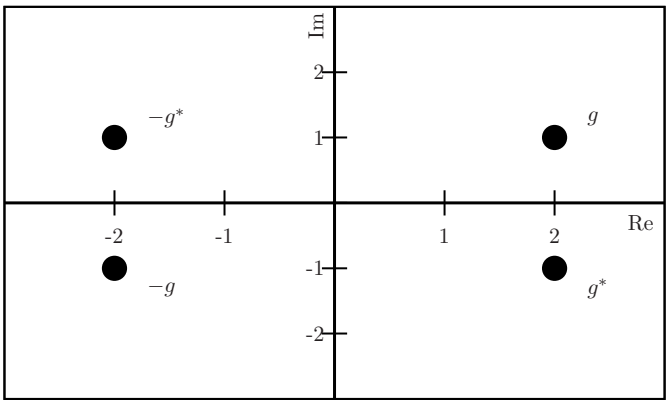

Figure 2.1: The four phase space points that correspond to the four coherent states which appear in the sum for the two-mode Schrödinger cat states. The weights of the coherent states are of equal magnitude, with possibly opposite signs. (Here the coherent amplitude is $g = 2 + i$.)

2.2.1 Two-mode Schödinger cat states by discretisation

Remarkably, if we consider the one-dimensional coherent state representation (1.72) of the squeezed vacuum, reducing the (continuous) integral to a discrete sum of appropriately chosen two terms we retain much of the original squeezing. A possible selection are the even Schrödinger cat states

$$|\alpha, +\rangle = \mathcal{N}_+(\alpha)^{-1}(|\alpha\rangle + |-\alpha\rangle) \tag{2.41}$$

introduced in Eq. (1.69). Interestingly $|\alpha, -\rangle$ has similar squeezing properties, however, is not related to the squeezed vacuum in a simple manner. Nevertheless, it is worthwhile to examine it from the point of view of discretised one-dimensional coherent state representations.

In a similar manner, we may consider discretisations of the one-complex-plane coherent state representation of the two-mode squeezed vacuum, and concentrate on the entanglement of the resulting states. For practical purposes, we consider states symmetric in the two modes. Since the representation contains the coherent state pairs $|\alpha\rangle$ and $|\alpha^*\rangle$, for a general α a similar and symmetrical superposition would involve four phase space points as depicted on Fig. 2.1. The natural superposition following the two-mode squeezed vacuum (2.19) is therefore

$$|g, ++++\rangle := \mathcal{N}_{++++}(g)^{-1}(|g^*\rangle|g\rangle + |g\rangle|g^*\rangle + |-g^*\rangle|-g\rangle + |-g\rangle|-g^*\rangle), \tag{2.42}$$

where the normalisation factor is $\mathcal{N}_{++++}(g) = 2\sqrt{2}\sqrt{\cosh(2|g|^2) + \cosh(2\,\mathrm{Re}\,g^2)}\,\mathrm{e}^{-|g|^2}$. A

straight-forward generalisation of the notation is

$$|g, s_1s_2s_3s_4\rangle := \mathcal{N}_{s_1s_2s_3s_4}(g)^{-1}[(-1)^{s_1}|g^*\rangle|g\rangle + (-1)^{s_2}|g\rangle|g^*\rangle + (-1)^{s_3}|-g^*\rangle|-g\rangle + (-1)^{s_4}|-g\rangle|-g^*\rangle], \quad (2.43)$$

where s_i are binary parameters, and the normalisation factor must be calculated accordingly. Of course, the parameters s_i are not completely independent: the freedom of selecting an arbitrary overall global phase must be taken into account. Note, that in the more general notation, the state $|g, ++++\rangle$ corresponds to $|g, 0000\rangle$.

On the other hand, not all combinations of s_i and g comply with our requirement of being symmetrical for the two modes. In fact there are two such combinations for arbitrary g: the above mentioned $|g, 0000\rangle$ and $|g, 0101\rangle$, together with their equivalents considering the global phase factor. There is no way to make the state symmetric if the number of 1's in the binary string $s_1s_2s_3s_4$ is odd. However, there are two superpositions $|g, 0011\rangle$ and $|g, 1001\rangle$ that yield such a solution for a pure real $g = x$, and pure imaginary $g = iy$, respectively. Indeed, the two resulting states

$$|x, 0011\rangle = 2\mathcal{N}_{0011}(x)^{-1}(|x\rangle|x\rangle - |-x\rangle|-x\rangle), \quad (2.44)$$

$$|iy, 1001\rangle = 2\mathcal{N}_{1001}(iy)^{-1}(|iy\rangle|-iy\rangle - |iy\rangle|-iy\rangle) \quad (2.45)$$

are locally equivalent to $\mathcal{N}_-(\sqrt{2}\alpha)^{-1}(|\alpha\rangle|\alpha\rangle - |-\alpha\rangle|-\alpha\rangle)$ which was considered in Refs. [94, 151]. This equivalence under local unitary operations shall become an important property when we consider entanglement.

2.2.2 Generation of two-mode Schrödinger cat states

In the present section, we shall demonstrate that the two-mode Schrödinger cat states (2.43) can be generated from two ordinary Schrödinger cat states (1.69) using a simple beam splitter. To begin, we consider a beam splitter (2.4) and its action on coherent states (1.77). It is straight-forward to apply these formulae on the input states

$$|\psi_{\text{in}}(\sigma_1, \sigma_2)\rangle = \mathcal{N}_{\sigma_1}(x)^{-1}\mathcal{N}_{\sigma_2}(y)^{-1}\left(|x\rangle + (-1)^{\sigma_1}|-x\rangle\right) \otimes \left(|iy\rangle + (-1)^{\sigma_2}|-iy\rangle\right), \quad (2.46)$$

and find that with $g := (x + iy)/\sqrt{2}$ we have

$$|g, 0000\rangle = U_R|\psi_{\text{in}}(00)\rangle, \quad (2.47a)$$

$$|g, 0101\rangle = U_R|\psi_{\text{in}}(11)\rangle, \quad (2.47b)$$

$$|g, 0011\rangle = U_R|\psi_{\text{in}}(01)\rangle, \quad (2.47c)$$

$$|g, 0110\rangle = U_R|\psi_{\text{in}}(10)\rangle. \quad (2.47d)$$

With the understanding that the parameters s_i are not independent, we discover that every two-mode Schrödinger cat state with even number of 1's in the binary string $s_1s_2s_3s_4$ can be generated this way.

2.2.3 Entanglement in a non-orthogonal basis

Evaluation of the entanglement of a pure state given in a non-orthogonal basis does not pose a conceptually difficult task. A standard solution is to find an orthogonal basis — using e.g. the Gram–Schmidt procedure — and simply solve the problem in that basis. For certain cases, however, this may obscure the underlying symmetry or other properties of the original problem, well exhibited in the non-orthogonal basis. In our case, for example, with countable non-orthogonal but linearly independent states, a direct method is more useful. In the following, we present a simple way to formulate the eigenvalue problem and hence the computation of the entanglement of a pure state.

Given a pure state $|\psi\rangle$ in two Hilbert spaces $\mathcal{H}_a$ and $\mathcal{H}_b$, to calculate its entanglement, we must compute the von Neumann entropy (1.98) of the reduced density operator $\varrho_a := \mathrm{Tr}_b\, |\psi\rangle\langle\psi|$,

$$E(|\psi\rangle) = S(\varrho_a) = -\,\mathrm{Tr}(\varrho_a \log_2 \varrho_a). \tag{2.48}$$

To evaluate Eq. (2.48), we essentially need to determine the eigenvalues λ_i of ϱ_a and use

$$E(|\psi\rangle) = -\sum_i \lambda_i \log_2 \lambda_i = H(\{\lambda_i\}). \tag{2.49}$$

Now the question is, how to solve the eigenvalue equation in a non-orthogonal basis.

Let our basis states be $|a_i\rangle \in \mathcal{H}_a$ $i = 0, 1, \ldots, N_a$ and $|b_i\rangle \in \mathcal{H}_b$ $i = 0, 1, \ldots, N_b$. Their non-orthogonality properties are completely characterised by the matrices

$$G^{(a)}_{kl} := \langle a_k | a_l \rangle\,, \quad \text{and} \quad G^{(b)}_{kl} := \langle b_k | b_l \rangle\,, \tag{2.50}$$

which we shall call *metric tensors* in the following. We chose a representation more suitable for our problem, and introduce the representation of elements and operators in $\mathcal{H}_a$ (same for $\mathcal{H}_b$) as

$$|x\rangle = \sum_k x_k\, |a_k\rangle\,, \quad \text{and} \quad A = \sum_{kl} A_{kl}\, |a_k\rangle\langle a_l|\,. \tag{2.51}$$

Note, that this is not the same as the usual representation, since e.g. $\langle a_i | x\rangle \neq x_i$. In this representation the scalar product can be written in terms of N_a dimensional vector algebra:

$$\langle x | y\rangle = \mathbf{x}^\dagger \mathbf{G} \mathbf{y}, \tag{2.52}$$

where † denotes the adjoint. Similarly, the action of an operator can be expressed using the metric tensors,

$$|y\rangle = A\, |x\rangle\,, \quad \text{with} \quad \mathbf{y} = \mathbf{A}\mathbf{G}\mathbf{x}, \tag{2.53}$$

given $\mathbf{x}$ and $\mathbf{y}$ are representations of $|x\rangle$ and $|y\rangle$, respectively. Hence we may write the eigenvalue equation in the similar algebraic form: the eigenvalues λ_i of A can be calculated from the equation

$$(\mathbf{A}\mathbf{G})\mathbf{x} = \lambda \mathbf{x}. \tag{2.54}$$

Indeed the eigenvectors $\mathbf{x}$ from Eq. (2.54) are representations (2.51) of the eigenstates of A.

It is straight-forward to apply this formalism to calculation of entanglement of a pure bipartite state. We write this state as

$$|\psi\rangle = \sum_{k,l} \psi_{kl} \, |a_k\rangle|b_l\rangle \, , \tag{2.55}$$

hence our density operator becomes $\varrho = \sum \psi_{ij}\psi^*_{kl} \, |a_i\rangle|b_j\rangle \, \langle a_k|\langle b_k|$, that yields the reduced density operator

$$\varrho_a = \mathrm{Tr}_b \, \varrho = \sum_{ik} \left(\sum_{jl} \psi_{ij}\psi^*_{kl} G^{(b)}_{lj} \right) |a_i\rangle\langle a_k| \, . \tag{2.56}$$

Therefore, according to Eq. (2.49), we must find the eigenvalues of the operator defined in the non-orthogonal basis with $A_{ik} := \sum \psi_{ij}\psi^*_{kl} G^{(b)}_{lj}$, or in matrix representation $\mathbf{A} := \boldsymbol{\psi}\mathbf{G}^{(b)*}\boldsymbol{\psi}^\dagger$. (In writing this expression, we have used the property $\mathbf{G}^* = \mathbf{G}^T$, where * denotes complex conjugate, and ^{T} denotes transposition.) To find these eigenvalues, we use Eq. (2.54), and obtain the entanglement of (2.55) in terms of the eigenvalues λ_i of the $N_a \times N_a$ complex matrix

$$R := \boldsymbol{\psi}\mathbf{G}^{(b)*}\boldsymbol{\psi}^\dagger\mathbf{G}^{(a)}. \tag{2.57}$$

These eigenvalues can then be determined using simple algebra, either by analytical or numerical methods, depending on the complexity of the problem.

2.2.4 Entanglement of two-mode Schrödinger cat states

We calculate the entanglement of the two-mode Schrödinger cat states (2.43) using Eq. 1.103, which calls for determining the eigenvalues of the reduced density matrix. The main result Eq. (2.57) of the previous section can be used to do this efficiently. The dimensionality of the problem is 4×4, and we enumerate the basis states as

$$\begin{aligned} |a_1\rangle &:= |g\rangle \, , & |a_2\rangle &:= |g^*\rangle \, , \\ |a_3\rangle &:= |-g\rangle \, , & |a_3\rangle &:= |-g^*\rangle \, . \end{aligned} \tag{2.58}$$

Similar definitions with $|b_i\rangle$ also work for the second mode, hence in the notation of the previous section we have $\mathbf{G}^{(a)} = \mathbf{G}^{(b)}$. The matrix elements can be obtained by using Eq. (1.61).

Before blindly starting to solve the eigenvalue problem for all states in Eq. (2.47), let us pause for a moment and examine the entanglement properties of $|g, 0011\rangle$ and $|g, 1001\rangle$. We know from the theory of entanglement that if there exist local operations that transform one state into the other, their entanglement properties are the same. Also, since we are dealing with a manifold of states (parametrised by g), if there exist some mapping F on g that transforms one state into the other, the two manifolds have similar entanglement properties, and to go from one to another we just need to change our coordinate system using this mapping F. Indeed, a combination of these two bears

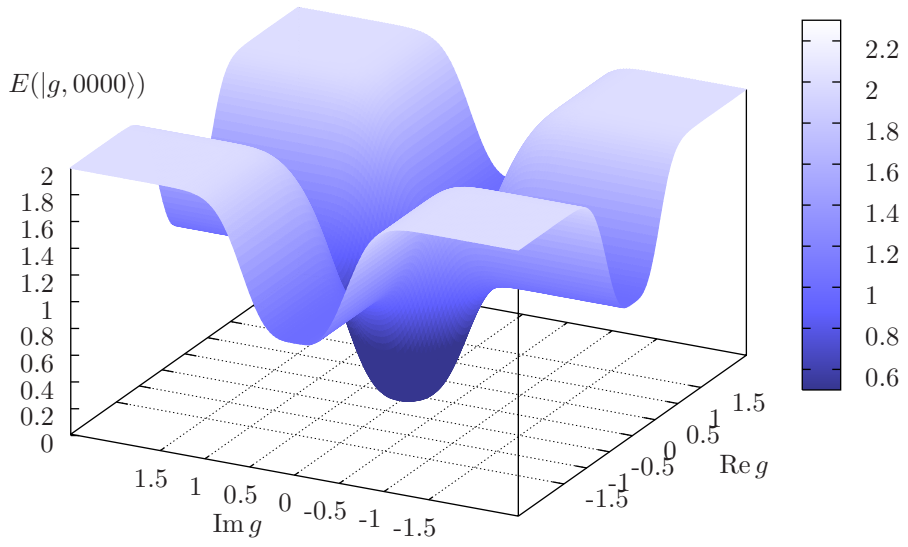

Figure 2.2: Entanglement of the two-mode Schrödinger cat state $|g, 0000\rangle$ in ebits. We observe that it starts from 0 at the origin and reaches almost 2 ebits for large amplitudes far from the axes, however, shows half the entanglement in the vicinity of the two axes.

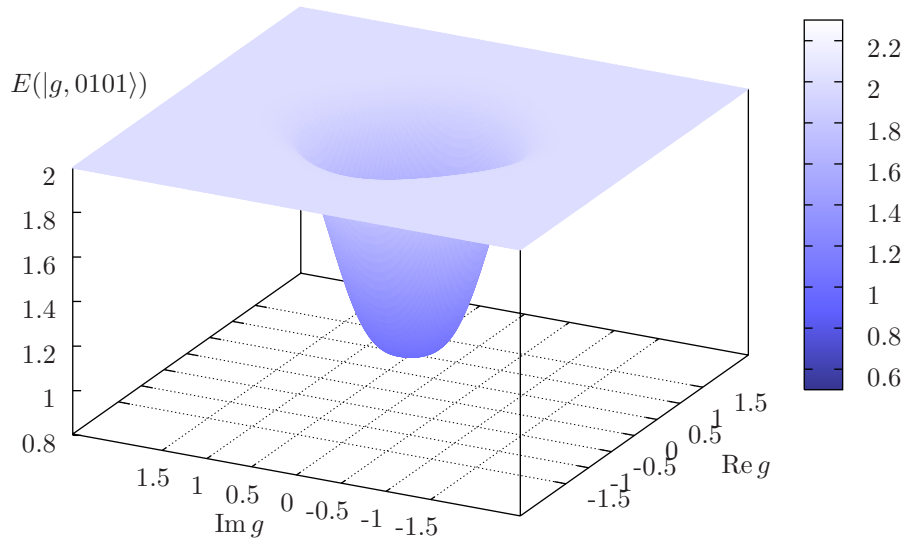

Figure 2.3: Entanglement of the two-mode Schrödinger cat state $|g, 0101\rangle$ in ebits. This class of states exhibit the most entanglement. The entanglement of these states ranges from 1 to 2 ebits, therefore they could be used in a conditional teleportation of 2 qubits with high efficiency.

fruit in our case: it can be shown that $|ig, 0011\rangle$ is equivalent to $|g, 1001\rangle$ up to the local unitary operation $\exp(i\pi a^\dagger a)\,|\alpha\rangle|\beta\rangle = |-\alpha\rangle|\beta\rangle$.

After this lesson, we proceed to solve the eigenvalue problems yielded by the states $|g, 0000\rangle$, $|g, 0011\rangle$ and $|g, 0101\rangle$. It turns out that the eigenvalue problem can be solved exactly. For example, for $|0101\rangle$ there are two, doubly degenerate eigenvalues

$$\lambda_\pm = N\left\{\exp(-4|g|^2 + 2\,\mathrm{Re}\,g^2) + \exp(2\,\mathrm{Re}\,g^2) - \exp(2|g|^2) - \exp(-2|g|^2 + 4\,\mathrm{Re}\,g^2)\right.$$
$$\left. \pm \exp(-2|g|^2)\left[\exp(2\,\mathrm{Re}\,g^2) - 2\,\mathrm{Cosh}\,2g^2\right]\right\}, \quad (2.59)$$

where N has been introduced for simplicity, and plays the role of a normalisation factor necessary for fulfilling $2\lambda_+ + 2\lambda_- = 1$. The expressions of eigenvalues for the other two states are more lengthy, and provide little insight on their own. Much more instructive are the plots of their entanglement on Figs. 2.2–2.4.

The entanglement of each two-mode Schrödinger cat state calculated according to Eq. 1.103 is plotted on Figs. 2.2–2.4, which allows a good visual assessment of the applicability of the respective states. Note, that although the Hilbert space is infinite dimensional, we only work in a subspace spanned by four explicitly given coherent states, therefore the maximum entanglement we can expect is 2 ebits. Indeed, for special choices of g the dimensionality may reduce to only two (e.g. when $g = g^*$), which corresponds to

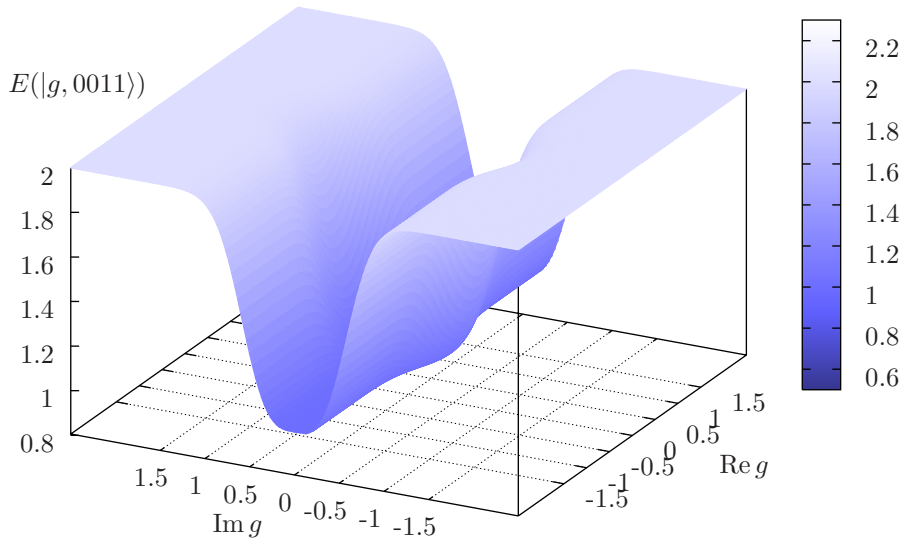

Figure 2.4: Entanglement of the two-mode Schrödinger cat state $|g, 0011\rangle$ in ebits. This class of states show a stable 1 ebit entanglement along the real axis, therefore these states (more precisely states equivalent to these) have found application earlier in the literature.

1 ebit of maximal entanglement. As we can observe on the plots, all three states exhibit entanglement arbitrary close to 2 ebits for certain parameter ranges.

It is clear from the plots, that the most entanglement is exhibited by $|g, 0101\rangle$ (Fig. 2.3). For sufficiently large amplitudes, its entanglement is arbitrarily close to the maximum. It must be noted, however, that $|g, 0101\rangle = 0$ when g is real or pure imaginary, hence the entanglement function $E(|g, 0101\rangle)$ is discontinuous at the axes. However, this discontinuity can be removed since the function has the same limit, independently from which side of the axis we approach to the discontinuity. Another nice property of this class of states is that

$$E(|g, 0101\rangle) > 1 \qquad \text{(almost everywhere)}, \tag{2.60}$$

hence it can always be used for (conditional) teleportation of up to two quantum bits. In this respect, $|g, 0000\rangle$ (Fig. 2.2) can be regarded as the least useful state of all three, since for small $|g|$, its entanglement drops below 1 ebit, and eventually reaches 0 at $g = 0$. The third state, $|g, 0011\rangle$, is also highly entangled, with the property that on the real axis its entanglement is exactly 1 ebit, and due to the degeneracy of the basis states (2.58) this indicates a maximally entangled state. Hence with $\mathrm{Im}\, g = 0$ it allows for *exact* teleportation of 1 qubit (but no more). As it has been mentioned earlier, this is the property that has been exploited in Ref. [94].

2.2.5 Teleportation using the four-qubit Schrödinger cat states

According to the previous section, the states in (2.47) exhibit more than 1 ebit of entanglement for certain parameters, hence they can be used in a 2 qubit quantum teleportation scheme. However, since their entanglement is never equal to 2 ebits, the protocol can only be conditional. For our setup we select $|g, 0101\rangle$ as our quantum channel, and we determine the optimal measurement for this non-maximally entangled resource based on the ideas of the anti-linear operator method of Ref. [140].

The formalism that we shall use in the following has been formulated on basis independent ground. However, since we intend to apply the machinery to a specific case, which happens to be most conveniently described in the non-orthogonal basis (2.58), we decided to drop basis independence. This also makes the anti-linearity condition unnecessary. However, the formal results of [140] remain valid as long as we do not change our initial basis.

To characterise our input state, we define the 4×4 matrix

$$\mathbf{C} = \begin{pmatrix} 0 & 1 & 0 & 0 \\ -1 & 0 & 0 & 0 \\ 0 & 0 & 0 & 1 \\ 0 & 0 & -1 & 0 \end{pmatrix} \tag{2.61}$$

acting on the basis (2.58). This corresponds to the operator L of the anti-linear formalism since our (unnormalised) entangled state can be expressed as

$$|g, 0101\rangle = \sum_i |a_i\rangle \sum_j C_{ji} |a_i\rangle . \tag{2.62}$$

Incidentally, after bringing both sums to the front we see that this definition is in accordance with the definitions (2.51), but this is now valid for a bipartite system.

As we have previously demonstrated on examples of quantum teleportation (Sec. 1.5), Bob has to apply a unitary transformation to fully recover the input state. What unitary he has to apply depends on the measurement outcome obtained by Alice. In a special case, the unitary operation is the identity, or it only differs from it by an irrelevant phase factor. The state to which this projection was made has therefore a special role, hence we shall call it ideally matching Bell state.

In a fashion similar to (2.62) let $|\text{Bell}\rangle = \sum B_{ij} |a_i\rangle |a_j\rangle$ denote our ideally matching Bell state. Similarly for the single party system, we can use the coefficient matrices to represent our states. In this formalism, the ideally matching Bell state $|\text{Bell}\rangle$ can be expressed as

$$\mathbf{B} = (\mathbf{G}^T \mathbf{C}^T \mathbf{G})^{-1}. \tag{2.63}$$

The formula can be evaluated analytically, and gives us a matrix with 8 non-zero elements. The calculations are straight-forward but give a rather lengthy result. A great simplification can be made, however, when

$$\cos(2 \operatorname{Im} g^2) = 1, \tag{2.64}$$

since this makes four more elements vanish. In addition, the other elements also get significantly simplified, and the ideally matching Bell state turns out to be the same as the entangled resource:

$$|\mathrm{Bell}\rangle = |g, 0101\rangle\,. \tag{2.65}$$

Now the restriction $\cos(\mathrm{Im}\, g^2) = 1$, which actually implies (2.64), allows for a convenient definition of an orthogonal basis

$$\begin{aligned} |e_0\rangle &= \mathcal{N}_0(g)(|g\rangle + |g^*\rangle - |-g\rangle - |-g^*\rangle), \qquad & |e_2\rangle &= \mathcal{N}_2(g)(|g\rangle + |g^*\rangle + |-g\rangle + |-g^*\rangle), \\ |e_1\rangle &= \mathcal{N}_1(g)(|g\rangle - |g^*\rangle - |-g\rangle + |-g^*\rangle), \qquad & |e_3\rangle &= \mathcal{N}_3(g)(|g\rangle - |g^*\rangle + |-g\rangle - |-g^*\rangle), \end{aligned} \tag{2.66}$$

using simple superpositions of our coherent-basis states reminiscent of the Schrödinger cat states (1.69). The normalisation factors here in Eq. (2.66) may be expressed as:

$$\mathcal{N}_s(g) = \mathcal{N}_{\sigma_1}(\mathrm{Re}\, g^2)\mathcal{N}_{\sigma_0}(\mathrm{Im}\, g^2), \tag{2.67}$$

where $\sigma_1\sigma_0$ denotes the binary string representation of s, i.e. $s = 2\sigma_1 + \sigma_0$, and we use the natural identifications $\mathcal{N}_+(\alpha) \equiv \mathcal{N}_0(\alpha)$ and $\mathcal{N}_-(\alpha) \equiv \mathcal{N}_1(\alpha)$. Later we shall see why the orthogonality of these states is important.

Now that we have obtained the ideally matching Bell state explicitly, we can use it as a starting point to obtain other states that yield successful teleportation. Since our entangled resource is only partially entangled, our teleportation must be conditional, i.e. the states corresponding to successful teleportation do not form a complete basis in our bipartite Hilbert space.

To construct a good approximation to a Bell basis, we first consider a possible setup for a projection onto the ideally matched Bell state. This case we have an easy task: we only need to reverse the scheme which generates the two-mode Schrödinger cat state $|g, 0101\rangle$. This scheme has been already discussed in Sec. 2.2.2, and the conclusion there was that we need two Schrödinger cats and a $50-50\%$ beam splitter. If we include the generation of the entangled pair in the teleportation scheme, then the detection part can be understood as consisting of the similar beam splitter, but turned around by 180^o. This setup is depicted on Fig. 2.5.

If we consider the setup on Fig. 2.5 with an input state

$$|\psi_{\mathrm{in}}\rangle = A_1\,|g\rangle + A_2\,|g^*\rangle + A_3\,|-g\rangle + A_4\,|-g^*\rangle\,, \tag{2.68}$$

and look at the states after the BS_2 beam splitter transformation, we get in the modes A, B and c

$$\begin{aligned} |\psi_1\rangle_{ABc} = \frac{1}{4}\mathcal{N}_{0101}(g)^{-1}\,[&\mathcal{N}_{\mathrm{res}}^{-1}\,|\psi_{\mathrm{res}}\rangle_{ABc} + \\ &- \mathcal{N}_+(x)\mathcal{N}_+(y)\,|x,+\rangle_A\,|iy,+\rangle_B\,T_1\,|\psi_{\mathrm{in}}\rangle_c - \mathcal{N}_+(-)\mathcal{N}_+(y)\,|x,-\rangle_A\,|iy,+\rangle_B\,T_2\,|\psi_{\mathrm{in}}\rangle_c \\ &- \mathcal{N}_+(x)\mathcal{N}_-(y)\,|x,+\rangle_A\,|iy,-\rangle_B\,T_3\,|\psi_{\mathrm{in}}\rangle_c - \mathcal{N}_-(x)\mathcal{N}_-(y)\,|x,-\rangle_A\,|iy,-\rangle_B\,T_4\,|\psi_{\mathrm{in}}\rangle_c \\ &- \mathcal{N}_+(y)\mathcal{N}_+(x)\,|iy,+\rangle_A\,|x,+\rangle_B\,T_5\,|\psi_{\mathrm{in}}\rangle_c - \mathcal{N}_+(y)\mathcal{N}_-(x)\,|iy,+\rangle_A\,|x,-\rangle_B\,T_6\,|\psi_{\mathrm{in}}\rangle_c \\ &-\mathcal{N}_-(y)\mathcal{N}_+(x)\,|iy,-\rangle_A\,|x,+\rangle_B\,T_7\,|\psi_{\mathrm{in}}\rangle_c - \mathcal{N}_-(y)\mathcal{N}_-(x)\,|iy,-\rangle_A\,|x,-\rangle_B\,T_8\,|\psi_{\mathrm{in}}\rangle_c]\,, \end{aligned} \tag{2.69}$$

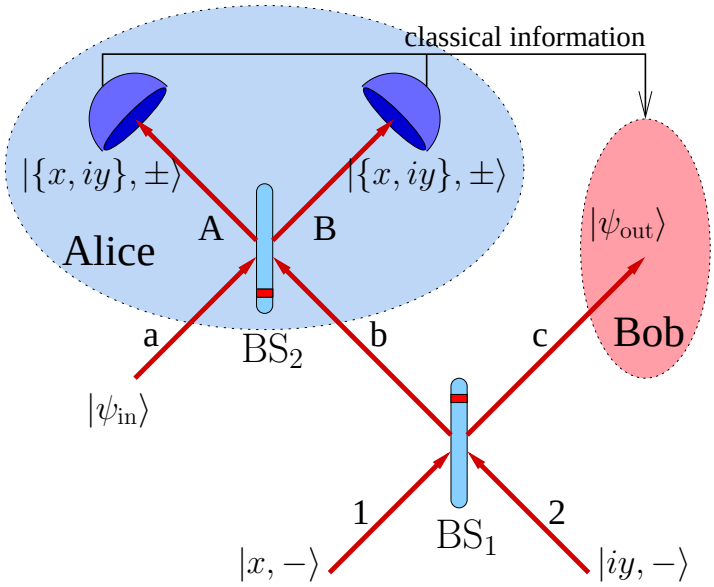

Figure 2.5: Teleportation scheme for teleporting four coherent state qubits. The input state can be written written $A_1 |g\rangle + A_2 |g^*\rangle + A_3 |-g\rangle + A_4 |-g^*\rangle$, the entangled state is the two-mode Schrödinger cat state $|g, 0101\rangle$. The detectors symbolise Schrödinger cat discriminators.

where $\mathcal{N}_\pm(\alpha)$ is given after Eq. (1.69), and the operators T_i correspond to the transfer operator of teleportation. For the sake of simplicity we give the matrix representation of these operators. In a representation that corresponds to the product matrix $\mathbf{AG}$ of Eq. (2.53), these can be written:

$$\mathbf{T}_1 = \text{Diag}(1, -1, 1, -1),\ \mathbf{T}_2 = \text{Diag}(1, -1, -1, 1),\ \mathbf{T}_3 = \text{Diag}(1, 1, -1, -1),\ \mathbf{T}_4 = \mathbb{1}, \tag{2.70}$$

and

$$\mathbf{T}_j = \begin{pmatrix} 0 & 0 & 1 & 0 \\ 0 & 0 & 0 & 1 \\ 1 & 0 & 0 & 0 \\ 0 & 1 & 0 & 0 \end{pmatrix} \mathbf{T}_{j-4}, \qquad \text{when } j > 4, \tag{2.71}$$

where Diag represents the diagonal matrix with the specified elements appearing on the diagonal in the specified order. We note, that for a representation that is fully conforming to that given in Eq. (2.51), we would need to consider the matrices $\mathbf{T}_j \mathbf{G}^{-1}$. If we choose to represent the transfer operators T_j in the orthogonal basis (2.66), we obtain

$$\tilde{\mathbf{T}}_j = \text{Diag}(\mathcal{N}_0, \mathcal{N}_1, \mathcal{N}_2, \mathcal{N}_3) \mathbf{P}_j \,\text{Diag}(1/\mathcal{N}_0, 1/\mathcal{N}_1, 1/\mathcal{N}_2, 1/\mathcal{N}_3), \tag{2.72}$$

where P_j are related to pairwise permutation matrices as

$$\mathbf{P}_1 = \mathbf{P}_{01}\mathbf{P}_{23}, \quad \mathbf{P}_2 = \mathbf{P}_{03}\mathbf{P}_{12}, \quad \mathbf{P}_3 = \mathbf{P}_{02}\mathbf{P}_{13}, \quad \mathbf{P}_4 = \mathbb{1}, \tag{2.73}$$

and $\mathbf{P}_j = \mathrm{Diag}(1,1,-1,-1)\mathbf{P}_{j-4}$ when $j > 4$. Here we have used $\mathbf{P}_{kl}$ to denote permutation of the coefficients corresponding to the basis states $|e_k\rangle$ and $|e_l\rangle$.

Now under what conditions, can we revert the operations T_j unitarily? First we note that the relationship between T_{j+4} and T_j ($j \leq 4$) is indeed unitary as it corresponds to a π rotation in the phase space. This means that we only need to consider the first four of the T_j operators. It is clear that since T_4 is the identity operator, for two measurement events we can reconstruct the input state with perfect fidelity for any g that complies with the general restriction Eq. (2.64). We can get more insight into which other transformations allow perfect reconstruction by considering Eq. (2.72) and using the orthogonality of the basis (2.66). Since $\mathbf{P}_j$ are simply permutation matrices, it suffices to consider the normalisation factors $\mathcal{N}_j$. The type of conditions that need to be fulfilled are pairwise

$$\mathcal{N}_k/\mathcal{N}_l = \mathcal{N}_l/\mathcal{N}_k \quad \text{and} \quad \mathcal{N}_{\bar{k}}/\mathcal{N}_{\bar{l}} = \mathcal{N}_{\bar{l}}/\mathcal{N}_{\bar{k}}, \tag{2.74}$$

where $k \neq l$ and $\bar{k} \neq k,l$ and $\bar{l} \neq k,l,\bar{k}$. Due to the properties of the cosh and sinh functions, this can only be fulfilled for $g \to \infty$. This is, however, not surprising since our quantum channel consists of a partially entangled state, and such states do not allow perfect teleportation.

In the light of the above, we see that only two terms of Eq. (2.69) allow for perfect teleportation. In fact, these are the only terms that require the simultaneous measurement of two odd coherent states. Since the residual contribution $|\psi_{\mathrm{res}}\rangle$ can be shown to have the form

$$|\psi_{\mathrm{res}}\rangle = |0\rangle_A |\psi_{\mathrm{res}}^{Bc}\rangle_{Bc} + |0\rangle_B |\psi_{\mathrm{res}}^{Ac}\rangle_{Ac} \tag{2.75}$$

we have no contribution to the output state from $|\psi_{\mathrm{res}}\rangle$ in case we obtain by measurement the desired pair of odd coherent states. Therefore, it can be easily verified using the identity $\mathcal{N}_{0101}(g) = \mathcal{N}_-(x)\mathcal{N}_-(y)$ that the probability of successful teleportation is $1/8$.

It is worthwhile to mention that although this setup is not optimal since the probability of successful teleportation approaches only $1/2$ instead of the desired 1, it consists of simple elements which can be easily implemented, or as in the case of detecting Schrödinger cats, well approximated.

2.2.6 Conclusions

We have seen that coherent state qubits can be generalised to four dimensions using a recipe that might be easily generalised further. We have developed a formalism for working in a non-orthogonal basis that has proved to be handy for the calculation of entanglement of pure states. The study of a certain class of relatively easily preparable entangled states, termed two-mode Schrödinger cat states, yielded a simple teleportation scheme with a $1/8$ success probability. We note that the success probability may be increased by using a different measurement protocol, however, unconditional teleportation is not possible since the state used for quantum channel is never maximally entangled.

2.3 Decoherence and distinguishablity of optical Schrödinger cat states

In the previous section we have studied the representation problem of coherent state quantum bits. One of our findings was that it is possible to work in a non-orthogonal basis, e.g. coherent states, and the added overhead to calculations may well be compensated by the advantage we gain by using a representation that is natural to the particular system. On the other hand, at the read-out stage of a quantum algorithm, the output state is generally projected onto an orthogonal basis. The most suggestive choice of orthogonal basis for a coherent state qubit consist of the Schrödinger cat states (1.69) used extensively in the previous section.

The distinction between "internal" representation used during computation, and "external" representation used at the read-out may sound artificial at first. However, it is well justified, if we consider the fact that during computation every effort is made to isolate the system from the surroundings, whereas during the read-out process, information about the quantum state is transferred to the environment.

In the present section we shall be concerned exclusively with the read-out problem of coherent state quantum bits. We shall consider a scenario which is similar to that in the Deutsch and Deutsch–Jozsa algorithms; that is we seek an answer which is either "yes" or "no" and hence the output of such a computation is always exactly one of the basis states. In such a scenario superpositions of computational basis states are not expected to appear at the output.

Under these conditions, we need only to be concerned about distinguishing the two basis states from each other using the measurement outcomes. The degree to which this distinction can be accurate can be calculated using the quantum version of Sanov's theorem, that uses quantum relative entropy (see Sec. 1.6.3).

2.3.1 Decoherence model

We consider a decoherence model where the source of decoherence is the interaction of our quantum bit in the signal mode with an environment modelled by a single mode bosonic field. We use a model often used in optics to describe inefficient detection. In this scheme the interaction with the environment is represented by highly transparent beam splitter as depicted on Fig. 2.6. The environmental bosonic mode is usually considered to be a thermal state, that in the case of an optical mode, can generally be regarded being the vacuum. There are more sophisticated models for loss, derived e.g. from investigation of dispersing and absorbing media [152, 153] that allow a phononic interpretation of the environmental mode. In many of the cases, however, the simple model with a single beam splitter is satisfactory (c.f., for instance Ref. [147]).

Therefore, for the sake of simplicity we stick to the beam splitter model, and assume that the state of environment is somewhat under our control. In this approach we assume having no control over the interaction between the environment and the quantum bit,

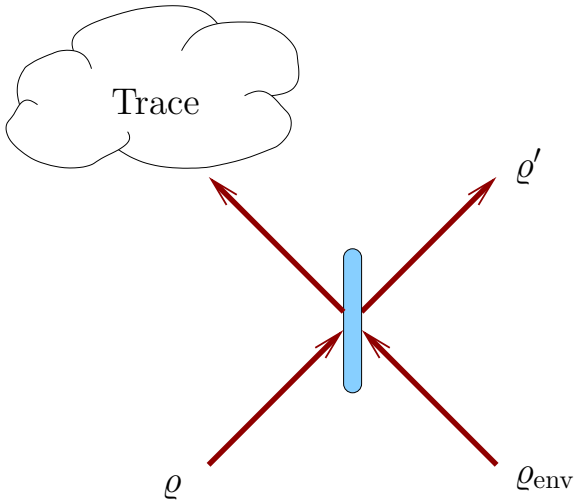

Figure 2.6: The model for loss. The signal mode interferes with an auxiliary "environmental" mode on a nearly transparent beam splitter.

however, we can apply squeezing to the immediate environment. Whether squeezing is a viable option in a particular setup or not, would require a specific study in each case. But as a general remark, we add that squeezed light is a cheap resource that may be used e.g. to influence the state of phononic modes in a system similar to that studied in Refs. [152, 153]. Other examples of using squeezing to suppress noise may be found in Ref. [154] and references therein.

Since we consider a squeezed vacuum state for the environment, the phase relations in the system become important. Therefore we consider the beam splitter parameters as $t = \mathrm{e}^{i\varphi_t}\cos\tau$ and $r = \mathrm{e}^{i\varphi_r}\sin\tau$, where the modulus of the transmittance is $|t| \approx 1$ that corresponds to a weak interaction with the environment.

To calculate the state of our qubit after decoherence we adopt the one-dimensional coherent state representation of the squeezed vacuum. Using Eqs. (1.72) and (1.69) we can express the possible states of the system including the environment and the quantum bit before the interaction as

$$|\psi_s^{\mathrm{in}}\rangle = |\alpha, s\rangle|Sq, \zeta\rangle = \tilde{\mathcal{N}}_s^{-1}(\alpha,\gamma)\sum_{\lambda=\pm1}\lambda^s\int_{\mathbb{R}}\mathrm{e}^{-\gamma x^2}\,|\lambda\alpha\rangle|x\,\mathrm{e}^{i\varphi}\rangle\,\mathrm{d}x. \tag{2.76}$$

The squeezing parameters γ and φ can be expressed using the Radmore and Barnett notation [116] as $\gamma = 1/\left(\exp(2|\zeta|) - 1\right)$ and $\varphi = \arg(\zeta)/2 + \pi$. The normalisation factor is $\tilde{\mathcal{N}}_s(\alpha,\gamma) = \mathcal{N}_s(\alpha)\mathcal{N}(\gamma)$, where $\mathcal{N}(\gamma)^2 = \pi/\sqrt{\gamma^2+\gamma}$.

In coherent state representation it is easy to describe the action of the beam splitter since coherent states interfere the same way as classical fields: the output amplitude for each coherent state pair is the sum of the transmitted and reflected amplitudes. To obtain the state remaining from the Schrödinger cat after the interference, this output density operator must be traced out for the environment mode. Hence that density operator for

the state the output mode of the beam splitter with $|\alpha, s\rangle$ on the input reads

$$\varrho_s = \tilde{\mathcal{N}}_s(\alpha,\gamma)^{-2} \sum_{\lambda,\nu=\pm1} (\lambda\nu)^s \int_{\mathbb{R}^2} \mathrm{e}^{-\gamma x^2}\, \mathrm{e}^{-\gamma y^2}\, \langle -\nu r^*\alpha + t^*\, \mathrm{e}^{i\varphi}\, y| - \lambda r^*\alpha + t^*\, \mathrm{e}^{i\varphi}\, x\rangle \times |\lambda t\alpha + r\, \mathrm{e}^{i\varphi}\, x\rangle\langle \nu t\alpha + r\, \mathrm{e}^{i\varphi}\, y|\, \mathrm{d}x\, \mathrm{d}y, \quad (2.77)$$

where the complex numbers r and t stand for the reflectance and transmittance of the beam splitter, including phase shifts as defined earlier. In our interpretation, we can make measurements on the density operator ϱ_s when the result of the algorithm was $|\alpha, s\rangle$. To be able to decide which state was the actual result, the two density operators we have to able to distinguish the ϱ_0 and ϱ_1 from each other. In the following we shall calculate this distinguishablity. For aesthetic purposes, we shall use the notation $\varrho_0 \equiv \varrho_+$ and $\varrho_1 \equiv \varrho_-$ for the two density operators in Eq. (2.77).

2.3.2 Calculation of distinguishablity

As mentioned earlier, the quantification of distinguishablity of two quantum states is possible using the quantum Sanov theorem. This theorem tells us the distinguishablity based on a series of measurements on the same quantum state. This approach is suitable for our purposes since we consider a deterministic algorithm that may be repeated as many times as we wish.

The quantum Sanov theorem has already been briefly introduced in Sec. 1.6.3. Using the reasoning there, to obtain the probability of not being able to distinguish the two outcomes ϱ_+ and ϱ_- we have to calculate the relative entropies $S(\varrho_\pm \| \varrho_\mp)$ and consider the smaller.

In order to calculate relative entropy we take its power series around the identity. For two arbitrary density matrices ϱ and ϱ', this reads

$$S(\varrho\|\varrho') = \sum_{n=1}^{\infty} \sum_{k=1}^{n} \binom{n}{k} \frac{(-1)^k}{n} \left(\operatorname{Tr} \varrho \varrho'^k - \operatorname{Tr} \varrho^{k+1} \right). \quad (2.78)$$

Considering the density matrices ϱ_s and $\varrho_{s'}$ of a pair of Schrödinger cat states after decoherence, the two traces in Eq. (2.77) produce a sum of Gaussian integrals:

$$\operatorname{Tr}\{\rho_s \rho_{s'}^k\} = \tilde{\mathcal{N}}_s(\alpha,\gamma)^{-2} \tilde{\mathcal{N}}_{s'}(\alpha,\gamma)^{-2k} \sum_{\lambda_1,\nu_1=\pm1} (\lambda_1\nu_1)^s \times \sum_{\lambda_2,\nu_2=\pm1} (\lambda_2\nu_2)^{s'} \cdots \sum_{\lambda_{k+1},\nu_{k+1}=\pm1} (\lambda_{k+1}\nu_{k+1})^{s'} G_{k+1}(\lambda_1,\nu_1,\ldots,\lambda_{k+1},\nu_{k+1}), \quad (2.79)$$

where, assuming modulo k on all indices, we have

$$G_k(\{\lambda_i\},\{\nu_i\}) = \int_{\mathbb{R}^{2k}} \prod_{l=1}^{k} \exp\left[-\gamma(x_l^2 - y_l^2)\right] \langle -\nu_l r^*\alpha + t^*\, \mathrm{e}^{i\varphi}\, y_l| - \lambda_l r^*\alpha + t^*\, \mathrm{e}^{i\varphi}\, x_l\rangle \times \langle \nu_l t\alpha + r\, \mathrm{e}^{i\varphi}\, y_l|\lambda_{l+1} t\alpha + r\, \mathrm{e}^{i\varphi}\, x_{l+1}\rangle\, \mathrm{d}^k x\, \mathrm{d}^k y. \quad (2.80)$$

To simplify the following formulae we shall pack the variables such as x_l and y_k into single vectors as the following:

$$(\mathbf{x})_i := \begin{cases} x_i, & \text{if } i \leq k \\ y_{i-k}, & \text{otherwise} \end{cases}, \quad (\boldsymbol{\lambda})_i := \begin{cases} \nu_i, & \text{if } i \leq k \\ \lambda_{i-k}, & \text{otherwise} \end{cases}, \quad \theta_i := \begin{cases} 1 & \text{if } i \geq 0 \\ 0 & \text{otherwise} \end{cases}, \tag{2.81}$$

Since this introduces a little complication with the indices, we use the short-hand notation $[n]_k$ for $n \mod k$. Now we can expand the coherent state products in Eq. (2.80), and with

$$\begin{aligned} (\mathbf{A})_{lm} &= -\left(\gamma + \frac{1}{2}\right)\delta_{lm} + |t|^2\theta(k-m)\delta_{l,m+k} + |r|^2\theta(k-m)\delta_{l,[m-1]_k+k}, & \text{(2.82a)} \\ (\mathbf{b})_l &= \theta_{k-l}(\lambda_{[l-1]_k} - \lambda_l)rt^*\alpha^*\,\mathrm{e}^{i\varphi} + \theta_{l-(k+1)}(\lambda_{k+[l-k+1]_k} - \lambda_l)r^*t\alpha\,\mathrm{e}^{-i\varphi}, & \text{(2.82b)} \\ c &= \sum_{l=1}^{k}\left(\lambda_l\lambda_{[l+k+1]_k+k}|r|^2 + \lambda_l\lambda_{l+k}|t|^2\right)|\alpha|^2 - k|\alpha|^2, & \text{(2.82c)} \end{aligned}$$

and $\mathbf{Q} = \frac{1}{2}(\mathbf{A} + \mathbf{A}^T)$, we can express it as

$$G_k(\boldsymbol{\lambda}) = \int_{\mathbb{R}^{2k}} \exp\left[\mathbf{x}^T\mathbf{A}\,\mathbf{x} + \mathbf{b}^T\mathbf{x} + c\right]\mathrm{d}^{2k}\mathbf{x} = \frac{\pi^k}{\sqrt{\det\mathbf{Q}}}\,\mathrm{e}^{-\frac{1}{4}\mathbf{b}^T\mathbf{Q}^{-1}\mathbf{b}+c}\,. \tag{2.83}$$

Using this result and Eqs. (2.78) and (2.79) we obtain the relative entropy of two Schrödinger cat states undergone decoherence ϱ_s and $\varrho_{s'}$ as

$$S(\rho_s\|\rho_{s'}) = \sum_{n=1}^{\infty}\frac{1}{n}\sum_{k=1}^{n}\binom{n}{k}\frac{(-1)^k\pi^{k+1}}{\sqrt{\det\mathbf{Q}}}F_k, \tag{2.84}$$

where

$$\begin{aligned} F_k = &\sum_{\boldsymbol{\lambda}\in\{\pm1\}^{2k+2}} \tilde{\mathcal{N}}_s(\alpha,\gamma)^{-2}(\lambda_{k+1}\lambda_{2k+2})^s \\ &\times\left[\tilde{\mathcal{N}}_{s'}(\alpha,\gamma)^{-2k}\prod_{l=1}^{k}(\lambda_l\lambda_{k+1+l})^{s'} - \tilde{\mathcal{N}}_s(\alpha,\gamma)^{-2k}\prod_{l=1}^{k}(\lambda_l\lambda_{k+1+l})^{s}\right]\mathrm{e}^{-\frac{1}{4}\mathbf{b}^T\mathbf{Q}^{-1}\mathbf{b}+c}\,. \end{aligned} \tag{2.85}$$

The series expansion in equation (2.84) is convergent in norm, and its evaluation is straight-forward on a computer. The data plots presented in this dissertation are results from such evaluation. We note that for $|\alpha| \ll 1$, the convergence of the series in equation (2.84) is slow. Our method is suitable for larger values of $|\alpha|$, which are anyway the physically more interesting cases. Therefore the $|\alpha|$ scales of the figures start at 1.

2.3.3 Optimal parameters for conserving distinguishablity

For simplicity, in what follows, the two relative entropies of interest will be denoted by $S(+\|-)$ and $S(-\|+)$, respectively. For the plots we chose the beam splitter transmittance to be 0.95. At smaller values of transmittance (i.e. higher loss), the behaviour of the entropies are similar, but the actual values are smaller.

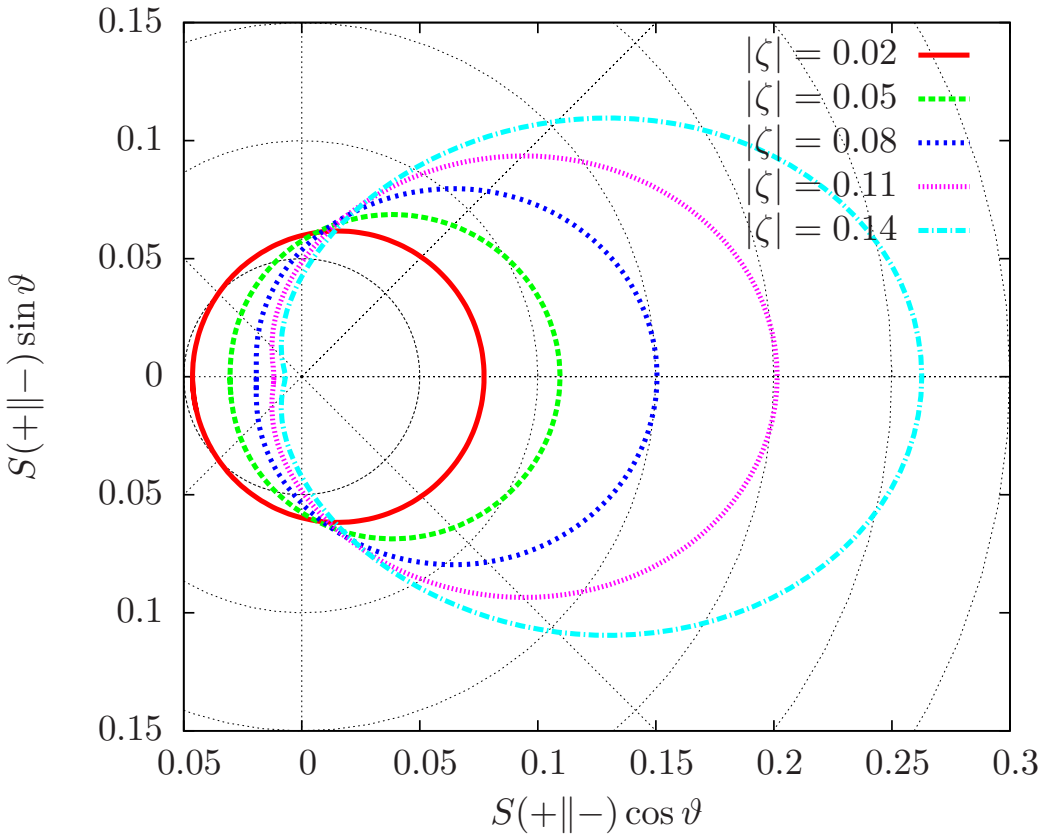

Figure 2.7: Polar plot of the dependence of the relative entropy $S(+\|-)$ on the relative phase-space orientation angle ϑ of equation (2.86) of the cat state and the squeezing of the environment for different magnitudes of squeezing. Beam splitter transmittance is $t = 0.95$, $|\alpha| = 3$.

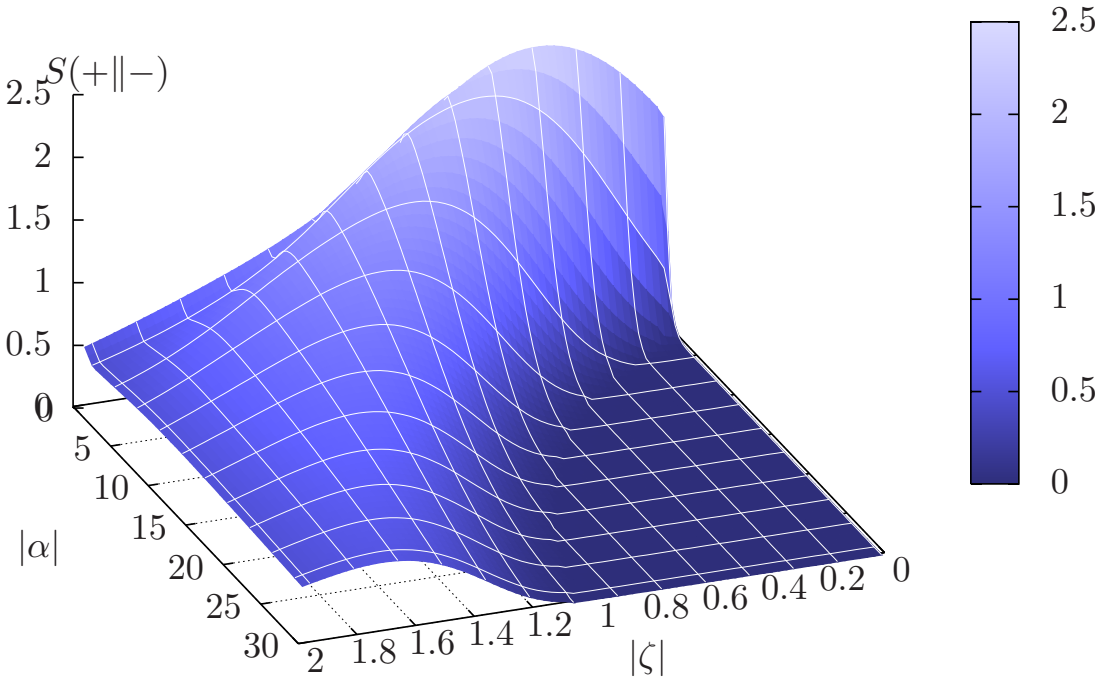

Figure 2.8: Plot of relative entropy $S(+\|-)$ versus magnitude of squeezing $|\zeta|$ and the magnitude of coherent amplitude $|\alpha|$ of the coherent state constituting the Schrödinger cats. The plot corresponds to the optimal phase $\vartheta = 0$, and beam splitter transmittance $t = 0.95$.

As it can be verified in Eqs. (2.82), these relative entropies depend only on a single phase variable

$$\vartheta = \arg(r) - \arg(t) - \arg(\alpha) + \arg(\zeta)/2. \tag{2.86}$$

Since on the output the input mode appears as transmitted and the environment mode as reflected, ϑ describes the direction of the squeezing relative to the orientation of the Schrödinger cats. The dependence of the relative entropy $S(+\|-)$ on ϑ for several squeezing parameters is plotted on Fig. 2.7. It is reasonable to assume that the behaviour observable on this numerically generated plot is general, and compared to the vacuum case ($\zeta = 0$) we always obtain improvement of the relative entropy when $\vartheta = 0$. We note that the case of $\vartheta = \pi$ corresponds to squeezing orthogonal to the optimal because of the $1/2$ factor in (2.86). This is typical for squeezing phenomena. Our studies show that the reverse case $S(-\|+)$ displays exactly the same behaviour.

In what follows, we treat only the case of maximal improvement, i.e. when $\vartheta = 0$. In figure 2.8 we have plotted the maximally improved entropy $S(+\|-)$ versus the magnitude of squeezing $|\zeta|$ and magnitude of coherent amplitude $|\alpha|$. Note that $|\alpha|$ is the distance in phase space between the two superposed coherent states in the optical Schrödinger cat states. Larger values of $|\alpha|$ correspond to quantum superpositions of more macroscopical states.

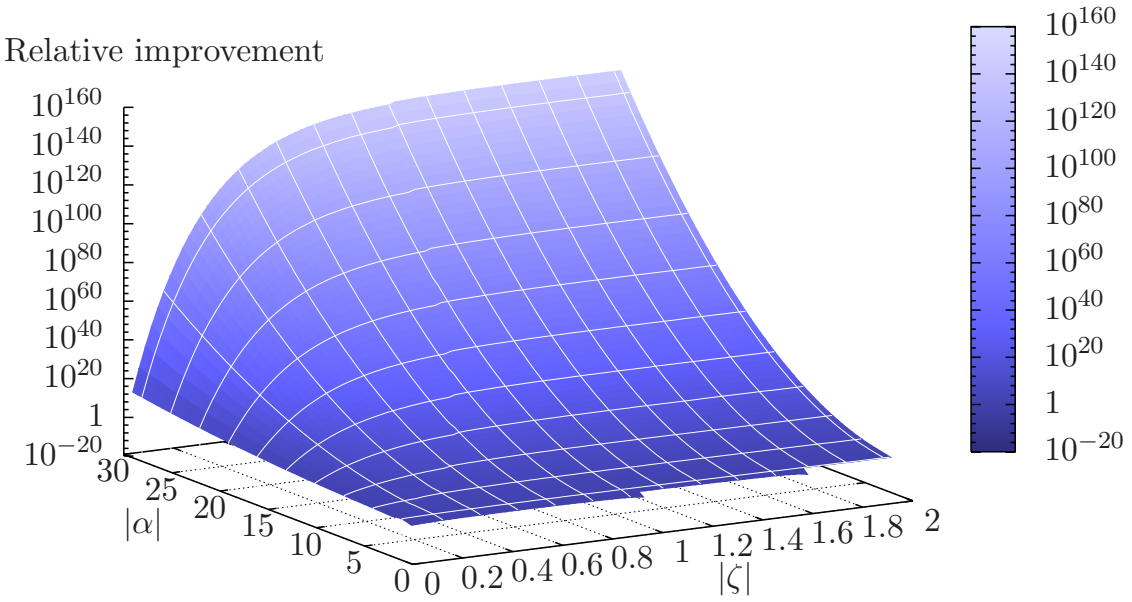

Figure 2.9: Relative improvement of distinguishablity compared to vacuum with no squeezing according to the formula $[S_\zeta(+\|-) - S_0(+\|-)]/S_0(+\|-)$. Beam splitter transmittance is $t = 0.95$. In contrast to Fig. 2.8, the existence of an optimal $|\zeta|$ parameter cannot be easily observed, due to the logarithmic scale on the vertical axis.

The entropy $S(+\|-)$ is so similar to $S(-\|+)$ that the difference would not be visible in a plot like Fig. 2.8. To illustrate this, on Fig. 2.10 we have plotted both entropies as a function of $|\alpha|$. It can be seen that the difference between the two entropies is relevant mainly for small $|\alpha|$'s, which is the less interesting case. This is somewhat expectable, since for larger $|\alpha|$'s the two states are more similar albeit keep their orthogonality. The similarity is more suggestive when one compares the shape of the two corresponding Wigner functions, and therefore we expect the probability of making a mistake to become more symmetric.

Returning to Fig. 2.8, we find that for a given $|\alpha|$, there is an optimal magnitude of squeezing where the improvement in the distinguishablity of the two cats is the most. For larger $|\alpha|$, i.e. for superpositions of more macroscopical coherent states, this optimal value of squeezing is higher. This is not surprising since the difference between the two orthogonal cat states is mostly concentrated in phase space within the well-known interference pattern between the two coherent states, and the band where these patterns are located is narrower for larger coherent amplitudes. On Fig. 2.8 it is also visible that the improvement is more significant for lower values of $|\alpha|$. However, on Fig. 2.9 where we have plotted the difference relative to the vacuum, we see dramatic improvement of distinguishablity as the coherent amplitude is increased.

It is remarkable that at $|\alpha| = 3$, when the achievable improvement is still rather significant, the average number of photons present in in the two Schrödinger cat state is

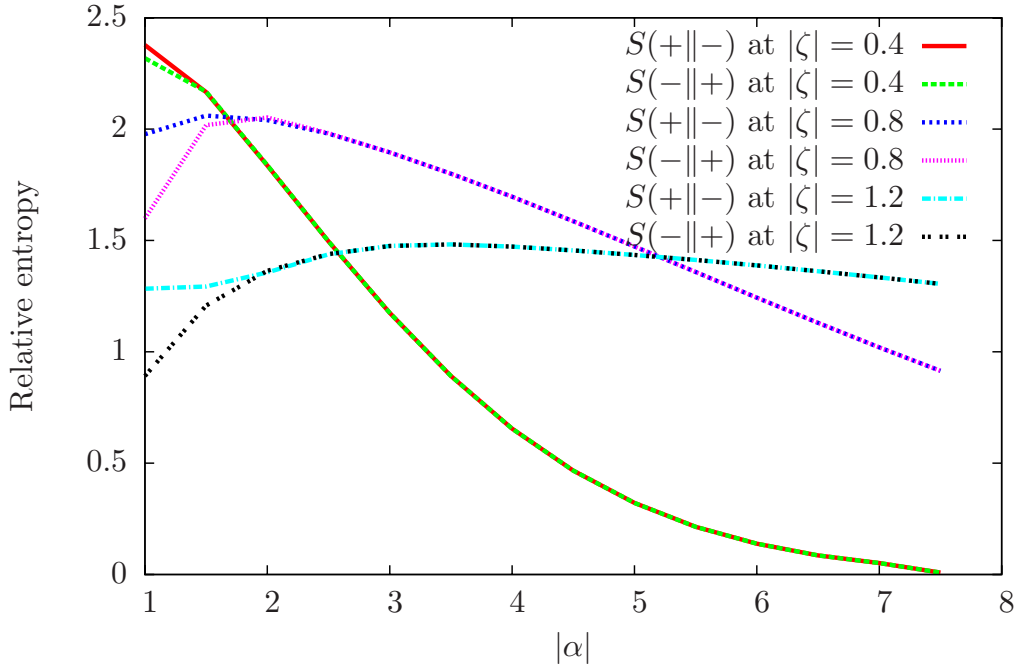

Figure 2.10: Plots of both relative entropies $S(+\|-)$ and $S(-\|+)$ versus the magnitude of parameter α of the cats, for different magnitudes $|\zeta|$ of the squeezing. Beam splitter transmittance is $t = 0.95$.

about 10. This means that states with relatively high photon numbers can play the role of computational basis states, in contrast to the traditional representations such as the polarisation or the dual rail where only a single excitation is present.

2.3.4 Conclusions

In this section we have studied a non-traditional representation of quantum bits, the optical Schrödinger cat states, and their response to decoherence. These quantum bits have the advantage that they are very natural to our experimental tools. We have been concerned with the analysis of a technique to suppress decoherence based on controlling the immediate environment. We have chosen this approach to fight decoherence because despite all their good qualities the theoretical description of the interaction of coherent state quantum bits with the environment can become quite complex. Therefore finding techniques to suppress the effect of noise based on identifying decoherence free subspaces or applying quantum error correction codes is also problematic.

The key of our approach is squeezing, and the special relation of optical Schrödinger cat states to it. As for the measurement part, we have taken the very general approach based on the quantum Sanov theorem, that eliminates all questions related to the optimality of measurements.

We have considered the read-out problem at the end of a deterministic, decision prob-

lem algorithm. In such case we only have to distinguish between the two basis states. Our calculations indicate that there are optimal parameters for the squeezing of the immediate environment. We have identified a single phase parameter of the system which combines all phase relations within, and characterises the effect of squeezing. The numerical results strongly suggest that the optimal value of this phase parameter is $\vartheta = 0$, and its optimality is independent of the rest of the parameters.

The optimal value for the amplitude of squeezing depends non trivially on the parameters of the basis states and of the decoherence, hence displays a more complicated behaviour. Our numerical calculations nonetheless proved that an optimal value of squeezing amplitude exists for every set of parameters we studied. We found that the distinguishablity achievable at the optimum is higher for low coherent amplitudes. Relative improvement in distinguishablity, however, always displayed a systematic increase with increasing $|\alpha|$. This provides a basis for possible applications of this technique.

Chapter 3

Quantum logic using trapped atoms and cavity systems

The previous chapter was dedicated to multi-partite systems consisting exclusively of optical modes. In the present section we turn to the possibilities of light–matter interactions for quantum computing. We may find several proposals already in the literature [105–107, 127, 155–166], however, these proposals generally lack scalability, or are very sensitive to decoherence. Here we shall discuss two different interaction schemes, both targeting computational scalability by increasing the number of atoms rather than employing more optical modes. What our two proposals also have in common is that the atoms involved are neutral, hence the optical modes play the role of mediating an interaction between the atoms that otherwise do not interact. In the first example the cavity acts as an "optical bus" that encodes quantum bits. In the second setup the cavity merely induces an effective Hamiltonian interaction between the atoms, and its quantum state does not show up explicitly in the calculations.

The theory of manipulation and read-out of atomic quantum bits with external laser pulses can be understood using the semi-classical theory of Sec. 1.3.2. On the other hand, the atom–cavity interaction requires the fully quantised treatment of Sec. 1.3.3.

The setup to be discussed in Sec. 3.1 consists of N atoms localised in a bi-modal cavity. The principle of operation remains the same regardless of the number of atoms N, hence from the theoretical point of view it is easily scalable. We shall assume that both the individual atoms and the cavity field can be individually manipulated, and we shall derive the universal two-qubit gates from the atom–cavity interaction. The atom–cavity interaction in this case manifests itself as shift in the ground state energy levels of the atoms [167]. Hence the effect of atomic decay in this system is greatly suppressed, and decoherence source is the one that scales with the size of the system. The requirements for the quality factor of the cavity is still strong, however, it is not amplified drastically by scaling.

The strength of the proposal set forth in Sec. 3.2 is that it places much lower demands on the quality of the cavity. The cavity field is considered to be in a thermal state, a state

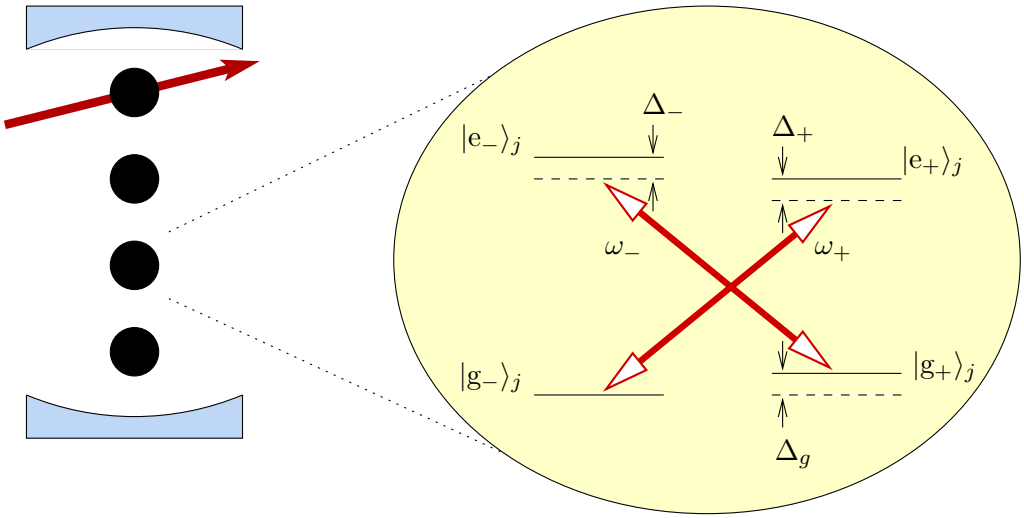

Figure 3.1: Physical arrangement, and schematic depiction of the atomic level structure and its relations to the cavity excitations. The red arrows symbolise the external Raman pulse used to realize single qubit rotations.

that usually develops during the interaction with the environment. We shall consider an arrangement where two-level atoms interact with this thermal field, such that the atomic transition is far detuned from the cavity mode with the closest frequency. The interaction manifests itself in the form of Stark shifts, and an effective interaction between the atoms can be derived [168]. The interaction is rather complex on the level of quantum bits, and to derive universal quantum gates we resort to the algorithmic search based on Ref. [169] as reformulated in Sec. 1.4.5. We present the solutions for the construction of universal quantum logic for $N = 2$ and $N = 3$ atoms. Further generalisation to more atoms might also be possible. Also, we assume a very simple atomic structure, therefore generalisations to more complex atomic structures to combat decoherence are also straight-forward.

3.1 Quantum gates in a system of four-level atoms and a cavity

In the present proposal we assume that good localisation of the atoms inside a cavity can be achieved. The time scale on which we require localised atoms is of the order of several several Rabi oscillations, the exact number depending on the complexity of the computational task. Such strong and stable the localisation of atoms for long time have only been achieved in ion traps [170, 171]. However, at least on the single atom level, outstanding trapping times inside cavities have been achieved [172–178]. In this section we shall show, that in exchange for the additional difficulty due to the cavity, we could obtain a system that scales in fairly robust way, while a simple formalism can be maintained. This is in contrast with the ion-trap quantum computer, where the formalism becomes hardly man-

ageable even for a couple of quantum bits. For ion-traps, the response to this theoretical challenge was a clever modification of the apparatus based on segmentation [170], that however, slows down the operation significantly. We also mention, that there is a certain analogy of super-conducting quantum bits in circuit quantum electrodynamics and cavity quantum electrodynamics [179–181]. In such systems the quantum bits are realised by accumulating cooper-pairs on a super-conducting island [182], therefore localisation is not an issue.

In the following proposal we employ the dispersive interaction between four-level atoms and a bimodal cavity field. We use the Hamiltonian derived in Ref. [167] for this system. The qubits are defined on an invariant subspace of the effective Hamiltonian that consists of ground states of the atoms, and the single photon excitation states of the cavity. The structure of the resulting Hamiltonian is similar to that of the interaction of nuclear spins, as used in NMR quantum computing [183–185]. We develop quantum gates along the same lines as it is generally followed in NMR, and explicitly construct the universal controlled-NOT gates between each pair of qubits.

3.1.1 Physical arrangement

We consider a system of N identical four-level atoms localised within a bimodal cavity. Localisation is needed for two reasons. First, motionless atoms experience time independent coupling to the electromagnetic field, which would not be true if they were moving. Second, we need individual addressability of the qubits. Since the atoms are identical, their position can be used to distinguish them from each other. In practice, this means that the external laser pulses that we use to make one-qubit operations can be directed to well known positions to address a particular qubit.

The level structure of the atoms involve four levels, between those pair-wise couplings can be induced using σ^+ and σ^- polarised light in an X-like shape, as depicted on Fig. 3.1 for the jth atom. The cavity modes are characterised by their polarisation and frequency. The frequencies of the σ^+ circular polarisation is denoted by ω_+, while that of the σ^- is ω_-. The two frequencies are not necessarily equal. The detunings of the cavity modes from the atomic transitions are $\Delta_\pm = \omega_0^\pm - \omega_\pm$. The complete atoms–cavity Hamiltonian in the rotating wave approximation reads:

$$\begin{aligned} H = \hbar\frac{\omega_0^-}{2}\sum_{j=1}^{N}\left(|e_-\rangle\langle e_-|_j - |g_+\rangle\langle g_+|_j\right) + \hbar\frac{\omega_0^+}{2}\sum_{j=1}^{N}\left(|e_+\rangle\langle e_+|_j - |g_-\rangle\langle g_-|_j\right) \\ + \hbar\Delta_g\sum_{j=1}^{N}\left(|e_-\rangle\langle e_-|_j + |g_+\rangle\langle g_+|_j\right) + \hbar\left(\omega^+ a_+^\dagger a_+ + \omega^- a_-^\dagger a_-\right) \\ + \hbar\left(a_-\sum_{j=1}^{N} g_j^-\,|e_-\rangle\langle g_+|_j + h.c.\right) + \hbar\left(a_+\sum_{j=1}^{N} g_j^+\,|e_+\rangle\langle g_-|_j + h.c.\right). \end{aligned} \quad (3.1)$$

Solving the equations of motion for this Hamiltonian is a daunting task. However, we

shall operate in the dispersive limit

$$\Delta_{\pm} \gg |g_j^{\pm}|, \tag{3.2}$$

and then the problem can be simplified greatly. In the next section we shall see in detail, what simplifications this assumption brings, and introduce a notation most suitable for quantum logic.

3.1.2 Effective dynamics

In the dispersive limit (3.2) the Hamiltonian (3.1) leads to an effective interaction between the two ground states and the two cavity modes. The effective Hamiltonian can be derived by noting that (3.1) can be regarded as a sum of two Hamiltonians each describing the interaction of a two level system with a single cavity mode. In the interaction picture, this effective Hamiltonian depends only on the detunings ($\Delta_{\pm}$), and possesses two invariant subspaces in the atomic part of the Hilbert space. One subspace contains only the excited and the other only the ground states[167]. Therefore if the initial states are superpositions of $|g_{\pm}\rangle_j$ ground states, the final state must be a similar superposition. If we denote the dipole coupling constants $g_j^{\pm} = g_j$ (g_j real), in the interaction picture the effective Hamiltonian acting on the ground states becomes

$$H_{\text{eff}} = -\frac{\hbar}{\Delta}\sum_{j=1}^{N} g_j^2 \left[a_-^{\dagger}a_-|g_+\rangle\langle g_+|_j + a_+^{\dagger}a_+|g_-\rangle\langle g_-|_j\right]. \tag{3.3}$$

With the help of the individual spin operators $S_z^{(j)} = |g_+\rangle\langle g_+|_j - |g_-\rangle\langle g_-|_j$, we define the modified collective spin operator

$$S_z = \sum_{j=1}^{N} g_j^2 S_z^{(j)}. \tag{3.4}$$

We note that the individual spin operators obey the identity $2|g_{\pm}\rangle\langle g_{\pm}|_j = 1 \pm S_z^{(j)}$, hence we have

$$\sum_{j=1}^{N} g_j^2 S_{\pm}^{(j)} = \frac{1}{2}\sum_{j=1}^{N} g_j^2 \pm S_z, \tag{3.5}$$

therefore Eq. (3.3) can be written as $H_{\text{eff}} = \frac{\hbar}{2\Delta}(a_+^{\dagger}a_+ - a_-^{\dagger}a_-)S_z + \frac{\hbar}{2\Delta}\sum_j g_j^2(a_+^{\dagger}a_+ + a_-^{\dagger}a_-)$. Since the second term does not describe any interaction, it can be included in the Hamiltonian H_0 used to go into the interaction picture, and we finally obtain

$$H_{\text{eff}} = \frac{\hbar}{2\Delta}N_z S_z, \tag{3.6}$$

where $N_z = a_+^{\dagger}a_+ - a_-^{\dagger}a_-$ stands for the usual Schwinger operator for the z direction.

To define quantum bits, we restrict our attention to the case when the cavity contains exactly one excitation. Then the cavity state can be written as a superposition of $|10\rangle$

and $|01\rangle$, where the first number corresponds to a Fock state of the σ^+ and the second to the σ^- polarisation mode. In other words, the two states for the quantum bit are the polarisation states of a photon. This concept has been used widely in the field, most remarkably for the experimental realization of quantum teleportation [114].

To obtain concise formulae later, we now introduce new notations for the states of the system. Namely, we adopt the dual-rail representation for the cavity

$$\begin{aligned} |0\rangle_0 &:= |10\rangle\,, \\ |1\rangle_0 &:= |01\rangle\,, \end{aligned} \tag{3.7}$$

and also make the definitions

$$\begin{aligned} |0\rangle_j &:= |g_+\rangle_j\,, \\ |1\rangle_j &:= |g_-\rangle_j\,, \end{aligned} \tag{3.8}$$

for the atomic states ($j = 1, \ldots, N$). Using these notations the effective Hamiltonian (3.6) can be written as

$$H_{\text{eff}} = \frac{\hbar}{2} \sum_{j=1}^{N} J_j \sigma_z^{(0)} \sigma_z^{(j)}, \tag{3.9}$$

where $J_j = g_j^2/\Delta$ and $\sigma_z^{(\alpha)} = |0\rangle\langle 0|_\alpha - |1\rangle\langle 1|_\alpha$ is a Pauli-z matrix for every $\alpha = 0, \ldots, N$. The free part of the total Hamiltonian we have used to go into the interaction picture can be written

$$H_0 = \frac{1}{2}\hbar\delta\sigma_z^{(0)} + \frac{1}{2}\hbar\Delta_g \sum_{i=1}^{N} \sigma_z^{(i)}, \tag{3.10}$$

where we have dropped the constant term $\frac{\hbar}{2\Delta}\sum_j g_j^2$. In the following, Latin indices (e.g. i, j) shall always run from 1 to N, and Greek indices (e.g. α, β) from 0 to N, unless otherwise indicated.

We know that the effective Hamiltonian (3.9) is universal together with all single qubit gates, using the bang-bang control technique [135, 136]. Crucial to this statement is complete unitary control at the single qubit level. In the next section we investigate which single qubit gates are available to us in the present system.

3.1.3 Simple quantum gates

The required single qubit gates for universality were briefly discussed in Sec. 1.4.4. It has been mentioned, that besides the CNOT gate it suffices to have two arbitrary unitary rotations about two orthogonal axes for exact universality. This is, however, not necessary, and having for example the single qubit gates H, S, and T of Eq. (1.108) is enough for approximate universality. In the following we collect the single qubit gates that can be conveniently carried out within our setup. These turn out to be less than the arbitrary rotations about two perpendicular axes, nevertheless, in Sec. 3.1.4 we shall show that with the interaction Hamiltonian (3.9) these still suffice for universality.

First we consider single qubit gates on the atomic qubits. Use of Rabi oscillations induced by external laser fields is a well-known technique to manipulate the quantum state

of atoms [161], and it can also be extended to Raman transitions between two ground states, involving some third level [107, 127]. In the present case we need a pair of pulses, one is π polarised and the other either σ^+ or σ^-. If we denote the two respective Rabi frequencies by Ω_1 and Ω_2, and the detuning from the intermediate level by $\Delta_{\rm R}$, then the effective Rabi frequency of the Raman pulse becomes $\Omega_{\rm R} = \Omega_1\Omega_2/\Delta_{\rm R}$. If $\Omega_{\rm R} \gg J_k$ holds for all k, the collective interaction can be neglected for the duration of the Raman pulse. This greatly simplifies the calculations, and we can think of applying either a one-qubit quantum gate or the multi-qubit gate coming from $H_{\rm eff}$ of (3.9). Technically, the laser pulses are used similarly as the RF pulses in NMR. The similarity is that these directly allow realisations of rotations about any axis in the x–y plane, in the way akin to those that led to the transformations listed in Eq. (1.92). Similarly to the NMR, rotations about z can be easily performed virtually, by adjusting the time reference frame, i.e. shifting the phase of the controlling laser pulse.

Now we turn to the possibility of implementing one-qubit gates on the cavity field. Although there is a wide range of techniques available to manipulate the polarisation state of a photon in free space, most of these techniques are not applicable to a cavity mode. There is, however, a successful method of modifying the state of a bimodal cavity. This is based on sending two-level circular Rydberg atoms through the cavity. A requirement is that the cavity modes are non-degenerate ($\omega_+ \neq \omega_-$), and the frequency difference

$$\delta = \omega_+ - \omega_- \tag{3.11}$$

is much greater than the dipole coupling of the transition of the Rydberg atom ($\delta \gg g_A$) and we have means of suddenly changing the resonance frequency of the atom. In the microwave regime, Stark shift can be induced by applications of a time-dependent static external electric field to the cavity. This technique has been proposed for preparing non-classical states of light [186], and used successful to create entangled states of the modes of a bimodal cavity [187]. In the optical regime, ac-Stark shifts can be induced by coupling one of the energy levels to a much higher excited state by a far detuned, intense laser pulse, and thereby altering the original resonance frequency. In either case, we may assume that it is possible to tune the atomic resonance from one cavity frequency to the other. For the realisation of quantum logic, the chosen external control field is changed in a step function manner, therefore we do not have explicit time dependence of the Hamiltonian for certain intervals. This feature keeps the calculation of the time evolution still quite simple.

The single qubit gates for the atoms could have been studied in the interaction picture defined by the free Hamiltonian (3.10). However, adding the traversing atom to the system, an additional term appears in the free part, and it becomes

$$H_0' = H_0 + \frac{1}{2}\hbar\omega_A\sigma_z^{(A)}, \tag{3.12}$$

where ω_A is the controllable transition frequency of the atom. If the atom is resonant to the cavity mode s ($s = \pm$), then the Hamiltonian in the interaction picture prescribed by

H_0' becomes

$$H'_{\text{eff}} = H_{\text{eff}} + \hbar g_A \left(\sigma_+^{(A)} a_s + \sigma_-^{(A)} a_s^\dagger \right), \tag{3.13}$$

and we can neglect the shifts caused by the other mode. When the atom is far detuned from both modes, then we assume $H'_{\text{eff}} = H_{\text{eff}}$. Since H_0' varies in time according to a step function, we must return to the Schrödinger picture before each frequency jump and go to a different interaction picture with the new transition frequency ω_A.

As the consequence of switchings between different interaction pictures we expect R_z rotations to show up. In addition, R_z rotations can be applied in controlled manner using the following scheme. The atom enters the cavity in its ground state $|g\rangle$, and there it interacts resonantly with one of the modes, say s ($s = \pm$), for a time t_π. We term this process a π pulse when t_π satisfies $g_A t_\pi = \pi$. The effect of a π pulse can be written as

$$\alpha\,|01\rangle\,|g\rangle + \beta\,|10\rangle\,|g\rangle \rightarrow |0\rangle\,(\alpha\,|1g\rangle + \beta\,|0e\rangle), \tag{3.14}$$

assuming that the atom was in resonance with the first mode. Following this interaction, by adjusting the external static electric field, the atomic transition frequency is tuned to some ω_{off} such that $|\omega_{\text{off}} - \omega_\pm| \gg g_A$. Now we wait for some time t, and tune the atom back into resonance with mode s and let it evolve for another t_π. This brings the atom back to its ground state, and the resulting transformation on the cavity qubit can be written

$$R_z(2\delta t_\pi + (\delta + s\delta_{\text{off}})t), \tag{3.15}$$

where $\delta_{\text{off}} = \omega_{\text{off}} - \omega_s$. To inhibit any further interaction between the cavity modes and the ground state atom, we may tune its transition far from any resonance condition. The time it takes to perform this rotation depends on how large δ_{off} can be made.

Realization of R_x rotations begin similarly. The atom enters the cavity in the ground state, it is tuned into resonance with the s mode and these interact for t_π. Then the atom is tuned into resonance with the orthogonal mode $\bar{s}$, and interact with it for some time t_φ ($2g_A t_\varphi = \varphi$). The atom is then tuned back to the s mode and another π pulse is applied. The resulting transformation is

$$R_z(\delta t_\pi - \pi) R_x(\varphi) R_z(\delta t_\pi + \pi). \tag{3.16}$$

The π and $-\pi$ terms enter the formula because of the orthogonality of the two polarisations. We can combine this scheme with the realization of R_z rotations: before and after tuning the atom resonant with $\bar{s}$ we tune it to some off-resonant frequency ω_{off}, and let it evolve for some times t_1 and t_2, respectively. The net transformation can be written

$$R_z(\delta t_\pi - \pi + (\delta + s\delta_{\text{off}})t_2) R_x(\varphi) R_z(\delta t_\pi + \pi + (\delta + s\delta_{\text{off}})t_1). \tag{3.17}$$

For example, if $t_1 = t_2 = t_\pi$, $\delta_{\text{off}} = -2s\delta$ and $\varphi = \pi/2$ then the above sequence can be used to realize the pseudo Hadamard transformation

$$H_p = \frac{1}{\sqrt{2}} \begin{pmatrix} 1 & 1 \\ -1 & 1 \end{pmatrix}, \tag{3.18}$$

and when $\varphi = -\pi/2$, its adjoint $H_p^\dagger$. We shall see in the next section the significance of H_p.

We can briefly recall the results for the present section. We saw that using external control we can apply any $SU(2)$ transformation to the atomic qubits, and among other transformations we can perform the pseudo Hadamard gates H_p and $H_p^\dagger$ on the cavity qubit. There is an important difference, however, in using the different qubits. Manipulation of atomic states can be considered cheap and without complications compared to that of the cavity state. The cavity qubit gates are more expensive since they require a precisely timed atom to be in the cavity, and mathematically more complicated since the Hamiltonian used to go into the interaction picture changes in time. It is the time dependence of the free Hamiltonian that prohibits in the case of on the photonic qubits the virtual realisation of R_z rotations, that are possible for the atoms.

3.1.4 Universality

In this section we shall show how the interaction described by (3.9) can be used to generate the universal CNOT gate using the single qubit operations described in Sec. 3.1.3.

First, we recall that (3.9) is a special case of the NMR Hamiltonian [183–185] with the general coupling coefficients $J_{\alpha\beta}$ taking the values $J_{\alpha\beta} = J_\beta$ while $\alpha = 0$ and $\beta > 0$, and $J_{\alpha\beta} = 0$ otherwise. Since the commutator is $[\sigma_z^{(\alpha)}, \sigma_z^{(\beta)}] = 0$, all terms in (3.9) commute. Therefore, the time evolution operator $U(t) = \mathrm{e}^{-\frac{i}{\hbar}H_{\mathrm{eff}}t}$ may be written as a product of

$$U_{0k}^J(t) = \mathrm{e}^{-iJ_k\sigma_z^{(0)}\sigma_z^{(k)}t/2} \tag{3.19}$$

operators. We shall refer to this operator as J-coupling evolution, borrowed from NMR terminology. The time evolution operator of the complete system in the interaction picture can therefore be expressed as

$$U(t) = \mathrm{e}^{-\frac{i}{\hbar}H_{\mathrm{eff}}t} = \prod_{k=1}^{N} U_{0k}^J(t). \tag{3.20}$$

We can use the technique called refocusing in NMR to cancel any of the J-coupling operators in the time evolution (3.20). This involves casting single-qubit rotations on some qubits thereby interrupting the time evolution governed by H_{eff}. The following identity lies at the heart of the technique:

$$R_x^{(\beta)}(\pi)U_{\alpha\beta}^J(t)R_x^{(\beta)}(\pi)U_{\alpha\beta}^J(t) = \mathbb{1}. \tag{3.21}$$

Here $R_x^{(\beta)}(\varphi)$ denotes the x rotation on the β qubit, defined as $R_x^{(\beta)}(\varphi) = \mathrm{e}^{-i\sigma_x^{(\beta)}\varphi/2}$ with $\sigma_x^{(\beta)} = |0\rangle\langle 1|_\beta + |1\rangle\langle 0|_\beta$. Now we have chosen an x rotation, however, any rotation in the x–y plane would be suitable. Eq. (3.21) highlights a very important property of the J-coupling interaction: it can be cancelled by manipulating only one of the qubits. We can use this to spare "expensive" transformations of the photonic qubit, and perform the cancellation by operating exclusively on the atoms.

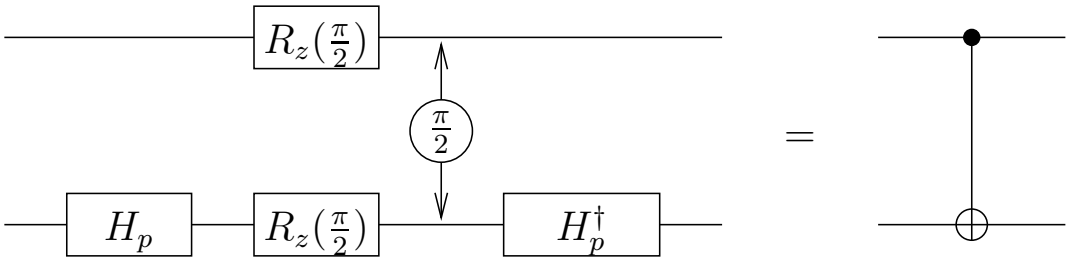

Figure 3.2: Construction of CNOT gate using a J-coupling interaction

Since the rotation operator for the kth atom commutes with the rest of the J-coupling operators, the terms in (3.20) can be cancelled individually as

$$R_x^{(k)}(\pi)U(t/2)R_x^{(k)}(\pi)U(t/2) = R_x^{(k)}(\pi)U_{0k}^J(t/2)R_x^{(k)}(\pi)U_{0k}^J(t/2)\prod_{j\neq k}U_{0j}^J(t) = \prod_{j\neq k}U_{0j}^J(t). \tag{3.22}$$

It is straight-forward to show that successive or even simultaneous applications of similar pairs of π rotations on different atomic qubits can be used to cancel any number of terms in (3.9). In particular, all terms but one can be cancelled, therefore H_{eff} can be used to realize time evolution described by a single U_{0k}^J. When $J_k t = \pi/2$ this operator is equivalent[169] to the controlled-NOT gate, and hence can be used to generate it. This is a well-known construction in NMR (see the references [183, 184]), and for completeness we have depicted it on Fig. 3.2.

The procedure depicted on Fig. 3.2 requires rotations about the two axes x and z. Since the J-coupling evolution is symmetric with respect to the two qubits, the role of qubits in the resulting CNOT gate is determined by the single-qubit gates which precede and follow $U_{0k}^J(J_k^{-1}\pi/2)$. Specifically, the qubit to which the H_p and $H_p^\dagger$ sequence is applied becomes the target quantum bit, while the other becomes the control. We note, that the R_z operations commute with U_{0k}^J, therefore the duration of the J-coupling is determined by the time elapsing between the two operations H_p and $H_p^\dagger$.,For the same reason, the R_z operations can be shifted in time as long as the single qubit operation commutation rules permit it.

This technique allows us to implement CNOT gates directly between the cavity qubit and any atomic qubit. We can extend this ability using SWAP gates the way it is depicted on Fig. 3.3, and arrive to applying a CNOT between any two atomic qubits. This property allows us to think of the atomic qubits as computational registers on which we perform computational operations, and consider the role of the cavity qubit that may be called an "optical bus."

Hidden in the scheme, however, there are single qubit operations that need to be performed on the cavity qubit. The cover-up is the elegant notion of the SWAP gate. What are the requirements for realising a SWAP gate regarding the cavity qubit? Considering the well-known construction using three CNOT gates, the requirements are the same as for

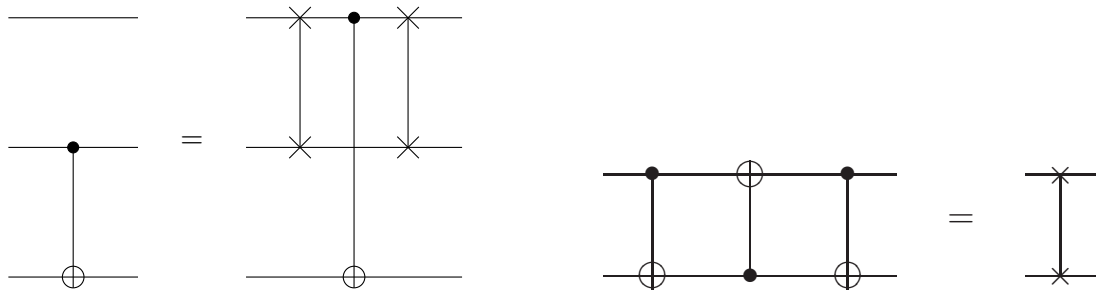

Figure 3.3: Construction of a CNOT gate between two atomic qubits, using two SWAP gates (left). And the well-known construction of a SWAP gate using three CNOT gates (right).

a CNOT. Inspecting the expanded diagram for a SWAP gate we find that altogether two single-qubit transformations are needed for the photonic qubit: $R_z(\pi/2)H_pR_z(\pi/2)$ and $R_z(\pi/2)H_p^\dagger$ which both fit perfectly into the scheme of Eq. (3.17), we only need to adjust t_1 and t_2 appropriately for the extra R_z rotations.

3.1.5 Conclusions

In this section we have demonstrated the universality of the considered N atom and cavity system, and gave explicit recipes for constructing CNOT and single qubit gates. The mathematical description of the effective interaction is similar to the NMR Hamiltonian, therefore we could borrow some ideas from the theory of NMR quantum computing. However, there are subtle differences compared to the NMR quantum computing even from a more abstract theoretical point of view. The role of photonic and atomic quantum bits in this setup is very different from each other. While the photon interacts with each atom, the atoms do not interact with each other at all. Due to the inherent difficulties to manipulate the quantum state of the cavity field, we proposed a scheme in which all the computation is carried out on the atomic quantum bits, and the cavity functions only as an "optical bus" used only in SWAP gates. A major advantage of the setup is that the Hamiltonian remains simple even for large number of atoms. Due to this simple scaling property, if the requirements on trapping and individual addressing can be met, the system could, in principle, be scaled up to a many qubits.

3.2 Quantum gates on two-level atoms and dispersive cavity

The greatest challenge with using a cavity for quantum computation is the relatively short decoherence time of photons. In every proposal where the state of the cavity field is used to realize a quantum bit, its decoherence time usually dominates that of the entire system. Examples of such implementations can be found in Refs. [107, 127, 155–161, 163–166], and also in Sec. 3.1. The in-depth study of the situation in Sec. 3.1 highlighted the importance

of the cavity as a mediator when neutral atoms are used in the implementation.

In the present section we shall discuss a scheme where the cavity is used solely as a mediator, and its quantum state does not play any role during the computation process. Such a scheme is expected to be very robust against cavity losses. For the atomic quantum bits we have similar demands as in the previous setup: The atoms must be localised and distinguishable on the basis of their position, i.e. their centre of mass wave functions must be non-overlapping. As it has been mentioned before, such trapping of several atoms is becoming more realistic with recent advances [172–178].

A similar idea to our proposal has been used in a proposition to prepare entangled atomic states in a cavity [188]. Here we are taking a more general approach, however, not only by demonstrating computational universality, which itself incorporates state preparation, but also in terms of including the loss coefficient κ of the cavity. These losses can be included in the discussion by using the results of Ref. [168], where it has been shown that the κ coefficient merely reduces the strength of the effective interaction between the atoms. Although we shall only be concerned with the notions within the cavity QED framework, it is worth noting that the interaction Hamiltonian we shall be using is a special case of the Lipkin model [189]. Similar Hamiltonians can be associated with the dynamics of ion traps [190] and Fe^{3+} ions of a large magnetic molecule [191], therefore our considerations may be adopted when one attempts to do quantum logic using those systems.

The technique we shall propose here is based on the collective interaction of the atoms, induced by the cavity, and single-qubit rotations, realized e.g. by selective laser pulses. We shall derive explicit results for systems of two and three atoms, and provide direct constructions of important quantum gates for both configurations. Our results imply that arbitrary quantum gates could be realized for the two and three qubit systems. In the latter case this is demonstrated by first deriving a universal two-qubit gate from the collective interaction of the three atoms. The obtained two-qubit gate is constructed solely from the collective three-atom interaction and single-qubit rotations. In particular, we do not use any techniques involving other auxiliary states, or select pairs of atoms to interact in any way, as it is common in the literature of cavity QED quantum computing [155–160, 165, 166].

To obtain an appropriate collective interaction, we work in the dispersive limit of the atom–photon interaction. Although this reduces the number of sources of decoherence, calculations for implementing universal gate sets become more involved. The difficulty arises from the fact that the CNOT gate is derived from a more complex three-qubit gate, and other than using lengthy and approximate Trotter formulae [129, 135, 136], no general solution to this reduction problem is known yet.

3.2.1 Physical arrangement

We consider N two-level atoms trapped inside a cavity as depicted on Fig. 3.4. The cavity resonance frequency ω is detuned from the atomic transition frequency ω_0 by some value

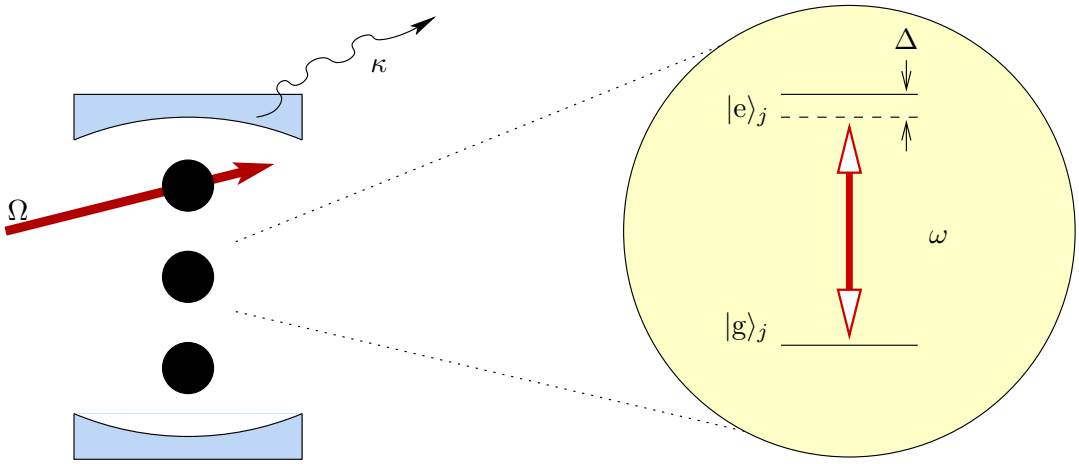

Figure 3.4: Physical arrangement of the atoms and the cavity. Also shown is the energy level configuration of the jth atom, and the closest cavity mode. ($\Delta = \omega - \omega_0$)

Δ, and we denote the dipole coupling constant for the atom–photon interaction by g. We also take the cavity loss rate into account, and introduce the parameter κ to characterise it.

In the present scope we do not consider the impact of spontaneous decay of the excited state to the ground state. Considering the number of many ways to work around this problem (e.g. deriving effective two-level atoms from a Λ type system) we do not regard it as essential. We stress, however, that the cavity is not expected to *enhance* this decay, since we assume the resonances to be far detuned from each other, and in such cases the Purcell effect is negligible. We also assume that the individual atoms are addressable by external highly focussed, monochromatic, resonant (with the atomic transition) laser pulses, hence single-qubit operations can be implemented selectively.

The most convenient way to describe the dynamics of the atomic system is to use the collective spin-$N/2$ operators

$$S_i = \frac{1}{2}\sum_{k=1}^{N} \sigma_i^{(k)}, \tag{3.23}$$

were $\sigma_i^{(k)}$ are the Pauli operators defined in Eqs. (1.83). The computational basis is introduced as

$$\begin{aligned} |0\rangle_j &:= |g\rangle_j\,, \\ |1\rangle_j &:= |e\rangle_j\,, \end{aligned} \tag{3.24}$$

therefore one qubit is assigned to each atom inside the cavity.

3.2.2 Effective dynamics

A simple effective dynamics can be derived for the atoms, if we assume the cavity to be far detuned and in a thermal state. The effective dynamics have been derived independently

using two different techniques in Refs. [168] and [188]. Here we use the results of Agarwal [168] because it is more general, and also gives a better account to why the cavity can be assumed to be in a thermal state. In this approach, the evolution of the cavity is given by a master equation of the form in Eq. (1.123) with the parameters being $\Gamma = 2\kappa$ and $\Gamma' = \Gamma\bar{n}$, where $\hbar n$ is the average number of photons in the thermal state. The interaction between the atoms and the field is given by a term $S_+a + S_-a^\dagger$, which must also be incorporated into the master equation for the entire atoms–cavity system.

As it has been shown in [168], in the limit $g\sqrt{N} \ll |i\Delta + \kappa|$, the cavity field remains in a thermal state throughout the entire process. This limit can be reached either by having a high loss rate, or a large detuning Δ. Under these condition, the cavity field operators may be replaced by their expectation values corresponding to the thermal state. It has also been pointed out that when the detuning is much larger than the loss rate, i.e.

$$|\Delta| \gg \kappa, \tag{3.25}$$

the evolution of the atomic system is approximately unitary. The Hamiltonian associated to this evolution can be written as

$$\begin{aligned} H_N &= \hbar\eta(S_+S_- + 2\bar{n}S_z) && \text{(3.26a)} \\ &= \hbar\eta\left[S^2 - S_z^2 + (2\bar{n}+1)S_z\right], && \text{(3.26b)} \end{aligned}$$

using the total angular momentum square operator S^2, and introducing the effective coupling constant

$$\eta = \frac{g^2\Delta}{\kappa^2 + \Delta^2}. \tag{3.27}$$

We note that the condition under which we could eliminate the cavity state, and still have a Hamiltonian evolution, can now be reformulated in accordance with Eq. (3.25) as

$$|\Delta| \gg g\sqrt{N}. \tag{3.28}$$

We see in Eqs. (3.26) and (3.27) that the cavity decay factor affects only the coupling strength η. Hence, the higher the loss rate, the "slower" the interaction is. We also mention, that the indirect effect of a lossy cavity on the atomic decay rate could also be interesting in this context. Although the atomic decay has not been included in this treatment, from the case-study of simpler systems we can safely assume that the enhancement scales with $g^2\kappa/(\kappa^2 + \Delta^2)$, hence its contribution is negligible under the condition (3.25).

Our Hamiltonian (3.26) being quadratic, satisfies the conditions for being universal for any number of qubits. Therefore, we know that given we have complete local unitary control [135, 136] it must be universal. In the following, our goal shall be to find an efficient implementation framework up to $N = 3$ atoms that involves only few applications of the local controlling gates to achieve exact realisation of quantum gates. We shall do this by explicitly showing how CNOT gates in all possible configurations can be generated using this interaction and single-qubit rotations. The single qubit rotations can be carried out

using external resonant laser pulses in the following way. The transformations such as those in Eq. (1.92) can be directly realized provided the Rabi frequency of the pulse is much greater than the effective coupling $\Omega \gg \eta$. The Rabi frequency is proportional to the amplitude of the classical field, and can therefore be easily controlled. Just as in Sec. 3.1 the single qubit rotations interrupt the evolution of the collective system and therefore can be used to control virtually the duration for which this interaction is effective. However, due to the more complicated structure of the Hamiltonian (3.26), we do not have such an efficient cancellation as the refocussing technique used in section 3.1 and in NMR technology [183–185].

During the following calculations we shall often be concerned with the invariants as recollected in Sec. 1.4.5 following Ref. [169]. These invariants rely on the notion of *local invariance*, which means that transformations which can be brought to be equal using single qubit operations are regarded as being equivalent. This simplification can immediately be applied to the Hamiltonian (3.26). Inspection shows that the last terms of Eqs. (3.26a) and (3.26b) commute with the rest of the Hamiltonians, and therefore both expressions constitute z rotations with an angle proportional to the average photon number. Also notice that according to the definition of the collective operators, rotation operators of the collective system are simply tensor products of rotations of the individual spins. In the notations of 1.4.4, after time t the effect of the last terms in Eq. (3.26a) and Eq. (3.26b) are the transformations $R_z(2\eta\bar{n}t)$ and $R_z\left(\eta(2\bar{n}+1)t\right)$, respectively. In a rigorous treatment these rotations should be cancelled individually. Here we adopt a less precise terminology, and simply say that $\bar{n}$ is to be set to a certain value that renders our calculations simpler. This simplification is well justified since the compensation can be easily done if single qubit rotations can be easily realized. One only needs to know precisely the mean photon number (i.e. temperature) of the cavity, and keep good track of the application times of the collective Hamiltonian (3.26).

3.2.3 Quantum logic for two atom system

Dicke states [192, 193] span the entire Hilbert space. In the simplest interesting case, the cavity contains only two atoms and the collective spin operators describe a spin-1 system. The value of the total angular momentum and the z component are sufficient to identify the collective eigenstates, and no additional labels are necessary.

The time evolution operator can be calculated promptly by observing that the operator

$$G = (S^2 - S_z^2 + S_z)/2 \tag{3.29}$$

is a projection, i.e. $G^2 = G$, and the Hamiltonian (3.26) can be expressed as

$$H_N = \hbar\eta 2G, \qquad \text{when } \bar{n} = 0. \tag{3.30}$$

As we mentioned before, if the required value of $\bar{n}$ is not equal to the actual value in the implementation, it can be corrected by applying single qubit R_z rotations to every

qubit. Therefore we continue with this setting, which corresponds to considering only the nonlinear term in (3.26a). After a brief algebra we arrive at the expression

$$U^{(2)}(t) = e^{-\frac{i}{\hbar}H_2 t} = 1 - e^{-i\eta t} 2iG \sin(\eta t) \tag{3.31}$$

for the time evolution operator. Using a matrix notation in the computational basis, this evolution operator corresponds to

$$U^{(2)}(t) = e^{(-i\varphi)} \begin{pmatrix} e^{-i\varphi} & 0 & 0 & 0 \\ 0 & \cos\varphi & -i\sin\varphi & 0 \\ 0 & -i\sin\varphi & \cos\varphi & 0 \\ 0 & 0 & 0 & e^{i\varphi} \end{pmatrix}, \tag{3.32}$$

where we have set $\varphi = \eta t$ for brevity. The invariants (1.111) of this matrix turn out to be

$$[\cos^4\varphi, 4\cos^2\varphi - 1]. \tag{3.33}$$

To achieve universality, we look for parameters when $U^{(2)}(t)$ is equivalent to a CNOT gate. However, the invariants of CNOT are $[0, 1]$, and this is not attainable by any real φ. Therefore, we extend our search to seeking a CNOT equivalent gate in the form $U^{(2)}(t)O_f U^{(2)}(t')$, where O_f is the combination of some single qubit operations. In a general case, this task can be quite non trivial. For each qubit the arbitrary SU(2) rotation has three parameters, and O_f represents the tensor product of such two. We use the same parametrisation of the SU(2) transformations as in Eqs. (1.75) and (1.76), with superscript indices denoting the respective qubit.

In the course of search, we calculate the invariants of the operator $U^{(2)}(t)O_f U^{(2)}(t')$, and require that they are equal to those of the CNOT. The resulting requirement is by nature in the form a non-linear equation that may yield several solutions. We shall not present the full set of equations here due to space considerations. These can be obtained by simple algebra following the recipe outlined in Sec. 1.4.5. Furthermore, the verification of the validity of solutions is also straight-forward.

To obtain a solution of the non-linear equation we made certain simplifications. First, we realized that the phase dependence of expressions is only through the combinations $\varphi_r^{(1)} - \varphi_r^{(2)}$ and $\varphi_t^{(1)} - \varphi_t^{(2)}$. We decided to assume the respective phases to be equal, and it makes these phase differences zero. To further simplify, we also restricted our search to the equal time case $t = t'$. With these conditions, the equivalence requirement yielded two distinct solutions, one with application time corresponding to $\varphi = \pi/2$, and another to $\varphi = \pi/4$. Since the total computation time is dominated by the application time of the collective interaction, choosing the result with less time cost seems to be more practical. In this spirit we define

$$U^{(2)}_{\frac{\pi}{4}} = U^{(2)}\left(\frac{\pi}{4}\eta^{-1}\right). \tag{3.34}$$

It can be easily verified that the operator

$$\tilde{U}^{(2)} = U^{(2)}_{\frac{\pi}{4}} O_f U^{(2)}_{\frac{\pi}{4}}, \tag{3.35}$$

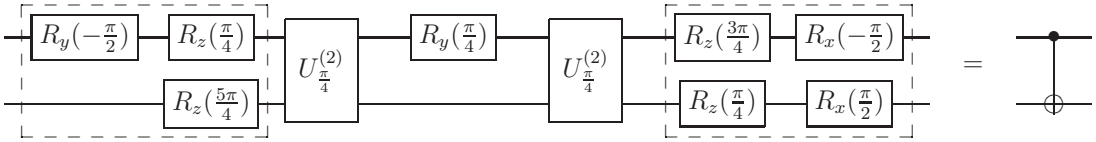

Figure 3.5: Quantum circuit diagram depicting the sequence to prepare CNOT gate from the time-evolution operator in (3.32).

with $O_f = R_y(\pi/4) \otimes \mathbb{1}$ is equivalent to the CNOT gate. In other words, if we apply an $R_y(\pi/4)$ transformation after the atoms interacted for a time $t_{\frac{\pi}{4}} = \pi/(4\eta)$ and again wait for time $t_{\frac{\pi}{4}}$ the resulting transformation will be equivalent to a CNOT gate up to local operations. Note that the role of qubits in this expression is so far interchangeable, although the CNOT is non-symmetric with regard to its input. This is well expected, since CNOT (either case) can be generated from the symmetric controlled-Z gate using only local operations.

To provide a universal quantum gate compatible with the existing formalism, we have to go one step further, and explicitly give the local operations that transform $\tilde{U}^{(2)}$ to an exact CNOT. In particular, CNOT with first bit as control and second as target bit can be produced as

$$\text{CNOT} = \mathrm{e}^{i\pi/4}\, O_c' \tilde{U}^{(2)} O_c, \tag{3.36}$$

with the local operations being

$$O_c' = [R_x(-\pi/2)R_z(3\pi/4)] \otimes [R_x(\pi/2)R_z(\pi/4)] \tag{3.37}$$

$$O_c = [R_z(\pi/4)R_y(-\pi/2)] \otimes R_z(5\pi/4). \tag{3.38}$$

We have included the irrelevant phase factor just to be able to use the equal sign. The entire construction is depicted as a quantum circuit diagram on Fig. 3.5. We note here, that assuming two-qubit gates $U^{(2)}$ with equal t, this construction is optimal in terms of operation time for the complete CNOT gate.

3.2.4 Quantum logic for three atom system

In the present section we shall show how universal quantum logic can be realized when three atoms interact via the cavity. The situation shall turn out to be different from the $N = 2$ atom case, and it therefore needs an approach different from the more usually adopted in earlier proposals. The usual approach is to concentrate on pair-wise interactions between qubits, and derive universal two qubit gates from these interactions. However, in the following we shall derive the universal two-qubit gates directly from the collective interaction.

To construct quantum logic operations of the system in Sec. 3.1 we already dealt with a collective interaction. There, however, the problem could have been tackled much easier.

A pair-wise interaction was derived using the well-known NMR technique of refocussing, and the obtained set of two-qubit unitaries includes the universal controlled phase gate.

Since no invariants are known for three qubit gates, we take here an approach similar to that of Sec. 3.1. As a first step, we set out to obtain unitaries in the form

$$U_{23}^{(3)} = \mathbb{1} \otimes U_{23}, \tag{3.39}$$

using only combinations of the three qubit evolution operator $U^{(3)}(t)$ and single-qubit gates. The requirement (3.39) is more than what is actually necessary. It would equally be useful to find an operator that can be written as $O_1 \otimes U_{23}$, where O_1 is a single qubit operator acting on the first qubit. However, the condition that an operator has the form (3.39) is simpler to express in terms of matrix elements, therefore the equations of the upcoming calculation are easier to solve.

The collective evolution is according to the Hamiltonian in Eq. (3.26b). For simplicity we shall drop its linear terms, that corresponds to taking

$$\bar{n} = -1. \tag{3.40}$$

Since this corresponds to a negative temperature reservoir, it can never be met directly by any experimental apparata. Instead, we assume that this condition is satisfied by using appropriate compensating rotations, as discussed earlier.

Despite the simplifications made above, our search space for finding an operator of the form (3.39) is still large. To tackle the problem, we follow a path similar to the spin-echo scheme and consider operators, that can be written

$$U_{23}^{(3)}(t) = X_1 U^{(3)}(t) X_1 U^{(3)}(t'), \tag{3.41}$$

using $U^{(3)}(t) = \exp(-\frac{i}{\hbar} t H_3)$, that denotes time-evolution generated by the chosen Hamiltonian, and $X_1 = R_x(\pi) \otimes \mathbb{1} \otimes \mathbb{1}$, that is essentially a NOT gate. Our search is now limited to finding the appropriate values of t and t', such that the operator (3.41) satisfies the condition (3.39).

To be able to efficiently formulate the condition (3.39) for (3.41) we consider the three atom system as a product of a spin-1/2 and a spin-1 system. We start with the matrix of $U^{(3)}(t)$ in the Dicke state basis, where it is diagonal, then we use the Clebsch-Gordan coefficients and the theory of angular momentum addition to transform it into the product basis. In this notation, Eq. (3.39) translates to the requirement that the operator in Eq. (3.41) acts on the spin-1/2 subsystem as the identity. With some algebra we obtain that this condition is fulfilled when $t' = t$ and $\sin(3/2\eta t) = 0$. This yields a different solution at each $i = -1, 0, 1$ for U_{23} through

$$\eta t = 2/3\pi(3k + i), \quad \forall k \in \mathbb{Z}. \tag{3.42}$$

Note, that $i = 0$ corresponds to the identity operator and is therefore irrelevant. The interesting cases are $i = -1$ and $i = 1$, and these yield operators being adjoint of one

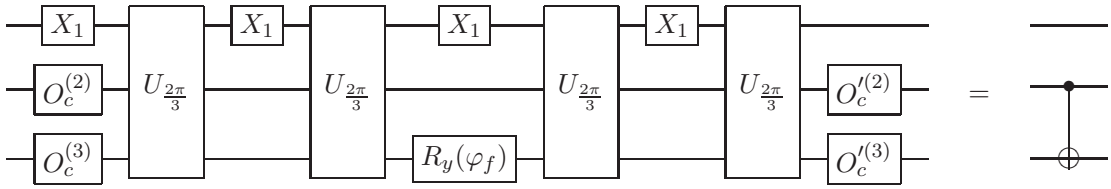

Figure 3.6: Construction of CNOT gate using the operator $U_{\frac{2\pi}{3}} = U^{(3)}(\eta^{-1}2\pi/3)$ generated by the collective Hamiltonian (3.26) with $\bar{n} = -1$. The single qubit operations are according to Eqs. (3.46) such that $O_c = O_c^{(2)} \otimes O_c^{(3)}$ and $O_c' = O_c'^{(2)} \otimes O_c'^{(3)}$.

another. The two operators are also equivalent in the sense of (1.109) as they both have invariants $[1/4, 3/2]$. Since, just like in Sec. 3.1, the time cost is essentially determined by the length of application of the collective interaction, we again prefer shorter times. Therefore, in the following we work out the CNOT gate for $i = 1$, and assume $k = 0$.

Returning to the computational basis, the resulting two qubit unitary turns out to be a diagonal matrix,

$$U_{23} = \mathrm{Diag}(e^{-i\pi/3}, e^{i\pi/3}, e^{i\pi/3}, e^{-i\pi/3}). \tag{3.43}$$

We note that using an operator notation, (3.43) can be written as

$$U_{23} = \exp\left(-i\frac{\pi}{3}\sigma_z \otimes \sigma_z\right), \tag{3.44}$$

which is exactly what we have for a Heisenberg spin-spin interaction. However, it is a very important difference here that the "application time" is fixed to what corresponds to a $\pi/6$ pulse. Hence the techniques used in NMR cannot be applied here. To obtain a CNOT gate, we resort to the invariant method.

Plugging in the operator (3.43) into the equations of Sec. 1.4.5 produces a satisfactory result in the second order. With straight-forward algebra we obtain the three local operators by means of those we can express the CNOT as

$$\mathrm{CNOT} = \mathrm{e}^{-i\pi/4}\, O_c' U_{23} O_f U_{23} O_c. \tag{3.45}$$

The control bit for this CNOT is the 2nd and the target is the 3rd qubit. Controlled NOT gates acting on different qubits can be obtained by exchanging the role of qubits at the time of application of single qubit operations. The explicit form of the local operations is

$$\begin{aligned} O_f &= \mathbb{1} \otimes R_y(\varphi_f), && \text{(3.46a)} \\ O_c &= R_x(-\pi/2) \otimes [R_z(\pi) R_x(\varphi_c)], && \text{(3.46b)} \\ O_c' &= [R_z(-\pi/2) R_y(-\pi)] \otimes [R_z(\varphi_c') R_y(-\pi/2) R_z(\pi/2)], && \text{(3.46c)} \end{aligned}$$

where the angular parameters must satisfy

$$\begin{aligned} \tan(\varphi_f/2) &= 1/\sqrt{2}, && \text{(3.47a)} \\ \tan(\varphi_c/2) &= \sqrt{2/3} - 1, && \text{(3.47b)} \\ \tan(\varphi_c'/2) &= (1 - \sqrt{3})/\sqrt{2}. && \text{(3.47c)} \end{aligned}$$

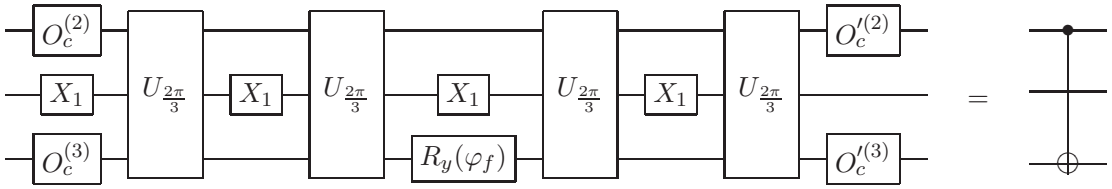

Figure 3.7: Constructing CNOT between the first and the third qubit, using the same notation as on Fig. 3.6.

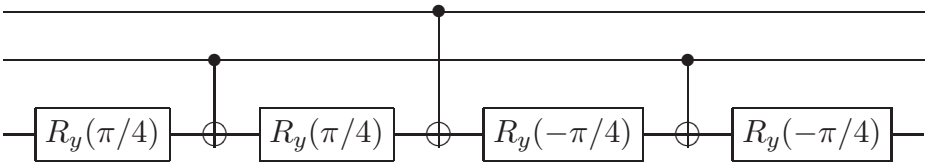

Figure 3.8: Quantum circuit diagram for the simplified Toffoli gate requiring only three CNOT gates [67].

Recall that only the 2nd and the 3rd qubits are considered in the notation of Eqs. (3.46). Fig. 3.6 depicts the complete sequence for all three qubits as a quantum circuit diagram.

3.2.5 A demonstration of universality

To have universality we need CNOT gates in all possible configurations. For example, if we are to construct the simplified Toffoli gate [67], we could realize a quantum circuit depicted on Fig. 3.8. Already for this relatively simple circuit we need two different CNOT operations. One of these we have worked out in Sec. 3.2.4, and the CNOT in the middle can also be constructed doing the straight-forward modification that means exchanging the role of the first and the second qubit. This exchange is reflected only in the application of single qubit gates, since the collective Hamiltonian is invariant to permutations of the qubits. This modified sequence of operations is depicted on Fig. 3.7.

The simplified version of the Toffoli gate differs from the Toffoli gate only in a conditional phase shift, however, it requires only half the CNOT gates. In certain situations Toffoli gates can be replaced by the simplified versions without altering the effect of the overall circuit [67]. Moreover, the simplified Toffoli gate is itself also a universal gate.

To calculate the total time cost for a quantum circuit, we need only to consider the number of $U_{\frac{2\pi}{3}}$ operations. Simple arithmetic yields the time $8\pi/\eta$ for the simplified Toffoli and $16\pi/\eta$ for the Toffoli gate. Following DiVincenzo's criteria [194], for efficient error-free quantum computation these gate times should be much shorter than the coherence time of the complete system, which in the present case is dominated by the decay of the excited atomic state.

3.2.6 Conclusions

We have explicitly demonstrated how the collective interaction affecting all atoms in the cavity can be used to generate a universal gate set without using lengthy and approximate Trotter formulae. A peculiar feature of the scheme that the collective interaction arises from the cavity enclosing all the atoms, therefore turning "on" and "off" the interaction selectively is not possible. This is in contrast to the generally preferred schemes, where selective two qubit interactions are available, and these are used directly to generate two-qubit gates.

In the considered system, up to three atoms we showed that using single qubit rotations, how the Hamiltonian of the system can be used to generate a universal set of CNOT gates. With this proposal we also successfully address the most challenging problem in cavity QED quantum logic proposals, the short cavity lifetime. In this proposal, we place only modest requirements on the quality of the cavity. The field in the cavity can be in any thermal state, and the cavity loss rate affects only the strength of the interaction but not the decoherence time. Therefore spontaneous decay remains as the main source of decoherence. However, the atomic level structure we have considered here is the simplest of all. This makes it possible to apply techniques that combat the spontaneous decay. These features can make our proposal a possible candidate for experimental realisation.

Összefoglalás (Summary in Hungarian)

Bevezetés

A kvantuminformáció-elmélet forradalmian új elméleti eredményeket alkotott a gépi számítások hatékonyságának növelése és a telekommunikáció biztonságosabbá tételének terén. Ezen eredményeket azonban eddig még nem követték nagymérvű kísérleti megvalósítások. Minden kvantuminformáció-feldolgozási protokoll megvalósításának egyik előfeltétele, hogy megtaláljuk a kiválasztott fizikai rendszer megfelelő reprezentációját. Különösen kvantumszámítások megvalósítása esetén, ezzel párhuzamosan szükség van kvantuminformáció nagy hibatűrésű módon történő kezelésére is.

Kvantumoptikai megvalósításokban, a fizikai rendszer rendszerint egy vagy több elektromágneses módusból, esetleg üregrezonátorban lévő atomokból áll. Ezek a jelöltjeink kvantumbitek megvalósításához. A tisztán optikai kvantumrendszerek többnyire számos elektromágneses módust alkalmaznak, és a legnagyobb sikerrel alkalmazott alapösszetevőik passzív lineáris eszközök (pl. nyalábosztók) és fotodetektorok. Ezekben a rendszerekben, a kvantumbiteket az elektromágneses módusok kvantumállapotaiban kódolják, és a kvantumlogikai műveleteket a lineáris eszközökkel valósítják meg. Bizonyos elrendezésekben, ezeket továbbkombinálják detektormérésekből vett visszacsatolásokkal. Minthogy az elektromágneses tér szabadsági fokainak száma rendkívül nagy, kvantumbitek ábrázolásának módjai is hasonlóan tágak. Már egyetlen kvantumbit ábrázolásának megválasztásánál is szembesülünk azzal, hogy egy, kettő vagy akár több módust is felhasználhatunk. Sőt, ha döntöttünk is valamelyik módus mellett, még akkor is választhatunk diszkrét, illetve folytonos ábrázolások között, miközben rendelkezésünkre áll az ábrázolásra használt lineáris altér dimenziójának megválasztása is.

Azon megvalósításokban, melyek az üregrezonátor kvantum-elektrodinamikáját használják ki, a rezonátorban lévő atomok is használhatók kvantumbitek ábrázolására. Ilyen esetekben, az elektromágneses tér tulajdonságaiból fakadó választási szabadság tovább bővül azzal, hogy az atomok releváns elektronállapotainak energiaszint-szerkezete is megválasztható azzal, hogy milyen atomot és annak melyik spektrális rezonanciáját használjuk. További gazdag lehetőségek tárulnak fel előttünk, amint a kvantuminformáció-kezelés megvalósításához alapot nyújtandó, a tárgyalásban figyelembe vesszük a rezonátorban éb-

redő atom–foton kölcsönhatást. Elméleti oldalról tekintve, a rendszer rengeteg elrendezést tesz lehetővé az atomi szintek szerkezetének, a közel rezonáns rezonátormódusok frekvenciájának és polarizációjának, illetve a külső pumpáló lézerek paramétereinek megválasztásával. Az üregrezonátor kvantum-elektrodinamikáján alapuló kvantumszámítástechnikai kutatás célja, a különböző feltételek mellett legmegfelelőbb elrendezés megtalálása.

Nagyon fontos feltételt jelentenek a rendszer dekoherencia jelenségei. Mivel ezen jelenségek gördítik a legkomolyabb akadályokat a kísérleti megvalósítások elé, ezért ezeket a lehetőség szerint figyelembe kell venni minden elméleti javaslatban. Dekoherencia általában a kvantumbitek környezettel vagy egymással történő nemkívánt kölcsönhatása miatt lép fel, és eredményeképpen akár a teljes kezdetben kódolt információ is elveszhet. Az üregrezonátoros kvantumrendszerek jellemző dekoherencia-csatornái a fotonveszteség és a gerjesztett atomi állapotok spontán bomlása.

Koherens-állapot kvantumbitek

A koherens-állapotok több szempontból is érdekes osztályát képezik az elektromágneses tér kvantumállapotainak. Fontosak egyrészt a kvantumállapot-reprezentációt illetően, mivel egy teljes folytonos bázist alkotnak, másrészt mert természetes bázisként használhatóak a fény szokványos dekoherencia jelenségeinek leírásánál. Továbbá, koherens-állapotok előállíthatóak ideális lézerekkel, így ezek az állapotok könnyen rendelkezésre állnak. A koherens-állapot kvantumbitekkel kapcsolatos eredményeinket a 2. fejezetben gyűjtöttük össze.

A koherens-állapotok egyetlen komplex változóval jellemezhetőek, ami a klasszikus amplitúdónak és fázisnak feleltethető meg. A kvantumállapot-reprezentáció szempontjából érdekes, hogy a koherensállapot-bázis túlteljes, azaz a koherens-állapotok szerinti kifejtés nem egyértelmű, továbbá hogy minden koherens-állapot átfed egymással. Az egydimenziós koherensállapot-reprezentáció alkalmazásakor az elektromágneses tér állapotait olyan koherens-állapotok szerint fejtjük ki, amelyek a fázistérben egyetlen folytonos görbe mentén helyezkednek el. Ezt a reprezentációt azért nevezzük egydimenziósnak, mert ezt a folytonos görbe egyetlen valós változóval paraméterezhető. Ezen reprezentáció reprezentáció működésének hátterében is ez a túlteljesség áll. Az egydimenziós koherensállapot-reprezentáció egyik speciális esete, amikor a kiválasztott körbe egy origón áthaladó egyenes. Ebben az esetben egy diszkrét bázis is kifejezhető Hermite polinomok segítségével.

Az egydimenziós koherensállapot-állapot reprezentáció általánosításának igénye összefonódott állapotok leírásának szükségességénél merül fel. A mi általánosításunk a kétmódusú összenyomáson alapul. Eredményeinket a 2.1. szakaszban ismertettük, amelyben először megadtuk a kétmódusú-összenyomott vákuum egyetlen komplex paraméter felhasználásával történő, $|\alpha\rangle|\alpha^*\rangle$-hez hasonló alakba írható, kétmódusú koherens-állapotok szerinti kifejtését. A kifejtés súlyfüggvényére egy Gauss-eloszlás adódott, majd a továbbiakban megmutattuk, hogyan definiálható egy diszkrét bázis Laguerre-2D polinomok segítségével. Az így értelmezett egykomplexsík-reprezentáció teljességét a Laguerre-2D

polinomok teljességét felhasználva bizonyítottuk.

Az egykomplexsík-reprezentáció kétmódusú-összenyomott állapotok tárgyalásakor és dekoherencia leírásánál bizonyult különösen hasznosnak. Ezt a reprezentációt használták a folytonos változós kvantumteleportáció ideális és veszteséges eseteinek tanulmányozásánál is.

A 2.2. szakaszban, az egykomplexsík-reprezentációból kiindulva bevezettünk kétmódusú Schrödinger-macska állapotokat. Ezek az állapotok a szokásos optikai Schrödinger-macska állapotoknak olyan általánosításai, amelyek akár két ebit összefonódottságot is mutatnak. Kidolgoztunk egy formalizmust nemortogonális bázisban megadott tiszta kvantumállapotok összefonódottságának kiszámítására. A kétmódusú Schrödinger-macska állapotok összefonódottságát ezen formalizmus segítségével számítottuk ki. Meghatároztuk, hogy melyik típusú Schrödinger-macska állapot szolgálhat megbízhatóan a legnagyobb mértékű összefonódottsággal, és felhasználtuk ezt az állapotot, mint kvantumcsatornát egy teleportációs eljárásban. Pontosan meghatároztuk melyik a használandó Bell-projekció, és elméletileg készítettünk egy optikai optikai összeállítást, amivel a sikeres teleportáció valószínűsége 1/8.

A 2.3. szakaszban koherens-állapot kvantumbitek dekoherencia-problémáját vizsgáltuk egy, az optikában bevetten használt modell segítségével. A használt modellben a környezettel való kölcsönhatást egy nyalábosztóval helyettesítjük, aminek az egyik bemeneti portján a rendszer állapota, a másikon a környezetet leíró módus lép be. A nyalábosztón történt kölcsönhatás után a környezethez tartozó módust elvetjük, ami egy részleges nyom képzésnek felel meg. Természetes körülmények között a környezet egy vákuumhoz közeli termális állapotban van, ám bizonyos esetekben a vizsgált rendszer közvetlen környezetét valamely más állapotba is hozhatjuk.

Egy determinisztikus döntési algoritmus kiolvasási problémáját tanulmányoztuk a fent említett dekoherencia mechanizmus tükrében. Az ilyen algoritmusok egyik különlegessége, hogy eredményük kizárólag valamelyik bázisállapot lehet, és nem azok szuperpozíciója. Jó példa erre a Deutsch- és a Deutsch—Jozsa-algoritmus. Ezen esetekben tehát, egy koherens-állapotokon alapuló megvalósításban a kiolvasási probléma a két optikai Schrödinger-macska állapot megkülönböztetését követeli meg. A megkülönböztethetőséget a Sanov-tétel kvantummechanikára vonatkozó változatának segítségével számszerűsítettük. Ezt a tételt felhasználva, az optimális mérésekkel elérhető sikeres megkülönböztetés valószínűségét kvantum-relatíventrópiák kiszámításával határozhattuk meg.

Megvizsgáltuk azt az esetet, amikor a környezet összenyomott vákuum állapotba preparálható, és megkerestük az összenyomási paraméter azon optimális értékét, amely az adott reprezentáció és dekoherencia mellett a legnagyobb megkülönböztethetőséget adja. Azt találtuk, hogy a megkülönböztetőségre vett hatásuk szempontjából, a rendszer összes fázisviszonya leírható egyetlen változóval. Ez a fázisváltozó a Schrödinger-macskák fázisát, a környezet összenyomásának szögét, és a nyalábosztó fázisait additívan tartalmazza. Átfogó numerikus eredményeink arról tanúskodnak, hogy ennek a fázisváltozónak az optimális értéke nulla. Vizsgáltuk, továbbá, hogy hogyan függ a megkülönböztethetőség

értéke a nyalábosztó áteresztőképességétől, az összenyomás mértékétől és a Schrödinger-macska állapotokat alkotó koherens-állapotok intenzitásától. Numerikus eredményeink, minden általunk vizsgált esetben azt mutatták, hogy az összenyomás mértékének létezik egy optimális értéke minden áteresztőképesség és intenzitás mellett. Eredményeink azt is mutatják, hogy a megkülönböztethetőség relatív javulásának optimális értéke növekszik a bázisállapotokat alkotó koherens-állapotok intenzitásával.

Kvantum-logikaihálózatok atom–rezonátor rendszerekben

A 3. fejezetben az üregrezonátor kvantum-elektrodinamikáján alapuló kvantumszámítógépre adott két javaslatunkat mutattunk be. Mindkét elrendezésben feltételeztük, hogy a jól lokalizált, semleges atomok, az erős csatolás tartományában hatnak kölcsön az üregrezonátor terével. Mivel az atomok semlegesek, nem lép fel közöttük közvetlen kölcsönhatás, és köztük az egyetlen számottevő közvetítő az üregrezonátor tere.

A 3.1. szakaszban egy olyan elrendezéssel foglalkoztunk, amelyben az atomok a kölcsönhatásban két alapállapottal és két gerjesztett állapottal, az üregrezonátor pedig két ellenkezően cirkulárisan polarizált módussal vesz részt. Amikor az üregrezonátor módusainak frekvenciái távol vannak hangolva az atomi átmenettől, továbbá, egy olyan kezdeti állapotból indulunk, amely a két alapállapot szuperpozíciója, valamint a rezonátortér egyetlen gerjesztést tartalmaz, akkor bizonyos közelítéseket alkalmazva a rendszer Hamilton-operátora nagyban leegyszerűsíthető. Ilyen körülmények között, a Hamilton-operátor egy csillag-szerű topológiájú spin z–z kölcsönhatásnak felel meg úgy, hogy egy központi spin páronként kölcsönhat a többi spinnel, de amazok egymással nem hatnak kölcsön. Ebben az analógiában a központi spin az üreg polarizált fotonjának, a többi spin pedig a kétállapotú atomoknak felel meg.

Kvantum-logikaihálózatok tárgyalásának előkészítése gyanánt egy-egy kvantumbitet feleltettünk meg minden atomnak, és egy további kvantumbitet az üregrezonátorban található polarizált fotonnak. Egy N atomot tartalmazó rendszer esetében, tehát, ez $N+1$ kvantumbitnek felel meg, amelyek közül a fotonikus kvantumbit megkülönböztetett szerepet játszik. A mag mágneses rezonanciáján alapuló kvantumszámítógép elméletéből ismert újrafokuszálás technikáját alkalmazva, effektív két-kvantumbites kapukat vezettünk le az említett spin z–z csatolásból. Az újrafokuszálás megvalósításához elegendő az atomokon végrehajtani egy-kvantumbites műveleteket, amely műveletek kivitelezhetők rezonáns Raman-impulzusok alkalmazásával. Javaslatot tettünk CNOT kapuk megvalósítására oly módon, hogy a szükséges egy-kvantumbites műveleteket úgy valósítjuk meg, hogy a Raman-impulzusokat kiegészítjük egy üregbe vitt kétállapotú atommal, melynek rezonancia frekvenciáját egy külső statikus elektromos térrel változtatjuk. Rámutattunk, hogy amennyiben rendelkezünk CNOT kapukkal a fotonikus kvantumbit és mindegyik atomi kvantumbit között, minden kvantumművelet megvalósítható egy olyan sémában, amelyben a fotonikus kvantumbit egy „optikai busz” szerepét tölti be.

Ebben a javaslatban egy olyan rendszert írtunk le, amely skálázhatóságának nincse-

nek elvi akadályai, hiszen N elvileg bármilyen nagyságrendű szám lehet. Továbbá, mivel az atomoknak csak az alapállapotát használtuk, az atomi szintek bomlásából származó dekoherencia hatása nem jelentős. A dekoherencia szempontjából az egyetlen komoly akadályt a rezonátor vesztesége jelenti, ami miatt a megfelelő jósági tényezőjű üregrezonátor készítése komoly kihívást jelenthet.

A 3.2. szakaszban egy másik elrendezéssel foglalkoztunk, amelyben az atomoknak két állapota hat kölcsön diszperzíven az üregrezonátor egyetlen módusával. Stark-eltolódások következtében az atomok között egy effektív kölcsönhatás jön létre, ami bizonyos feltételek mellett közelítőleg unitér időfejlődést jelent kizárólag az atomok rendszerét tekintve is. Ezen időfejlődés Hamilton-operátora a kollektív spin-operátorok egy négyzetes kifejezéseként írható, valamint a Dicke-állapotok bázisán egy diagonális mátrixnak felel meg.

Rámutattunk, hogy amennyiben teljes lokális kontrollal bírunk, ez a Hamilton-operátor univerzális kvantumlogikai hálózatok alapjául szolgálhat akár tetszőleges számú atom esetén. A tárgyalt elrendezésben teljes lokális kontroll szelektív, rezonáns lézerimpulzusokkal valósítható meg. A legföljebb $N = 3$ atomos esetre receptet adtunk kvantumlogikai műveletek egzakt megvalósítására. Megadtuk a megfelelő univerzális CNOT kapuk kifejtését egy-kvantumbit műveletek és a kollektív időfejlődés szerint.

Az $N = 3$ atomos esetben, első lépésként a három-kvantumbites kölcsönhatásból két-kvantumbites kaput származtattunk, egy az újrafokuszáláshoz hasonló eljárást alkalmazva. A második lépésben ezt a kvantumkaput használtuk fel, az invariáns technika segítségével, a különböző CNOT kapuk megalkotására. A rendszer műveleti univerzalitásának nyomatékosítása érdekében tárgyaltuk a három-kvantumbites Toffoli-kapu egyszerűsített változatának előállítását.

Az utóbbi kvantum-logikaihálózatok megvalósítására tett javaslat egyik érdekessége, hogy noha az üregrezonátor jelenléte elengedhetetlen a működéséhez, annak veszteségeire csak csekély mértékben érzékeny. Nagyobb fotonveszteségi ráta mellett csak gyöngül a kvantumbitek közötti effektív csatolás, míg a dekoherencia nem növekszik számottevően. Jelentős dekoherencia-forrásnak egyedül a gerjesztett atomi állapot bomlási mechanizmusa marad. Tekintettel, viszont, a javaslatban szereplő atomi szerkezet egyszerűségére, az adott kísérleti körülményeket figyelembe véve könnyen lehet olyan változtatásokat tenni az elrendezésen, amivel ez a hatás is csaknem teljesen megszüntethető.

A disszertáció tézisei

1. Bevezettük a kétmódusú elektromágneses tér állapotainak egy egyetlen komplex változójú függvényeket használó reprezentációját. Az ábrázolás $|\alpha\rangle|\alpha^*\rangle$ alakú kétmódusú koherensállapotok folytonos szuperpozícióján alapul. Ezért ezt a reprezentációt egykomplexsík koherensállapot-reprezentációnak neveztük. Megmutattuk, hogy létezik egy egy-egy leképezés a kétmódusú-összenyomott Fock-állapotok és a Laguerre-2D polinomok között. Ezt az eredményt felhasználva megmutattuk, hogy a kétmódusú elektromágneses tér minden állapota reprezentálható egy egyetlen komp-

lex változós függvénnyel. [I, II]

2. Optikai Schrödinger-macska állapotok kétmódusú általánosítására tettünk egy javaslatot. Kifejlesztettünk egy formalizmust nemortogonális bázisban megadott, tiszta állapotok kétrészű összefonódottságának kiszámítására, és a formalizmus segítségével kimutattuk, hogy a javasolt kétmódusú Schrödinger-macska állapotok általában összefonódottak. Szemléltetésül készítettünk egy teleportációs protokollt, amelyben a kvantumcsatornát egy kétmódusú Schrödinger-macska állapot alkotja. Tettünk egy javaslatot, ami alapul szolgálhat egy részleges Bell-mérés optikai megvalósításához, továbbá megmutattuk, hogy a javaslatot követve, egyidőben két kvantumbit feltételes teleportációja valósítható meg 1/8 valószínűséggel. [III]

3. A mérés egy általános általános megközelítésében, a Sanov-tétel kvantumos változatát használva megmutattuk, hogy az optikai Schrödinger-macska állapotok megkülönböztethetősége jobban megőrizhető ha a közvetlen környezetüket összenyomott állapotba tudjuk hozni. Egy jellemző helyzet, amikor a megkülönböztethetőségi probléma felmerül, az amikor egy döntési probléma determinisztikus kvantumalgoritmusának eredményét olvassuk ki. Numerikus eredményeinkre alapozva arra a következtetésre jutottunk, hogy létezik egy egyértelmű optimális beállítása a rendszer fázisviszonyainak, továbbá, hogy a Schrödinger-macska állapotok minden választásához és a dekoherencia minden erősségéhez létezik a környezetnek egy optimális összenyomottsági foka. [IV]

4. Javaslatot tettünk egy potenciálisan skálázható, üregrezonátor kvantum-elektrodinamikáján alapuló kvantum-logikaihálózat megvalósításra. A javasolt összeállítás N darab, kétmódusú üregrezonátorban csapdázott, négyállapotú atomból áll, amelyben minden atom, valamint a rezonátor fotonja egy-egy kvantumbitet valósít meg. Megmutattuk, hogy univerzális kvantum-logikaihálózat valósítható meg hasonló elven, mint a mag mágneses rezonanciáján alapuló kvantumszámítógép esetében. A működéshez szükséges egy-kvantumbit műveletek végrehajtása az atomokon rezonáns Raman-impulzusokkal, az üregrezonátor terén pedig egy segéd-atommal lehetséges. Mivel a fotonikus kvantumbit a séma egyetlen kvantumbitje, ami a többivel kölcsönhatásban van, ezért az egy „optikai busz” szerepét tölti be. [V]

5. Javaslatot tettünk egy atomokból és diszperzív üregrezonátorból álló rendszeren alapuló kvantum-logikaihálózat megvalósításra. Rámutattunk, hogy a rendszer műveletileg univerzális tetszőleges számú atom esetén. Két és három atomos esetben CNOT kapuk egzakt megvalósítását származtattuk. A több-kvantumbites kapukat a rezonáns lézerimpulzusokkal megvalósított egy-kvantumbites kapukból és az atomok közötti, üregrezonátor által keltett, kollektív kölcsönhatásból állítottuk össze. A javasolt rendszer hibatűrőképessége az üregrezonátor veszteségekkel szemben rendkívüli, márpedig általában ez a veszteség a dekoherencia legfőbb forrása az üregrezonátor kvantum-elektrodinamikáján alapuló elrendezésekben. A hibatűrőképesség

egyik megnyilvánulása, hogy az üregrezonátor tere tetszőleges termális állapotban lehet, továbbá, hogy a veszteség növelésével a dekoherencia nem nő, hanem csak az atomok közötti effektív csatolási állandó csökken. [VI]

Summary

Introduction

Quantum information science has produced revolutionary theoretical results to improve efficiency of computation, and security of communication. These results, however, remain promises until large scale experimental realizations emerge. For the implementation of quantum information processing protocols, first a right representation has to be found in the chosen physical system. In addition, specifically for quantum computation, the robust manipulation of quantum information is also necessary.

In quantum optical implementations the physical system generally consists of one or more electromagnetic modes, and possibly atoms in a cavity. These are the candidates for providing quantum bits. Presently, pure optical quantum systems usually consist of several electromagnetic modes, and the most successfully used basic components are passive linear elements (such as beam splitters), and photo detectors. In these systems quantum bits are encoded in the states of electromagnetic modes, and the transformations for quantum logic are realized using the linear elements. Certain schemes combine these with detector feedback. Since the number of degrees of freedom of the electromagnetic field is very large, the choices of representing quantum bits are equally numerous. One already has the choice to use either one, two or more modes to represent a single qubit. And even when only a single mode is selected, we have the choice of working in a discrete or a continuous representation, and the dimensionality of the subspace designated to the representation is also at our choice.

In cavity QED implementations, the atoms in the cavity can also be used to represent quantum bits. In this case, in addition to the freedom of choice regarding the electromagnetic field, also the relevant electronic energy level structure of the atoms can be varied by choosing which kind of atoms and which of their spectral resonances are used. We see a wealth of additional possibilities to unfold when, in order to provide a basis for manipulation of quantum information, the atom–photon interaction inside the cavity is included in the description. From the theoretical point of view, this system allows immense number of configurations by choosing the atomic level structure, the polarisations and frequencies of the near-resonant cavity modes, and external pump lasers. Research on cavity QED quantum computing is concerned with finding out of these configurations, the most suitable under the various conditions.

Very important ones of these conditions, are decoherence phenomena present in such systems. These phenomena pose great obstacle to experimental realizations, and therefore must be considered in every theoretical proposal in as much detail as possible. Generally, decoherence comes from unwanted interaction of quantum bits with the environment or each other, and ultimately can lead to the loss of all the information initially encoded in the qubits. The typical decoherence channels in cavity QED systems are photon loss, and spontaneous decay of the excited atomic states.

Coherent state quantum bits

Coherent states are an interesting class of quantum states of the electromagnetic field for several reasons. These are important from the point of quantum state representation, since these form a complete continuous basis, and are also the natural basis for discussing standard decoherence effects of light. Additionally, coherent states can be produced by ideal lasers, and therefore these states constitute a readily available resource. We have recollected our results related to coherent state quantum bits in Chapter 2.

Coherent states are labelled by a complex variable that corresponds to the classical amplitude and phase. Their important feature from the aspect of quantum state representation is that coherent state basis is over complete, therefore the expansion into coherent states is not unique, furthermore, all coherent states overlap. This property also implies that the In the one-dimensional coherent state representation, every quantum state of the electromagnetic field is expanded using only a set of coherent states that lie along a single continuous curve in phase space. It is called one-dimensional, because a curve can be parametrised using one real variable. This representation works because of the over completeness of the coherent basis. A special case of the one-dimensional coherent state representation is when the chosen curve is a straight line across the origin. In this case a discrete basis can be expressed using Hermite polynomials.

The need for a two mode generalisation of the one-dimensional coherent state representation arises from the need to describe entangled states. We have made a generalisation based on two-mode squeezing. This work has been presented in Sec. 2.1, where we have first given a coherent state expansion of the two mode squeezed vacuum in terms of two-mode coherent states such as $|\alpha\rangle|\alpha^*\rangle$, using only a single complex variable. The weight function turned out to be a Gaussian, and we have proceeded showing that a discrete basis can be defined in terms of Laguerre-2D polynomials. We have proven the completeness of the thus defined one-complex plane representation using the completeness property of the Laguerre-2D basis.

The one-complex plane representation is especially useful for discussing two-mode squeezed states and describing the effects of decoherence. These advantages had later been exploited in the study of continuous variable teleportation both in the ideal and in lossy case.

In Sec. 2.2 we have introduced two-mode Schrödinger cat states, starting from the

one-complex plane representation. These states are generalisations of the usual optical Schrödinger cat states that exhibit up to two ebits of entanglement. We have developed a formalism to calculate the entanglement of a pure quantum state given in a non-orthogonal basis. We have calculated the entanglement of four different type of two-mode Schrödinger cats using this formalism. We identified which kind can be considered to be the best resource of reliable entanglement, and used it as the quantum channel in a teleportation protocol. We calculated explicitly what is the required Bell projection, and theoretically constructed an optical scheme that may be used to obtain successful teleportation with probability 1/8.

In Sec. 2.3 we have considered the decoherence problem of coherent state quantum bits using a model often used to describe decoherence in optics. In this model the interaction with the environment is represented by a beam splitter, with the signal and the environment mode entering on its two input ports. The state of the environment after the interaction is discarded by partial tracing. Under natural conditions the environment of an electromagnetic field is a thermal state very close to the vacuum, however, in certain cases the immediate environment of the observed system could be prepared in an alternative state.

We have studied a read-out problem of a deterministic quantum decision problem algorithm, under the effect of the above mentioned decoherence mechanism. The speciality of such an algorithm is that its output can only be one of the basis states, and cannot be a superposition. Examples to these are the Deutsch and the Deutsch–Jozsa algorithms. Therefore, in case of a coherent state based implementation, the read-out problem involves the discrimination of the two optical Schrödinger cat states. We have used the quantum version of the Sanov theorem to quantify distinguishablity. We could therefore give the probability of successfully distinguishing the two outcomes using optimal measurements, by calculating quantum relative entropies.

We have studied a case when the environment can be prepared in a squeezed vacuum state, and searched for an optimal value of the squeezing parameter that yields the best distinguishablity for a given representation and decoherence. We have found that a single variable is sufficient to incorporate effect of phase relations on the distinguishablity. This phase variable additively contains the phase of the Schrödinger cats, the squeezed state of the environment, and the phases of the beam splitter. Strong numerical evidence suggests that the optimal value for the thus defined phase variable is zero. We have studied the dependence of distinguishablity on the beam splitter transmission coefficient, the intensity of the coherent states in the Schrödinger cat states, and the magnitude of squeezing. Our numerical studies have shown that for every value of transmittance and intensity, there is an optimal value of squeezing. The results also indicate that the optimal relative improvement, due to the squeezing of the environment, increases with intensity of the coherent states in the basis states.

Quantum logic in atom–cavity systems

In Chapter 3 we have presented two proposals for cavity quantum electrodynamics quantum computing. In both schemes we have assumed that we had well localised, neutral atoms strongly coupled to a cavity field. Since the atoms are neutral there is no direct interaction between them, and the cavity field may act as the only significant mediator.

In the proposal of Sec. 3.1 we have considered a scheme where the atoms have two ground states and two excited states, the cavity has two modes with opposite circular polarisation nearly resonant with the atomic transition. When the cavity resonance frequencies are far detuned from the atomic transitions, and we start from an initial state where the cavity contains only one excitation and the atoms are in a superposition of the two ground states, the Hamiltonian of the system can be greatly simplified using certain approximations. Under these conditions the Hamiltonian takes the form of a spin z–z interaction with a star shaped topology, where a central spin is pair-wise coupled to all the other spins, and the rest are not coupled to each other. In this analogy, the central spin corresponds to the polarised photon in the cavity, and the other spins to the two-level atoms.

To formulate quantum logic, we have associated one quantum bit to each atom, and an additional one to the polarised photon in the cavity. For N atoms this yielded $N + 1$ quantum bits, the photonic quantum bit playing a distinguished role. Using the refocussing technique from nuclear magnetic resonance quantum computing, we have derived effective two qubit gates based based on the above-mentioned spin z–z coupling. To perform refocussing, it is sufficient to realise single qubit operations on the atoms, and such operations can be carried out using resonant Raman pulses. We have suggested that to realize a CNOT gate, a sufficient set of single qubit operations could be realized, in addition to the Raman pulses, by injecting a two level Rydberg atom into the cavity, and varying its transition frequency using a static external field. We have pointed out that with CNOT gates between the cavity qubit and any atomic qubit, any quantum operation can be constructed, with the photonic qubit acting as an "optical bus."

In this proposal we have described a system where there are no theoretical limitations to scalability since N can be a number of any order. Also, since only the ground states of the atoms have been used in the proposal, the impact of atomic decay rate is weak. Related to the decoherence of the system, the only significant issue is cavity loss, that therefore places challenging requirements on the quality of the cavity.

In Sec. 3.2 we have considered an other configuration where the atoms have only two levels, and they interact dispersively with a single mode of the cavity electromagnetic field. Due to Stark shifts, an effective interaction between the atoms arises, that under certain conditions induces an approximately unitary time evolution regarding even only the atomic system. The Hamiltonian of this evolution is quadratic in terms of the collective spin operators, and diagonal in the Dicke state basis.

We have pointed out that this Hamiltonian can serve as a basis for universal quantum computing together with local unitary control for any number of atoms. In this system

complete local unitary control can be achieved by selectively addressing the atoms by resonant laser pulses. Up to $N = 3$ atoms we have given an explicit recipe for exact construction of quantum logic. We have given the respective decompositions of the universal CNOT gate in terms of applications of single qubit operations and the collective time evolution.

For the $N = 3$ atom system, in first step we have reduced the three qubit interaction to a two qubit gate using a technique similar to that of refocussing in nuclear magnetic resonance. In the second step, we have used this two qubit gate to construct various CNOT gates, with the aid of the invariant method. To underline the computational universality of this interaction for this system, we have discussed the construction of a simplified version of the three qubit Toffoli gate.

A peculiarity of the last proposal for realisation of quantum logic is that although its operation relies heavily on the presence of the cavity, it is very robust against cavity losses. A higher photonic decay rate only reduces strength of the effective coupling between the qubits, but it does not increase decoherence. The major source of decoherence remains the spontaneous decay of the excited atomic state. However, due to the simplicity of the atomic structure in the proposal, with considerations to the actual experimental circumstances, the scheme can easily be modified in a way that the impact of this effect can be almost completely eliminated.

Theses

1. We have introduced a representation of states of the two mode electromagnetic field, that uses functions depending on a single complex variable. The representation is based on continuous superposition of two-mode coherent states of the form $|\alpha\rangle|\alpha^*\rangle$. For these reasons, the representation has therefore been termed one-complex plane coherent state representation. We have shown that there exists a one-to-one mapping between two-mode squeezed Fock states and Laguerre-2D polynomials. We have used this result to demonstrate that every state of the two-mode electromagnetic field can be represented by a function of a single complex variable. [I, II]

2. We have proposed a two mode generalisation of optical Schrödinger cat states. We have developed a formalism to calculate bipartite entanglement of pure states in a non-orthogonal basis, and using this formalism we have shown that these two mode Schrödinger cat states are generally entangled. As an illustration we have devised a quantum teleportation protocol where the quantum channel is made up by a two-mode Schrödinger cat state. We have made a proposal that can serve as a basis for a linear optical implementation of the partial Bell detection, and shown that it simultaneously allows conditional teleportation of two quantum bits, with a probability 1/8. [III]

3. Taking a general approach to measurement, based on the quantum version of Sanov

theorem we have shown that distinguishablity of optical Schrödinger cat states can be better conserved by preparing their immediate environment in a squeezed state. A typical example where this distinguishablity problem arises is the read-out stage of a deterministic decision problem quantum algorithm. Based on numerical results, we have concluded that there is a unique optimal setting of the phase parameters in the system, and for every selection of Schrödinger cat states and strength of decoherence there is an optimal magnitude of squeezing for the environment. [IV]

4. We have proposed a potentially scalable cavity QED scheme for quantum logic. The proposed setup consists of N four-level atoms localised in a bimodal cavity, such that each atom and the cavity photon realises a quantum bit. We have shown that universal quantum logic can be realized along the same lines as for NMR quantum computing. The single qubit gates required for operation could be performed on the atomic quantum bits by resonant Raman pulses, and by an auxiliary atom on the photonic quantum bit. Since the photonic quantum bit is the only quantum bit in the scheme that interacts with the others, it plays the role of an optical bus. [V]

5. We have proposed a scheme for quantum logic on two-level atoms in a dispersive cavity. We have pointed out the computational universality of the system for any number of atoms. In the two atom and the three atom case we have derived CNOT gates exactly. The multi-qubit gates have been constructed using single qubit gates realised by resonant external laser pulses, and the collective interaction of the atoms induced by the cavity. The proposed system is particularly robust against cavity losses, and these losses are generally the main source of decoherence in cavity QED schemes. This robustness manifests itself in features, that the state of the cavity can be any thermal distribution, and an increase in the loss rate does not increase decoherence, it merely reduces the effective coupling between the atoms. [VI]

List of publications

Related publications

[I] József Janszky, Aurél Gábris, Mátyás Koniorczyk, András Vukics, and Péter Ádám, *Coherent-state approach to entanglement and teleportation*, Fortschr. Phys. **49**, 993 (2001).

[II] József Janszky, Aurél Gábris, Mátyás Koniorczyk, András Vukics, and János Asbóth, *One-complex-plane representation: a coherent state description of entanglement and teleportation*, J. Opt. B **4**, S213 (2002).

[III] József Janszky, János Asbóth, Aurél Gábris, András Vukics, Mátyás Koniorczyk, and Takayoshi Kobayashi, *Two-mode Schrödinger cats, entanglement and teleportation*, Fortschr. Phys **51**, 157 (2003).

[IV] Aurél Gábris, Péter Ádám, Mátyás Koniorczyk, and József Janszky, *Distinguishing Schrödinger cats in a lossy environment*, J. Opt. B: Quantum Semiclass. Opt. **6**, S84 (2004).

[V] Aurél Gábris and Girish S. Agarwal, *Controlled-NOT gates for four-level atoms in a bimodal cavity*, Acta Physica Hungarica B: Quantum Electronics **23**, 19 (2005).

[VI] Aurél Gábris and Girish S. Agarwal, *Vacuum induced Stark shifts for quantum logic using a collective system in a high quality dispersive cavity*, Phys. Rev. A **71**, 052316 (2005).

Other publications

[VII] Mátyás Koniorczyk, Zoltán Kurucz, Aurél Gábris, and József Janszky, *General optical state truncation and its teleportation*, Phys. Rev. A **62**, 013802 (2000).

[VIII] Ágnes Cziráki, Imre Gerőcs, Mercédesz Köteles, Aurél Gábris, Lajos Pogány, Imre Bakonyi, et al., *Structural features of the La-Sr-Fe-Co-O system*, Eur. Phys. J. B **21**, 521 (2001).

[IX] József Janszky, Mátyás Koniorczyk, and Aurél Gábris, *One-complex-plane representation approach to continuous variable quantum teleportation*, Phys. Rev. A **64**, 034302 (2001).

[X] A. Gábris and G. S. Agarwal, *Quantum teleportation with pair-coherent states*, Int. Journal of Quant. Inf. **5**, 17 (2007).

Acknowledgments

I would like to thank my supervisor Prof. József Janszky for his guidance throughout my years at the Research Institute for Solid State Physics and Optics. Without his professional and moral support this work could not have been completed. I would also like to thank Prof. Girish S. Agarwal, with whom the majority of work in Chapter 3 has been done during my visit to the Physical Research Laboratory, Ahmedabad.

I would like to express my gratitude towards Péter Domokos and especially Tamás Kiss, who have dedicated their valuable time to carefully reading the manuscript and adding their indispensable comments and suggestions to it. I am also indebted to my in-house opponents Péter Földi and Gábor Demeter for their thorough review, and helpful comments.

I would also like to thank all the present and past members of the Department of Nonlinear and Quantum Optics whom I had the opportunity to work with, for creating and maintaining an inspiring working and social atmosphere. In particular, I would like to thank our head Péter Ádám, who has a great share in creating this atmosphere. In addition to those already mentioned from our group, I would like to thank Zolán Kurucz with whom we had several memorable discussions during our student years, and also Mátyás Koniorczyk, Zsolt Kis, János Asbóth, Attila Kárpáti, Géza Tóth, András Vukics and Dávid Nagy.

I would also like to thank my family for their loving understanding and generous support they provided, despite the fact that I could never explain them well what is now written down in this dissertation.

Bibliography

[1] Marlan O. Scully and M. Suhail Zubairy, *Quantum Optics* (Cambridge, U.K., Cambridge University Press, 1997).

[2] William Henry Louisell, *Quantum Statistical Properties of Radiation*, Wiley Classics Library (John Wiley & Sons, 1990).

[3] Wolfgang P. Schleich, *Quantum Optics in Phase Space* (Wiley-VCH, Wiley-VCH Berlin, 2001).

[4] Claude Cohen-Tannoudji, Jacques Dupont-Roc, and Gilbert Grynberg, *Atom-photon interactions: basic processes and applications* (Wiley, New York, 1992).

[5] Claude Cohen-Tannoudji, Jacques Dupont-Roc, and Gilbert Grynberg, *Photons and atoms: introduction to quantum electrodynamics* (Wiley, New York, 1989).

[6] Leonard Mandel and Emil Wolf, *Optical coherence and quantum optics* (Cambridge University Press, Cambridge, 1995).

[7] Max Born and Emil Wolf, *Principles of optics; electromagnetic theory of propagation, interference and diffraction of light* (Pergamon Press, 1970).

[8] John David Jackson, *Classical Electrodynamics* (John Wiley & Sons, 1998), 3rd ed.

[9] Claude E. Shannon and Warren Weaver, *The Mathematical Theory of Communication* (University of Illinois Press, Urbana, IL, 1949).

[10] Rolf Landauer, *Information is physical*, Physics Today **May**, 23 (1991).

[11] Dirk Bouwmeester, Artur K. Ekert, and Anton Zeilinger, eds., *The physics of quantum information: quantum cryptography, quantum teleportation, quantum computation* (Springer, Berlin, 2000).

[12] Dieter Heiss, ed., *Fundamentals of quantum information: quantum computation, communication, decoherence, and all that*, no. 587 in Lecture notes in physics (Springer, New York, 2002).

[13] Hoi-Kwong Lo, Tim Spiller, and Sandu Popescu, *Introduction to Quantum Computation and Information* (World Scientific, Singapore, 1998).

[14] Jozef Gruska, *Quantum Computing* (McGraw-Hill, Maidenhead, Berkshire, 1999).

[15] Goong Chen and Ranee K. Brylinski, eds., *Mathematics of quantum computation* (Chapman and Hall/CRC, 2002).

[16] John Preskill, *Lecture Notes for Physics 219: Quantum Computation* (2004), `http://www.theory.caltech.edu/~preskill/ph219`.

[17] Alexei Yu. Kitaev, A. H. Shen, and M. N. Vyalyi, *Classical and quantum computation* (American Mathematical Society, Providence, R.I., 2002).

[18] Michael A. Nielsen and Isaac L. Chuang, *Quantum computation and quantum information* (Cambridge University Press, Cambridge, 2000).

[19] Benjamin Schumacher, *Quantum coding*, Phys. Rev. A **51**, 2738 (1995).

[20] Imre Csiszár and János G. Korner, *Information Theory - Coding Theorems for Discrete Memoryless Systems* (Academic Press, New York, 1981).

[21] Claude Cohen-Tannoudji, Barnard Diu, and Franck Laoë, *Quantum Mechanics* (Wiley-Interscience, New York, 1998).

[22] Albert Messiah, *Quantum Mechanics* (Dover, 1999).

[23] Asher Peres, *Quantum Theory: Concepts and Methods*, vol. 57 of *Fundamental Theories of Physics* (Kluwer Academic Publishers, 1995).

[24] Jun John Sakurai, *Modern Quantum Mechanics* (Addison-Wesley, Reading, Mass., 1994).

[25] David Bohm, *Quantum theory* (Prentice-Hall, New York, 1951).

[26] Károly Nagy, *Kvantummechanika* (Nemzeti Tankönyv Kiadó, Budapest, 2000).

[27] John von Neumann, *Mathematische Grundlagen der Quantenmechanik* (Springer, Berlin, 1932).

[28] Paul Busch, Pekka Lahti, and Peter Mittelstaedt, *The Quantum Theory of Measurement*, Lecture Notes in Physics New Series M (Springer-Verlag Telos, Berlin, 1991).

[29] Ervin Schrödinger, *Die gegenwärtige Situation in der Quantenmechanik*, Naturwissenschaften **23**, 807 (1935).

[30] John S. Bell, *On the Einstein-Podolsky-Rosen paradox*, Physics **1**, 195 (1964).

[31] John S. Bell, *Speakable and Unspeakable in Quantum Mechanics* (Cambridge University Press, Cambridge, 1987).

[32] Albert Einstein, Boris Podolsky, and Nathan Rosen, *Can quantum-mechanical description of physical reality be considered complete?*, Phys. Rev. **47**, 777 (1935).

[33] Michał Horodecki, Paweł Horodecki, and Ryszard Horodecki, *Separability of mixed states: necessary and sufficient conditions*, Physics Letters A **223**, 1 (1996).

[34] R. Simon, *Peres-Horodecki separability criterion for continuous variable systems*, Phys. Rev. Lett. **84**, 2726 (2000).

[35] Charles H. Bennett, David P. DiVincenzo, John A. Smolin, and William K. Wootters, *Mixed-state entanglement and quantum error correction*, Phys. Rev. A **54**, 3824 (1996).

[36] Scott Hill and William K. Wootters, *Entanglement of a pair of quantum bits*, Phys. Rev. Lett. **78**, 5022 (1997).

[37] Guifré Vidal and Reinhard F. Werner, *Computable measure of entanglement*, Phys. Rev. A **65**, 032314 (2002).

[38] Vlatko Vedral and Martin B. Plenio, *Entanglement measures and purification procedures*, Phys. Rev. A **57**, 1619 (1998).

[39] Michał Horodecki, Paweł Horodecki, and Ryszard Horodecki, *Limits for entanglement measures*, Phys. Rev. Lett. **84**, 2014 (2000).

[40] Géza Tóth and Otfried Gühne, *Detecting genuine multipartite entanglement with two local measurements*, Phys. Rev. Lett. **94**, 060501 (2005).

[41] Mohamed Bourennane, Manfred Eibl, Christian Kurtsiefer, Sascha Gaertner, Harald Weinfurter, Otfried Gühne, et al., *Experimental detection of multipartite entanglement using witness operators*, Phys. Rev. Lett. **92**, 087902 (2004).

[42] Zhi Zhao, Yu-Ao Chen, An-Ning Zhang, Tao Yang, Hans J. Briegel, and Jian-Wei Pan, *Experimental demonstration of five-photon entanglement and open-destination teleportation*, Nature **430**, 54 (2004).

[43] Zhi Zhao, Tao Yang, Yu-Ao Chen, An-Ning Zhang, Marek Żukowski, and Jian-Wei Pan, *Experimental violation of local realism by four-photon greenberger-horne-zeilinger entanglement*, Phys. Rev. Lett. **91**, 180401 (2003).

[44] Cass A. Sackett, David Kielpinski, Brian E. King, C. Langer, Volker Meyer, Christopher J. Myatt, et al., *Experimental entanglement of four particles*, Nature **404**, 256 (2000).

[45] Olaf Mandel, Markus Greiner, Artur Widera, Tim Rom, Theodor W. Hänsch, and Immanuel Bloch, *Controlled collisions for multi-particle entanglement of optically trapped atoms*, Nature **425**, 937 (2003).

[46] Richard Jozsa, in *The Geometric Universe*, edited by S. Huggett, L. Mason, K.P. Tod, S. T. Tsou, and N. M. J. Woodhouse (Oxford University Press, Oxford, 1998), p. 369.

[47] Artur Ekert, Richard Jozsa, and P. Marcer, *Quantum algorithms: Entanglement-enhanced information processing [and discussion]*, Phil. Trans.: Phys. Eng. Sci. **356**, 1769 (1998).

[48] Susana F. Huelga, Chiara Macchiavello, Thomas Pellizzari, Artur K. Ekert, Martin B. Plenio, and J. Ignacio Cirac, *Improvement of frequency standards with quantum entanglement*, Phys. Rev. Lett. **79**, 3865 (1997).

[49] David Deutsch, *Quantum theory, the Church-Turing principle and the universal quantum computer*, Proc. R. Soc. Lond. A **400**, 97 (1985).

[50] David Deutsch and Richard Jozsa, *Rapid solution of problems by quantum computation*, Proc. R. Soc. Lond. A **439**, 553 (1992).

[51] Peter W. Shor, in *35*$^{\text{th}}$ *Annual Symposium on the Foundations of Computer Science, Los Alamitos* (CA IEEE Computer Society Press, New York, 1994), p. 124.

[52] Don Coppersmith, in *IBM Internal Report No. RC19642* (1994), arXiv: quant-ph/0201067.

[53] Peter W. Shor, *Polynomial-time algorithms for prime factorization and discrete logarithms on a quantum computer*, SIAM J. Sci. Statist. Comput. **26**, 1484 (1997), arXiv: quant-ph/9508027.

[54] David Beckman, Amalavoyal N. Chari, Srikrishna Devabhaktuni, and John Preskill, *Efficient networks for quantum factoring*, Phys. Rev. A **54**, 1034 (1996).

[55] Artur Ekert and Richard Jozsa, *Quantum computation and Shor's factoring algorithm*, Rev. Mod. Phys. **68**, 733 (1996).

[56] Lov Grover, in *Proc. 28*$^{\text{th}}$ *Annual ACM Symposium on the Theory of Computing (STOC)* (ACM Press, New York, 1996), pp. 212–219, arXiv: quant-ph/9605043.

[57] Lov K. Grover, *Quantum mechanics helps in searching for a needle in a haystack*, Phys. Rev. Lett. **79**, 325 (1997).

[58] Charles H. Bennett and Gilles Brassard, in *Proceedings of IEEE International Conference on Computers, Systems and Signal Processing, Bangalore, India* (IEEE, New York, 1984), pp. 175 – 179.

[59] Charles H. Bennett, François Bessette, Gilles Brassard, Louis Salvail, and John Smolin, *Experimental quantum cryptography*, Journal of Cryptology **5**, 3 (1992).

[60] Charles H. Bennett, *Quantum cryptography using any two nonorthogonal states*, Phys. Rev. Lett. **68**, 3121 (1992).

[61] Artur K. Ekert, *Quantum cryptography based on Bell's theorem*, Phys. Rev. Lett. **67**, 661 (1991).

[62] Bruno Huttner and Artur K. Ekert, *Information gain in quantum eavesdropping*, Journal of Modern Optics **41**, 2455 (1994).

[63] David Deutsch, Adriano Barenco, and Artur Ekert, *Universality in quantum computation*, Proceedings: Mathematical and Physical Sciences **449**, 669 (1995).

[64] Richard Feynman, *Simulating physics with computers*, Int. J. Theor. Phys. **21**, 467 (1982).

[65] David Deutsch, *Quantum computational networks*, Proc. R. Soc. Lond. A **425**, 73 (1989).

[66] Ethan Bernstein and Umesh Vazirani, in *Proceedings of the 25$^{\text{th}}$ Annual ACM Symposium on Theory of Computing (STOC)* (ACM Press, New York, 1993), pp. 11–20, `http://portal.acm.org/citation.cfm?id=167097`.

[67] Adriano Barenco, Charles H. Bennett, Richard Cleve, David P. DiVincenzo, Norman Margolus, Peter Shor, et al., *Elementary gates for quantum computation*, Phys. Rev. A **52**, 3457 (1995).

[68] Camille Negrevergne, Rolando Somma, Gerardo Ortiz, Emanuel Knill, and Raymond Laflamme, *Liquid-state NMR simulations of quantum many-body problems*, Phys. Rev. A **71**, 032344 (2005).

[69] Lee Spector, *Automatic quantum computer programming: a genetic programming approach* (Kluwer, Boston, 2004).

[70] Emanuel Knill and Raymond Laflamme, *Quantum computing and quadratically signed weight enumerators*, Inf. Process. Lett. **79**, 173 (2001), arXiv: quant-ph/9909094.

[71] Howard Carmichael, *An open systems approach to quantum optics: lectures presented at the Université libre de Bruxelles, October 28 to November 4*, Lecture notes in physics (Springer-Verlag, Berlin, 1991).

[72] Wojciech H. Zurek, *Pointer basis of quantum apparatus: Into what mixture does the wave packet collapse?*, Phys. Rev. D **24**, 1516 (1981).

[73] Wojciech H. Zurek, *Environment-induced superselection rules*, Phys. Rev. D **26**, 1862 (1982).

[74] Barry M. Garraway, *Decay of an atom coupled strongly to a reservoir*, Phys. Rev. A **55**, 4636 (1997).

[75] William G. Unruh, *Maintaining coherence in quantum computers*, Phys. Rev. A **51**, 992 (1995).

[76] G. Massimo Palma, Kalle-Antti Suominen, and Artur K. Ekert, *Quantum computers and dissipation*, Proc. R. Soc. Lond. A **452**, 567 (1996).

[77] Erich Joos, ed., *Decoherence and the appearance of a classical world in quantum theory* (Springer, Berlin, 2003), 2nd ed.

[78] Peter W. Shor, *Scheme for reducing decoherence in quantum computer memory*, Phys. Rev. A **52**, 2493 (1995).

[79] Andrew M. Steane, *Error correcting codes in quantum theory*, Phys. Rev. Lett. **77**, 793 (1996).

[80] Andrew Steane, *Multiple-particle interference and quantum error correction*, Proc. R. Soc. Lond. A **452**, 2551 (1996).

[81] A. Robert Calderbank and Peter W. Shor, *Good quantum error-correcting codes exist*, Phys. Rev. A **54**, 1098 (1996).

[82] Daniel Gottesman, *Class of quantum error-correcting codes saturating the quantum hamming bound*, Phys. Rev. A **54**, 1862 (1996).

[83] A. Robert Calderbank, Eric M. Rains, Peter W. Shor, and Neil J. A. Sloane, *Quantum error correction and orthogonal geometry*, Phys. Rev. Lett. **78**, 405 (1997).

[84] Emanuel Knill and Raymond Laflamme, *Theory of quantum error-correcting codes*, Phys. Rev. A 55 **55**, 900 (1997).

[85] Mark Hillery, Robert F. O'Connell, Marlan O. Scully, and Eugene P. Wigner, *Distribution functions in physics: Fundamentals*, Physics Reports **106**, 121 (1984).

[86] József Janszky, Aurél Gábris, Mátyás Koniorczyk, András Vukics, and Péter Ádám, *Coherent-state approach to entanglement and teleportation*, Fortschr. Phys. **49**, 993 (2001).

[87] József Janszky, Aurél Gábris, Mátyás Koniorczyk, András Vukics, and János Asbóth, *One-complex-plane representation: a coherent state description of entanglement and teleportation*, J. Opt. B **4**, S213 (2002).

[88] József Janszky, Mátyás Koniorczyk, and Aurél Gábris, *One-complex-plane representation approach to continuous variable quantum teleportation*, Phys. Rev. A **64**, 034302 (2001).

[89] Charles H. Bennett, Gilles Brassard, Claude Crépeau, Richard Jozsa, Asher Peres, , et al., *Teleporting an unknown quantum state via dual classical and einstein-podolsky-rosen channels*, Phys. Rev. Lett. **70**, 1895 (1993).

[90] Samuel L. Braunstein and H. Jeff Kimble, *Teleportation of continuous quantum variables*, Phys. Rev. Lett. **80**, 869 (1998).

[91] H. Jeong and Myung Shik Kim, *Efficient quantum computation using coherent states*, Phys. Rev. A **65**, 042305 (2002).

[92] Timothy C. Ralph, Alexei Gilchrist, Gerard J. Milburn, William J. Munro, and Scott Glancy, *Quantum computation with optical coherent states*, Phys. Rev. A **68**, 042319 (2003).

[93] József Janszky, János Asbóth, Aurél Gábris, András Vukics, Mátyás Koniorczyk, and Takayoshi Kobayashi, *Two-mode Schrödinger cats, entanglement and teleportation*, Fortschr. Phys **51**, 157 (2003).

[94] Steven J. van Enk and Osamu Hirota, *Entangled coherent states: Teleportation and decoherence*, Phys. Rev. A **64**, 022313 (2001).

[95] Paul T. Cochrane, Gerard J. Milburn, and William J. Munro, *Macroscopically distinct quantum-superposition states as a bosonic code for amplitude damping*, Phys. Rev. A **59**, 2631 (1999).

[96] Masahito Hayashi, *Asymptotics of quantum relative entropy from a representation theoretical viewpoint*, J. Phys. A: Math. Gen. **31**, 3413 (2001).

[97] Fumio Hiai and Dénes Petz, *The proper formula for relative entropy and its asymptotics in quantum probability*, Commun. Math. Phys. **143**, 99 (1991).

[98] Aurél Gábris, Péter Ádám, Mátyás Koniorczyk, and József Janszky, *Distinguishing Schrödinger cats in a lossy environment*, J. Opt. B: Quantum Semiclass. Opt. **6**, S84 (2004).

[99] Tadamasa Kimura, Yoshihiro Nambu, Takaaki Hatanaka, Akihisa Tomita, Hideo Kosaka, and Kazuo Nakamura, *Single-photon interference over 150 km transmission using silica-based integrated-optic interferometers for quantum cryptography*, Jpn. J. Appl. Phys. **43**, L1217 (2004), arXiv: quant-ph/0403104.

[100] Michael Reck, Anton Zeilinger, Herbert J. Bernstein, and Philip Bertani, *Experimental realization of any discrete unitary operator*, Phys. Rev. Lett. **73**, 58 (1994).

[101] Bernard Yurke and David Stoler, *Generating quantum mechanical superpositions of macroscopically distinguishable states via amplitude dispersion*, Phys. Rev. Lett. **57**, 13 (1986).

[102] Gerard J. Milburn, *Quantum optical Fredkin gate*, Phys. Rev. Lett. **62**, 2124 (1989).

[103] Christopher C. Gerry, *Generation of optical macroscopic quantum superposition states via state reduction with a Mach-Zehnder interferometer containing a Kerr medium*, Phys. Rev. A **59**, 4095 (1999).

[104] Emanuel Knill, Raymond Laflamme, and Gerard J. Milburn, *A scheme for efficient quantum computation with linear optics*, Nature **409**, 46 (2001).

[105] Quentin A. Turchette, Christina J. Hood, Wolfgang Lange, Hideo Mabuchi, and H. Jeff Kimble, *Measurement of conditional phase shifts for quantum logic*, Phys. Rev. Lett. pp. 4710–4713 (1995).

[106] Arno Rauschenbeutel, Gilles Nogues, Stefano Osnaghi, Patrice Bertet, Michel Brune, Jean-Michel Raimond, et al., *Coherent operation of a tunable quantum phase gate in cavity QED*, Phys. Rev. Lett. **83**, 5166 (1999).

[107] Thomas Pellizzari, Simon A. Gardiner, J. Ignacio Cirac, and Peter Zoller, *Decoherence, continuous observation, and quantum computing: A cavity QED model*, Phys. Rev. Lett. **75**, 3788 (1995).

[108] Sergio M. Dutra, *Cavity Quantum Electrodynamics* (John Wiley & Sons, 2005).

[109] Paul R. Berman, ed., *Cavity Quantum Electrodynamics*, In series: Advances in Atomic, Molecular and Optical Physics (Academic Press, San Diego, 1994).

[110] Serge Haroche, in *Fundamental Systems in Quantum Optics*, edited by Jean Dalibard, Jean-Michel Raimond, and Jean Zinn-Justin (North-Holland, Amsterdam, 1992), Proceedings of the Les Houches Summer School, Session LIII, 1990.

[111] Aurél Gábris and Girish S. Agarwal, *Controlled-NOT gates for four-level atoms in a bimodal cavity*, Acta Physica Hungarica B: Quantum Electronics **23**, 19 (2005).

[112] Aurél Gábris and Girish S. Agarwal, *Vacuum induced Stark shifts for quantum logic using a collective system in a high quality dispersive cavity*, Phys. Rev. A **71**, 052316 (2005).

[113] Peter W. Milonni, *The Quantum Vacuum: An introduction to quantum electrodynamics* (Academic Press, San Diego, 1994).

[114] Dik Bouwmeester, Jian-Wei Pan, Klaus Mattle, Manfred Eibl, Harald Weinfurter, and Anton Zeilinger, *Experimental quantum teleportation*, Nature **390**, 575 (1997).

[115] Ulf Leonhardt, *Measuring the quantum state of light* (Cambridge University Press, Cambridge, 1997).

[116] Paul M. Radmore and Stephen M. Barnett, *Methods in Theoretical Quantum Optics* (Oxford University Press, Oxford, 1997).

[117] Roy J. Glauber, *Coherent and incoherent states of the radiation field*, Phys. Rev. **130**, 2766 (1963).

[118] Peter Adam, István Földesi, and József Janszky, *Complete basis set via straight-line coherent-state superpositions*, Phys. Rev. A **49**, 1281 (1994).

[119] Roy J. Glauber, *The quantum theory of optical coherence*, Phys. Rev. **130**, 2529 (1963).

[120] Géza Giedke and J. Ignacio Cirac, *Characterization of Gaussian operations and distillation of Gaussian states*, Phys. Rev. A **66**, 032316 (2002).

[121] Kevin E. Cahill, *Coherent-state representations for the photon density operator*, Phys. Rev. **138**, B1566 (1965).

[122] Péter Domokos, Peter Adam, and József Janszky, *One-dimensional coherent-state representation on a circle in phase space*, Phys. Rev. A **50**, 4293 (1994).

[123] Nicolas J. Cerf, Christoph Adami, and Paul G. Kwiat, *Optical simulation of quantum logic*, Phys. Rev. A **57**, R1477 (1998).

[124] Richard A. Campos, Bahaa E. A. Saleh, and Malvin C. Teich, *Quantum-mechanical lossless beam splitter: $SU(2)$ symmetry and photon statistics*, Phys. Rev. A **40**, 1371 (1989).

[125] János K. Asbóth, John Calsamiglia, and Helmut Ritsch, *Computable measure of nonclassicality for light*, Phys. Rev. Lett. **94**, 173602 (2005).

[126] Stephen M. Barnett and David T. Pegg, *Phase in quantum optics*, J. Phys. A: Math. Gen. **19**, 3849 (1986).

[127] Asoka Biswas and Girish S. Agarwal, *Transfer of an unknown quantum state, quantum networks, and memory*, Phys. Rev. A **70**, 022323 (2004).

[128] Edward Fredkin and Tommaso Toffoli, *Conservative logic*, Int. J. Theor. Phys. **21**, 219 (1982).

[129] Michael J. Bremner, Christopher M. Dawson, Jennifer L. Dodd, Alexei Gilchrist, Aram W. Harrow, Duncan Mortimer, et al., *Practical scheme for quantum computation with any two-qubit entangling gate*, Phys. Rev. Lett. **89**, 247902 (2002).

[130] Yuriy Makhlin, *Nonlocal properties of two-qubit gates and mixed states and optimization of quantum computations*, Quant. Info. Process. **1**, 243 (2002), arXiv: quant-ph/0002045.

[131] David P. DiVincenzo, *Two-bit gates are universal for quantum computation*, Phys. Rev. A **51**, 1015 (1995).

[132] Emanuel Knill, Isaac, Chuang, and Raymond Laflamme, *Effective pure states for bulk quantum computation*, Phys. Rev. A **57**, 3348 (1998).

[133] Seth Lloyd, *Almost any quantum logic gate is universal*, Phys. Rev. Lett. **75**, 346 (1995).

[134] Nik Weaver, *On the universality of almost every quantum logic gate*, J. Math. Phys. **41**, 240 (2000).

[135] Jennifer L. Dodd, Michael A. Nielsen, Michael J. Bremner, and Robert T. Thew, *Universal quantum computation and simulation using any entangling hamiltonian and local unitaries*, Phys. Rev. A **65**, 040301 (2002).

[136] Michael A. Nielsen, Michael J. Bremner, Jennifer L. Dodd, Andrew M. Childs, and Christopher M. Dawson, *Universal simulation of hamiltonian dynamics for quantum systems with finite-dimensional state spaces*, Phys. Rev. A **66**, 022317 (2002).

[137] Michael J. Bremner, Jennifer L. Dodd, Michael A. Nielsen, and Dave Bacon, *Fungible dynamics: There are only two types of entangling multiple-qubit interactions*, Phys. Rev. A **69**, 012313 (2004).

[138] Michael J. Bremner, Dave Bacon, and Michael A. Nielsen, *Simulating hamiltonian dynamics using many-qudit hamiltonians and local unitary control*, Phys. Rev. A **71**, 052312 (2005).

[139] Wan-Li Li, Chuan-Feng Li, and Guang-Can Guo, *Probabilistic teleportation and entanglement matching*, Phys. Rev. A **61**, 034301 (2000).

[140] Zoltán Kurucz, Mátyás Koniorczyk, Peter Adam, and József Janszky, *An operator description of entanglement matching in quantum teleportation*, J. Opt. B: Quantum Semiclass. Opt. **5**, S627 (2003).

[141] Akira Furusawa, Jens L. Sørensen, Samuel L. Braunstein, Christopher A. Fuchs, H. Jeff Kimble, and Eugene S. Polzik, *Unconditional quantum teleportation*, Science **282**, 706 (1998).

[142] Samuel L. Braunstein, Christopher A. Fuchs, and H. Jeff Kimble, *Criteria for continuous-variable quantum teleportation*, J. Mod. Opt **47**, 267 (2000).

[143] Samuel L. Braunstein, Christopher A. Fuchs, H. Jeff Kimble, and P. van Loock, *Quantum versus classical domains for teleportation with continuous variables*, Phys. Rev. A **64**, 022321 (2001).

[144] Girish S. Agarwal, *Quantum optics. Quantum statistical theories of spontaneous emission and their relation to other approaches*, vol. 70 of *Springer tracts in modern physics* (Springer Verlag, Berlin, 1974).

[145] Vlatko Vedral, *The role of relative entropy in quantum information theory*, Rev. Mod. Phys. **74**, 197 (2002).

[146] Alfred Wünsche, *Laguerre 2d-functions and their application in quantum optics*, J. Phys. A: Math. Gen. **66**, 8267 (1998).

[147] András Vukics, József Janszky, and Takayoshi Kobayashi, *Nonideal teleportation in coherent-state basis*, Phys. Rev. A **66**, 023809 (2002).

[148] Askold M. Perelomov, *Coherent states for arbitrary lie group*, Commun. Math. Phys **26**, 222 (1972).

[149] Szilárd Szabó, Péter Ádám, József Janszky, and Péter Domokos, *Construction of quantum states of the radiation field by discrete coherent-state superpositions*, Phys. Rev. A **53**, 2698 (1996).

[150] József Janszky, Péter Domokos, Szilárd Szabó, and Péter Ádám, *Quantum-state engineering via discrete coherent-state superpositions*, Phys. Rev. A **51**, 4191 (1995).

[151] Chin-Lin Chai, *Two-mode nonclassical state via superpositions of two-mode coherent states*, Phys. Rev. A **46**, 7187 (1992).

[152] Ludwig Knöll, Stefan Scheel, Eduard Schmidt, Dirk-Gunnar Welsch, and Aleksej V. Chizhov, *Quantum-state transformation by dispersive and absorbing four-port devices*, Phys. Rev. A **59**, 4716 (1999).

[153] Stefan Scheel, Ludwig Knöll, Tomáš Opatrný, and Dirk-Gunnar Welsch, *Entanglement transformation at absorbing and amplifying four-port devices*, Phys. Rev. A **62**, 043803 (2000).

[154] H. Jeff Kimble, Yuri Levin, Andrey B. Matsko, Kip S. Thorne, and Sergey P. Vyatchanin, *Conversion of conventional gravitational-wave interferometers into quantum nondemolition interferometers by modifying their input and/or output optics*, Phys. Rev. D **65**, 022002 (2001).

[155] S. J. van Enk, J. I. Cirac, and P. Zoller, *Purifying two-bit quantum gates and joint measurements in cavity qed*, Phys. Rev. Lett. **79**, 5178 (1997).

[156] X. X. Yi, X. H. Su, and L. You, *Conditional quantum phase gate between two 3-state atoms*, Phys. Rev. Lett. **90**, 097902 (2003).

[157] E. Solano, M. Fran ca Santos, and P. Milman, *Quantum phase gate with a selective interaction*, Phys. Rev. A **64**, 024304 (2001).

[158] Mang Feng, *Quantum computing with trapped ions in an optical cavity via raman transition*, Phys. Rev. A **66**, 054303 (2002).

[159] E. Jané, M. B. Plenio, and D. Jonathan, *Quantum-information processing in strongly detuned optical cavities*, Phys. Rev. A **65**, 050302(R) (2002).

[160] Jiannis Pachos and Herbert Walther, *Quantum computation with trapped ions in an optical cavity*, Phys. Rev. Lett. **89**, 187903 (2002).

[161] P. Milman, H. Ollivier, F. Yamaguchi, M. Brune, J. M. Raimond, and S. Haroche, *Simple quantum information algorithms in cavity qed*, J. Mod. Opt. **50**, 901 (2002).

[162] P. Domokos, J. M. Raimond, M. Brune, and S. Haroche, *Simple cavity-qed two-bit universal quantum logic gate: The principle and expected performances*, Phys. Rev. A **52**, 3554 (1995).

[163] Asoka Biswas and Girish S. Agarwal, *Quantum logic gates using stark-shifted raman transitions in a cavity*, Phys. Rev. A **69**, 062306 (2004).

[164] Marlan O. Scully and M. Suhail Zubairy, *Cavity qed implementation of the discrete quantum fourier transform*, Phys. Rev. A **65**, 052324 (2002).

[165] Chui-Ping Yang, Shih-I Chu, and Siyuan Han, *Simplified realization of two-qubit quantum phase gate with four-level systems in cavity qed*, Phys. Rev. A **70**, 044303 (2004).

[166] L. You, X. X. Yi, and X. H. Su, *Quantum logic between atoms inside a high-q optical cavity*, Phys. Rev. A **67**, 032308 (2003).

[167] Girish S. Agarwal, P. Lougovski, and H. Walther, *Multiparticle entanglement and the Schrödinger cat state using ground-state coherences*, J. Mod. Opt. **52**, 1397 (2005).

[168] Girish S. Agarwal, R. R. Puri, and R. P. Singh, *Atomic schrödinger cat states*, Phys. Rev. A **56**, 2249 (1997).

[169] Yu. Makhlin, *Nonlocal properties of two-qubit gates and mixed states and optimization of quantum computations*, Quant. Info. Process. **1**, 243 (2002).

[170] M. D. Barrett, J. Chiaverini, T. Schaetz, J. Britton, W. M. Itano, J. D. Jost, et al., *Deterministic quantum teleportation of atomic qubits*, Nature **429**, 737 (2004).

[171] M. Riebe, H. Häffner, C. F. Roos, W. Hänsel, J. Benhelm, G. P. T. Lancaster, et al., *Deterministic quantum teleportation with atoms*, Nature **429**, 734 (2004).

[172] P. Hyafil, J. Mozley, A. Perrin, J. Tailleur, G. Nogues, M. Brune, et al., *Coherence-preserving trap architecture for long-term control of giant Rydberg atoms*, Phys. Rev. Lett. **93**, 103001 (2004).

[173] W. Hänsel, P. Hommelhoff, T. W. Hänsch, and J. Reichel, *Bose–Einstein condensation on a microelectronic chip*, Nature **413**, 498 (2001).

[174] J. McKeever, J. R. Buck, A. D. Boozer, A. Kuzmich, H.-C. Nagerl, D.M. Stamper-Kurn, et al., *State-insensitive cooling and trapping of single atoms in an optical cavity*, Phys. Rev. Lett. **90**, 133602 (2003).

[175] Matthias Keller, Birgit Lange, Kazuhiro Hayasaka, Wolfgang Lange, and Herbert Walther, *Continuous generation of single photons with controlled waveform in an ion-trap cavity system*, Nature **431**, 1075 (2004).

[176] Stefan Nußmann, Markus Hijlkema, Bernhard Weber, Felix Rohde, Gerhard Rempe, and Axel Kuhn, *Submicron positioning of single atoms in a microcavity*, Phys. Rev. Lett **95**, 173602 (2005).

[177] Stefan Nußmann, Karim Murr, Markus Hijlkema, Bernhard Weber, Axel Kuhn, and Gerhard Rempe, *Vacuum-stimulated cooling of single atoms in three dimensions*, Nature Phys. **1**, 122 (2005).

[178] Karim Murr, Stefan Nußmann, T. Puppe, Markus Hijlkema, Bernhard Weber, S. C. Webster, et al., *Three-dimensional cavity cooling and trapping in an optical lattice*, Phys. Rev. A **73**, 063415 (2006).

[179] A. Wallraff, D. I. Schuster, A. Blais, L. Frunzio, R.-S. Huang, J. Majer, et al., *Strong coupling of a single photon to a superconducting qubit using circuit quantum electrodynamics*, Nature **431** (2004).

[180] Alexandre Blais, Ren-Shou Huang, Andreas Wallraff, S. M. Girvin, and R. J. Schoelkopf, *Cavity quantum electrodynamics for superconducting electrical circuits: An architecture for quantum computation*, Phys. Rev. A **69**, 062320 (2004).

[181] Yuriy Makhlin, Gerd Schön, and Alexander Shnirman, *Quantum-state engineering with josephson-junction devices*, Rev. Mod. Phys. **73**, 357 (2001).

[182] V. Bouchiat, D. Vion, P. Joyez, D. Esteve, and M. H. Devoret, *Quantum coherence with a single cooper pair*, Physica Scripta **T76**, 165 (1998).

[183] Isaac L. Chuang, Lieven M. K. Vandersypen, Xinlan Zhou, Debbie W. Leung, and Seth Lloyd, *Experimental realization of a quantum algorithm*, Nature **393**, 143 (1998).

[184] David G. Cory, Mark D. Price, and Timothy F. Havel, *Nuclear magnetic resonance spectroscopy: An experimentally accessible paradigm for quantum computing*, Physica D **120**, 82 (1998).

[185] T. S. Mahesh, Neeraj Sinha, K. V. Ramanathan, and Anil Kumar, *Ensemble quantum-information processing by nmr: Implementation of gates and the creation of pseudopure states using dipolar coupled spins as qubits*, Phys. Rev. A **65**, 022312 (2002).

[186] P. Domokos, M. Brune, J.M. Raimond, and S. Haroche, *Photon-number-state generation with a single two-level atom in a cavity: a proposal*, Eur. Phys. J. D **1**, 1 (1998).

[187] A. Rauschenbeutel, P. Bertet, S. Osnaghi, G. Nogues, M. Brune, J. M. Raimond, et al., *Controlled entanglement of two field modes in a cavity quantum electrodynamics experiment*, Phys. Rev. A **64**, 050301 (2001).

[188] Shi-Biao Zheng, *Generation of entangled states for many multilevel atoms in a thermal cavity and ions in thermal motion*, Phys. Rev. A **68**, 035801 (2003).

[189] H. J. Lipkin, N. Meshkov, and A. J. Glick, *Validity of many-body approximation methods for a solvable model*, Nucl. Phys. **62**, 188 (1965).

[190] R. G. Unanyan and M. Fleischhauer, *Decoherence-free generation of many-particle entanglement by adiabatic ground-state transitions*, Phys. Rev. Lett. **90**, 133601 (2003).

[191] Ersin Keçecioğlu and Anupam Garg, *Diabolical points in magnetic molecules: An exactly solvable model*, Phys. Rev. B **63**, 064422 (2001).

[192] R. H. Dicke, *Coherence in spontaneous radiation processes*, Phys. Rev. **93**, 99 (1954).

[193] F. T. Arecchi, Eric Courtens, Robert Gilmore, and Harry Thomas, *Atomic coherent states in quantum optics*, Phys. Rev. A **6**, 2211 (1972).

[194] David P. DiVincenzo, *The physical implementation of quantum computation*, Fortschr. der Phys. **48**, 771 (2000).